Preliminary Design of an Implantable Biosensor for the Detection and Differentiation of Acute Rejection, Vascular Occlusion, and Infection in the Liver or Kidney Transplant Graft

by

Megan M. Owens

B.S., Mechanical Engineering (1998)
Massachusetts Institute of Technology

Submitted to the Department of Mechanical Engineering
in Partial Fulfillment of the Requirements for the Degree of
Master of Science in Mechanical Engineering

at the

Massachusetts Institute of Technology

June 2000

Signature of Author .....
Department of Mechanical Engineering
May 5, 2000

Certified by .....
Thomas F. Marinis
Charles Stark Draper Laboratory
Thesis Supervisor

Certified by .....
Roger D. Kamm
Professor of Mechanical Engineering
Thesis Advisor

Accepted by .....
Ain A. Sonin
Chairman, Department on Graduate Students

ENG

Preliminary Design of an Implantable Biosensor for the Detection and Differentiation of Acute Rejection, Vascular Occlusion, and Infection in the Liver or Kidney Transplant Graft

by
Megan M. Owens
Submitted to the Department of Mechanical Engineering
on May 5, 2000 in Partial Fulfillment of the
Requirements for the Degree of Master of Science in
Mechanical Engineering

Abstract

Although organ transplant survival rates are encouraging from a historical perspective, they are not zero. Patient death is unacceptable in a perfect world, highly undesirable in reality. Currently, ailment detection is by external symptom exhibition, a late-stage event. This is non-ideal; earlier detection is preferable. Several common post-transplant complications evince similar and even identical symptoms, rendering doctors unable to diagnose with surety. In order to determine the correct ailment, a needle biopsy is performed and the results analyzed. Biopsy as a method of differentiation is flawed for several reasons, including time costliness, risk of complications, patient inconvenience, necessarily low number and frequency of sampling, and others. However, treatment regiments for different complications are specific and noninclusive. For example, if a doctor mistakenly prescribes immunosuppressive therapy to treat a case of supposed rejection when the ailment is truly infection, then the immune system will be crippled and the infection will worsen. A specialized sensor would be capable of eliminating ambiguities and would allow doctors to more rapidly prescribe an effective remedy with surety. The goal of this thesis is to present a preliminary design of an implantable sensor capable of detecting and distinguishing between liver or kidney graft acute immunorejection, vascular occlusion, and infection. These ailments may occur during the post-transplant critical period, the first month following surgery. Since the sensor resides within the organ of interest, it will allow the earliest possible detection of warning signs indicating an ailment. These warning signals are typically concentration surges or depletions of specific target molecules, most of which are cytokines. Since the sensor monitors the target concentrations in real-time, temporal profiles may be constructed correlating to ailment events. Currently, there is no product such as this available on the market. The proposed concept design consists of a sensing element, radiofrequency telemetry system, data display, power system, and biocompatible packaging. The design combines the chemical sensor technology of the flexural plate-wave gravimetric sensor with implantable biosensor technology to yield a feasible solution to a significant clinical problem.

Technical Supervisor: Thomas F. Marinis
Title: Principal Member of the Technical Staff

Thesis Advisor: Roger D. Kamm
Title: Professor of Mechanical Engineering

Acknowledgement

This thesis was prepared at the Charles Stark Draper Laboratory, Inc. under IR&D Number 15031. Publication of this thesis does not constitute approval by Draper of the findings or conclusions contained herein. It is published for the exchange and stimulation of ideas.

This is the product of a culmination of effort. Emotional support and technical direction has been generously proffered by many, to whom I extend my sincere gratitude. I am thankful to Phil Marfuta and to my family for their willingness to listen and motivate. To Homer Pien, Ph.D., Thomas F. Marinis, Ph.D., and Roger D. Kamm, Ph.D., I am grateful, for they have, all three, acted as technical contributor, reader, and advisor in my project. Without the time and dedication of all of these previous individuals, the presentation which follows would never have been.

In addition, the following people contributed their technical expertise in their specialized fields of knowledge to the production of this exploration. I thank each one for the effort they have extended. My appreciation is colossal.

Riccardo L. Benedetti, Ph.D. (Swiss Federal Institute of Technology in Zurich)
Charles B. Carpenter, M.D. (Brigham and Womens' Hospital)
Atif Chaudhry (Draper)
Brian Cunningham, Ph.D. (Draper, CIMIT)
Steve Dawson, M.D. (CIMIT)
Bill Kelleher (Draper)
Phil Marfuta (MIT)
Cathy McEleney (Draper)
Matt G. Paradise (Purging Talon Publishing)
Jane Pepper (Draper)
Anthony Petrovich (Draper)
Joseph Przyjemski (Draper)
Myron Spector, Ph.D. (MIT, Harvard Medical School, Brigham and Women's Hospital)
Sokwoo Rhee (MIT)
Joseph P. Vacanti, M.D. (CIMIT)
Paul VanBroekhoven (Draper)
Carlo Venditti (Draper)
Paul Ward (Draper)
Michael Watts (MIT, Draper)

Signature of Author .....

May 5, 2000

[This page intentionally left blank.]

Contents

List of Tables

List of Figures

1 Introduction

1.1 Problem

Despite the advent of immunosuppressive therapy and modern sterile surgical procedures, post-transplant surgery complications still occur. In 1998, roughly 12,000 kidney transplants were performed (Critical Data). The most current data shows that the three-month graft survival rate is 92.1% for cadaveric-donor kidneys and 95.7% for living-donor kidneys, while the three-month patient survival rates are 97.3% and 98.7%, respectively (1998 SR & OPTN Annual Report). These survival rates, while seemingly high, also indicate an implicit non-survival rate. Patient death is unacceptable in a perfect world, highly undesirable in reality.

After transplantation, many problems are possible. Within the first month, patients may experience acute immunorejection (Lachmann 861), vascular occlusion or perfusion (Humar 344), or infection, to name a few (Wong 1241, Munoz 294). Many post-transplant complications evince similar or even identical symptoms. Without an invasive and time-consuming biopsy procedure and analysis, the doctor is unable to diagnose with absolute surety (Berkow 834-835). In such cases it becomes possible for a prescribed treatment for an incorrectly-identified condition to severely exacerbate the ailment.

For instance, subsequent to a kidney transplant, both rejection and infection may produce a fever symptom (Berkow 586-587, 833). In order to determine the correct ailment, a needle biopsy must be performed and the results analyzed. One such analysis, of several, is for leucopenia, or an abnormal reduction in the number of leukocytes. If there is no inexplicable decrease in white blood cells, this indicates that the ailment is rejection, not infection. However, if the doctor mistakenly prescribes immunosuppressive therapy to treat a case of supposed rejection when the ailment is truly infection, then the immune system will be crippled and the infection will worsen. Once organ deterioration proceeds past a critical point, there are currently no known methods to prevent graft failure (Forsythe 65).

1.2 Solution

A specialized sensor would be capable of eliminating ambiguities and would allow doctors to more rapidly prescribe an effective remedy with surety. The sensor system inputs and outputs may be visualized as in the diagram below.

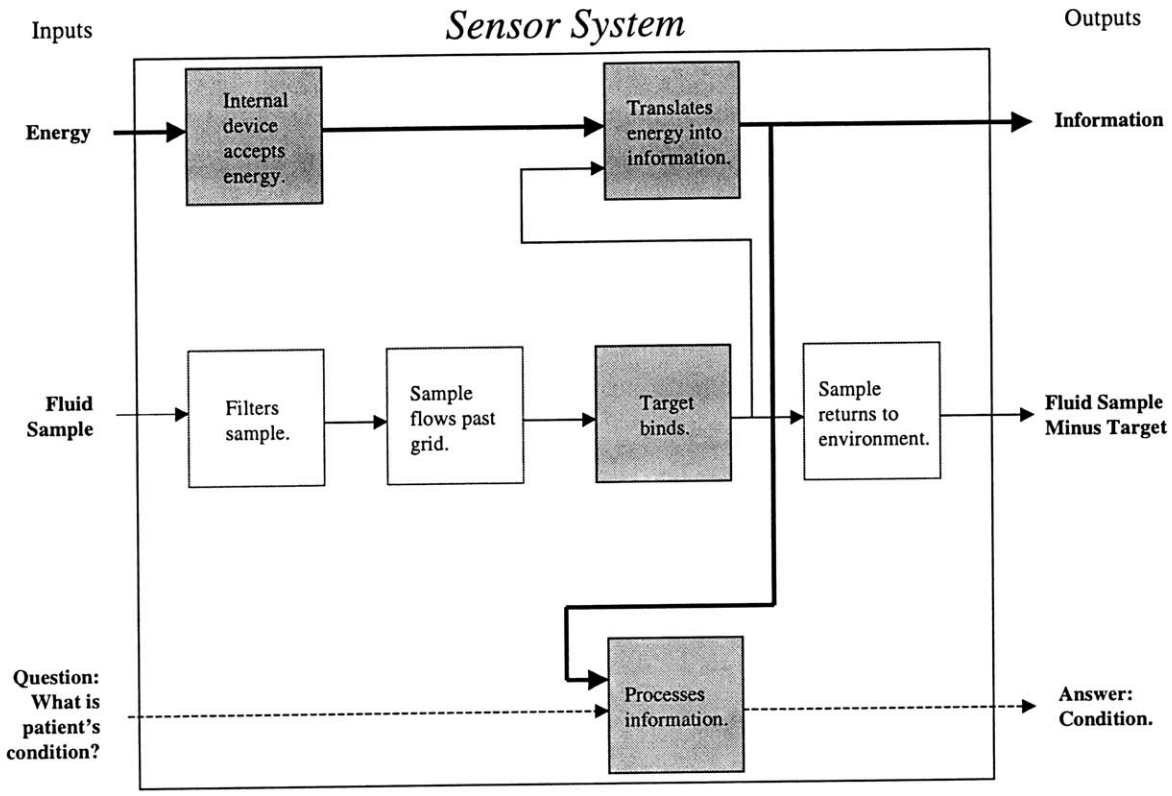

Figure 1: Sensor System Inputs and Outputs

The sensor described herein utilizes the flexural plate-wave gravimetric sensor to detect levels of cytokines and other chemical species indicative of acute rejection, infection, or vascular occlusion. The internal sensor is comprised of the sensing element, a semi-permeable membrane filter, a magnetic antenna, a battery power source, encapsulant, associated circuitry, and a biocompatible housing. It digitally emits concentration information to an external receiver once a day for four weeks. The information is received, processed, displayed, and stored. If target marker levels match levels which correlate with a problem, a visual and audio alert ensues. The patient is assured earliest detection of ailment. These operations might be physically characterized as in the following cartoon.

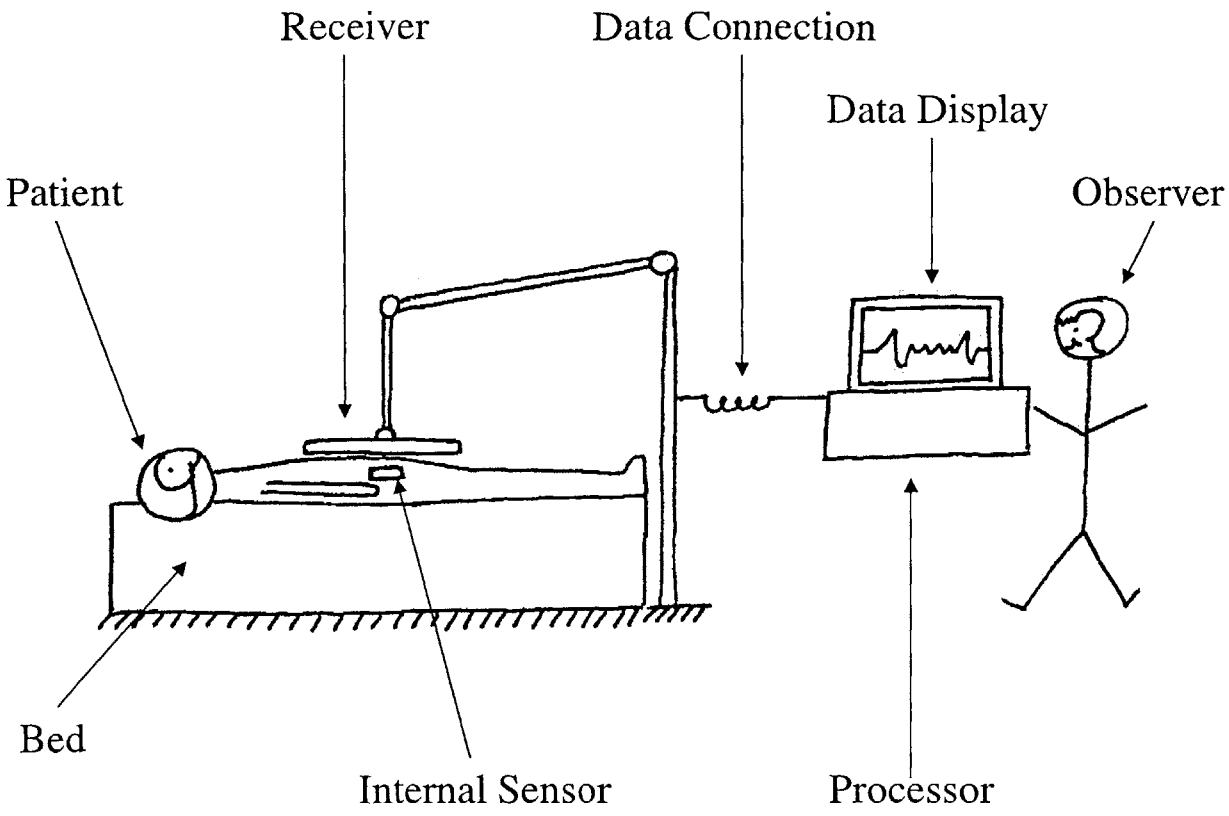

Figure 2: Operational Setup

Preliminary research results show that concentration surges of certain target molecules, often cytokines, may be able to predict immunorejection, as well as distinguish from infection and other ailments. For example, one of several well-documented studies involved the measure of serum or plasma interleukin-1 (IL-1), IL-1β, and IL-2 (Maury, Kutukculer). Typical results are shown in the form of a generic graph below.

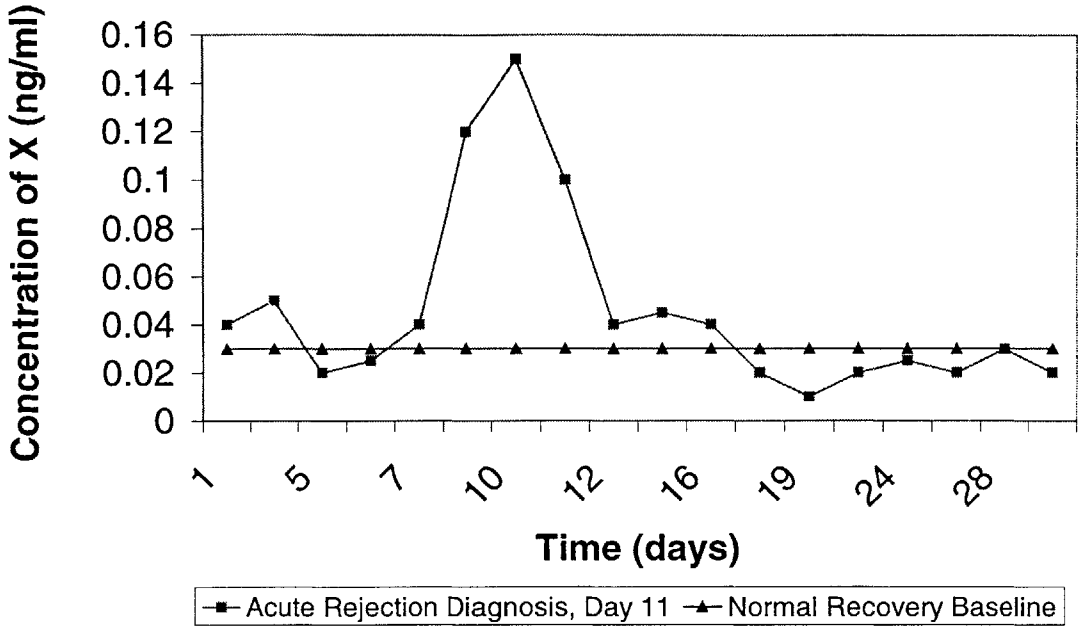

Figure 3: Typical Target Chemical Profile, Concentration vs. Time

Although research has shown promise regarding these molecules, in order to best understand rejection immunology and, thus, best treat patients, a series of studies must be undertaken in which all relevant molecules may be measured in a standardized fashion. The transplant organ biosensor may realize this goal. Once the best indicators have been revealed, the sensor may then be customized to detect these markers and monitor their concentration profiles over time. Transplant patients may then benefit from the final product.

1.3 Thesis Objective

The ultimate goal of this project is to design and implement an implantable biosensor capable of detecting and distinguishing between liver and renal graft acute immunorejection, vascular occlusion, and infection. Any of these ailments may occur within the first month following transplantation. Since the sensor is in direct contact with the organ's vascular system, it will allow the earliest detection of warning signs indicating a complication. These warning signals are typically concentration surges of specific target molecules. Currently, there is no

product such as this available to the surgical or research community.

The goals of this thesis are to (1) describe a medical problem of significant clinical importance, (2) explore the issues and challenges related to its solution, and (3) present a preliminary design of a novel solution.

First, relevant background information is included on the subjects of transplantation, kidney and liver anatomy, basic immunology, biomaterials-tissue interactions, and biosensor technology. Then, the design methodology is discussed, and the design is presented. Justifications for particular design choices also appear. Finally, future work is suggested and conclusions are given.

1.4 Contribution

This thesis offers three original and significant contributions to the field of biomedical engineering. First, it presents the concept of a specific and measurable molecular profile which correlates to a clinical event, in this case, acute immunorejection, infection, or vascular occlusion occurring in the post-transplant liver or kidney. Suspect molecular targets are identified. Second, it marries a particular chemical sensor technology, that of the flexural plate-wave gravimetric sensor, to implantable biosensor technology. This union results in the presentation of a unique application using both blocks of knowledge to solve a specific clinical problem. A logical design methodology is employed, yielding a mission statement pinpointing the project purpose, a set of customer-expressed product preferences, a set of product functional requirements, and a set of measurable metrics for the diagnostic device design. Using this newly developed knowledge, a preliminary feasible solution is designed and presented. Third, the thesis presents a solution formulation utilizing a step-by-step method which may be applied to any implantable biosensor radiotelemetry system design problem. Determination of optimal operating frequency, transmitter and receiver coil geometry, and power requirement are addressed.

2 Background Information

2.1 Anatomy

2.1.1 Kidney

The kidneys serve two main purposes: the excretion of both excess water and end

products of metabolic functions, and the production and release of several different endocrines. The first function is essential to the bodily maintenance of specific chemical concentrations, for example, electrolyte stasis within tissue fluids. The second function is responsible for products such as erythropoietin, an endocrine active in blood formation; and renin, which affects blood pressure. (Williams 1834)

The kidney has a distinctive shape. While its lateral edge is convex, its medial border is concave with a marked indentation called the hilus (Netter 2). In the average adult, a single kidney is about 11 cm long, 6 cm wide, and 3 cm in anteroposterior[1] direction. In men, a kidney weighs approximately 150 g, while in women, a kidney may weigh about 135 g. Healthy kidneys are a ruddy brown hue. (Williams 1834)

The kidney is overlaid by a thin capsule, mainly composed of collagen, along with some elastin and nonstriated muscle fibers (Williams 1819). The capsule vascular system is contiguous with the rest of the kidney's vessels (Williams 1820). This capsule may be easily removed from the kidney, except in some cases of renal failure (Williams 1819).

The kidney itself consists of two major parts, the medulla and the cortex. The medulla is the innermost portion of the kidney body and is comprised of conically-shaped renal pyramids, whose bases occupy the periphery of the medulla and whose vertices converge to the renal sinus, an area of the upper urinary tract consisting of major and minor calyces (Williams 1819). Minor calyces surround and grip groups of 7 to 14 renal pyramid papillae (Williams 1827). These calyces then lead to the ureter, a muscular pipe connecting to the urinary bladder (Williams 1828).

The cortex surrounds the medulla, capping the bases of the renal pyramids and reaching between them toward the renal sinus. The cortex may be further divided into an outer and an inner zone (Williams 1819). The inner zone is characterized by tangential blood vessels, including arcuate arteries and veins, while the outer zone is permeated by smaller interlobular arteries and veins (Williams 1827). The grainy texture of the cortex tissue is due to its composition of glomeruli and convoluted tubules, explained below, and many capillary nets (Netter 6).

The renal microstructure consists of dense uriniferous tubules packed in connective tissue laced with blood vessels, lymphatics, and nerves. Every tubule is comprised of two components:

---

[1] Bodily front to back, as illustrated in Gray's Anatomy (Williams 14).

a nephron and a collecting tubule. The nephron serves to produce urine, which the collecting tubule then gathers. A nephron is a unit consisting of a renal corpuscle, which filters the plasma; and a renal tubule, which selectively reabsorbs the filtrate. Blood enters the renal corpuscle through an afferent arteriole and winds through the turns of the capillary vessels, termed the glomerulus. Along the way, molecules and ions are filtered out through filtration slits in the capillary walls, and enter the urinary space. This space is of variable size depending on secretion levels and is enclosed by the glomerular capsule, an envelope of simple squamous[2] epithelium on the parietal wall and specialized epithelial podocytes[3] on the visceral wall. The filtered blood exits the glomerulus through the efferent arteriole. The renal tubule is the second component of the nephron and is comprised of (1) the glomerular capsule, (2) a proximal convoluted tubule, (3) the loop of Henle, (4) a distal convoluted tubule, (5) a junctional tubule, and (6) a collecting duct. The fluids course through these parts and then flow from the collecting duct, or collecting tubule, to a papillary duct of Bellini, which emerges from the vertex of a renal pyramid to penetrate one of the minor calyces.

The renal vasculature is fed by the renal arteries and drained by the renal veins. There are two renal arteries, a left and a right, each leading to its respective kidney. As each renal artery nears the hilus, it branches into four or five segments, one for each vascular lobe of the kidney. The branches, called segmental arteries, then superficially enter the kidney, immediately dividing again before plunging into the substance of the kidney. These branches feed the interlobular arteries running up between the pyramids of the medulla in the renal cortical columns. The interlobular arteries split into channels that flow roughly parallel to the kidney surface, the arcuate arteries. The arcuate arteries finally branch into interlobular arteries, which extend toward the cortex. Although many interlobular arteries actually feed capsular and extracapsular arteries, their primary purpose is to supply blood to the parenchyma and to deploy afferent arterioles into glomeruli. (Netter 16)

The venous pattern is noticeably different from the arterial network in that anastomoses between vessels do exist. This feature aside, the venous path is strikingly similar to the arterial

---

[2] Refers to cells with low cytoplasmic volume arranged in a single layer. Usually these cells are flattened and interlocking. (Williams 67-69)

[3] "Flat, stellate cells, their major processes curved around capillaries, interdigitating tightly with each other and attached to the basal lamina by numerous pedicels... [They] contain many mitochondria, microtubules, microfilaments and vesicles of various types, all of these being signs of active metabolism" (Williams 1822).

path. Small groups of radially-arranged subcapsular veins, called stellate veins, lie near the surface. These flow into interlobular veins, which proceed into arcuate veins, then interlobular veins. The interlobular veins converge into four to six vessels pointing toward the hilus. These large vessels lie anterior to the arteries and, once about 1 cm to 2 cm past the hilus, they merge to form the renal vein. (Netter 16)

The blood flow serves both regions of the kidney: the cortex and the medulla. Within the cortex, the cortical glomeruli are fed by afferent arterioles. The blood leaving the glomeruli exits through the efferent arteriole and circulates through a peritubular capillary net, supplying the tubular portion of the nephron with arterial blood. This net can occasionally anastomose with other glomeruli networks. Leaving the peritubular cortical net, the venous blood drains into vessels leading to the interlobular veins. These veins also accept the blood drained from the subcapsular stellate veins. (Netter 19)

Blood within the inner third portion of the medulla flows from the interlobular arteries or even arcuate arteries into the afferent arterioles of the juxtamedullary glomeruli. The efferent arterioles from these glomeruli descend directly inward, as opposed to the efferent arterioles of the cortical glomeruli, which flow into peritubular capillary nets. The efferent arterioles of the juxtamedullary glomeruli are just as large, or even larger, in diameter than the afferent arterioles. These descending efferent arterioles are referred to as vasa recta spuria. Plunging toward the hilus area, they often combine with other arterioles, forming new vessels. These vessels often tightly turn to ascend toward the pyramid bases, then empty into an arcuate vein. The ascending vessels are referred to as venulae rectae. Amidst the vasa recta spuria and venulae rectae, connections form, resulting in a network termed a rete mirabile conjugation. The outer portion of the medulla contains corticomedullary renal corpuscles, whose efferent vessels actually supply the outer medulla and part of the inner cortex, including the peritubular cortical nets. (Netter 19)

2.1.2 Liver

The hepar, or liver, is the most massive organ in the abdomen. It resides in the upper right portion of the viscera and is indispensable, responsible for a myriad of metabolic functions required for homeostasis,[4] alimentation,[5] and defense (Williams 1795).

---

[4] "The tendency to maintain, or the maintenance of, normal, internal stability in an organism by coordinated responses of the organ systems that automatically compensate for environmental changes" (Guralnik 671).

[5] "A nourishing or being nourished" (Guralnik 35).

Its position in the body may be specified with a fair amount of detail. The hepar resides in the upper portion of the abdomen, situated in the right hypochondriac[6] and epigastric[7] regions; its left lobe may protrude into the left hypochondrium space. The lungs overlap the liver, which overlaps the intestines and stomach. The diaphragm is also in close proximity. The upper right hand corner of the liver may rest as high as the fifth rib and the upper left hand corner as high as the sixth rib. Indeed, the ribcage covers most of the liver's right lobe and, with a body in the standing position, the liver comes down to the tenth or eleventh rib, while the pleura[8] extends only to the tenth rib and the lung to the eighth. Although the majority of the liver's bulk is covered by the ribcage, the portion in the epigastrium is not, and here the liver is situated about three fingers below the xyphoid process. The left lobe is partially guarded by the other half of the thoracic cage.

This normal placement of the liver may be altered by certain liver diseases, such as tumor infiltration, cirrhosis[9] or syphilitic hepar lobatum. It will also be affected by other bodily conditions. For example, subphrenic[10] abscesses[11] may push the liver downward, while ascites,[12] excessive colon dilation, and abdominal tumors may push it upward. Retroperitoneal tumors may even move it forward (Netter 4).

The organ shape may be described thusly:

> a wedge-shaped, rather rounded organ, its narrow end pointing left, and its anterior edge directed downwards. It is convex in front, to the right, above and behind, where it abuts the curved surfaces of the anterior body wall and diaphragm, and it is somewhat concave

---

[6] "Designating of the region of the hypochondrium," where the hypochondrium is "either side of the abdomen just below the lowest rib" (Guralnik 691).

[7] "Of or located within the epigastium," where the epigastrium is "the upper middle portion of the abdomen, including the area over and in front of the stomach" (Guralnik 470).

[8] "The thin serous membrane that covers a lung and lines that half of a chest cavity in mammals" (Guralnik 1094).

[9] "A degenerative disease in an organ of the body, especially the liver, marked by excess formation of connective tissue and subsequent contraction of the organ" (Guralnik 259).

[10] Refers to a space below the diaphragm (Guralnik 1073).

[11] "A swollen, inflamed area in body tissues, in which pus gathers" (Guralnik 5).

[12] "An accumulation of fluid in the peritoneal cavity of the abdomen" (Guralnik 80).

inferiorly where it is moulded to the shapes of the adjacent viscera (Williams 1796).

In men, the liver typically weighs between 1.4 kg and 1.8 kg, and in women, between 1.2 kg and 1.4 kg. A healthy liver is a reddish-brown color and is firm, but may be easily lacerated. In that case, bleeding is difficult to abate, due to the organ's great vascularity (Williams 1796). Save a small triangular part on the posterior surface, the organ is sheathed by peritoneum, connecting it to the stomach, duodenum, diaphragm, and anterior abdominal wall (Williams 1798-1800).

On a microstructural level, the organ is primarily composed of epithelial cells, in this case, hepatocytes.[13] Phagocytic macrophages also inhabit the liver, residing along the walls of the blood vessels. These cells are a part of the mononuclear phagocyte system and engulf and remove certain particles in the blood. The hepatocytes, the most prevalent cell type, provide many services: the breakdown and removal of toxins, the regulation of lipids and blood glucose, the storage of vitamins and ions, the breakdown or modification of amino acids, as well as other functions.

A number of cellular components exist within the liver cells. Fat droplets may appear within the cytoplasm. These are capable of gathering, being exported to the extracellular space, and gathering together to form fatty cysts in the tissue. Glycogen is another component in the cytoplasm. In severe disease of any kind, glycogen presence is drastically reduced. Hence, the glycogen content of the liver is able to act as an index of its functional status. Yet another component is vitamin A, the levels of which decrease as a result of malnutrition (Netter 7).

The hepatocytes are arranged throughout the liver in single-cell-thick plates called hepatic laminae or cords, which are mostly curved in many directions but may lie straight in some places. The endothelium-lined plates, riddled with holes of various sizes but usually larger in diameter than a single hepatocyte, fuse with other plates at various angles, forming an elaborate 3-dimensional mesh-like structure. Open spaces in the spongy structure are filled by connective tissue, blood vessels, and bile transfer ducts. The cell size within the plates ranges, the smallest being near plate holes and the largest residing at plate junctions. The holes in the plates link up to form tunnels, called lacunae, in which blood and bile transfer occur. Lacunae are lined with Kupffer cells, distinguished from other hepatocytes by their ability to greatly increase their size, thereby allowing increased macromolecule permeability. The small space

[13] The prefix "hepat-" or "hepato-" means "the liver," based on the Greek *hepar* (Guralnik 654).

through which this material flows, between the sinusoidal wall and the liver cell plate, is called Disse's space. *In vivo*, this space is very small and, indeed, the lacunae are virtually filled with blood. The vascular areas within the lacunae are termed hepatic sinusoids, the source of which is the hepatic portal vein and the hepatic arteries. Formed by the exterior walls of the hepatocytes themselves run tiny channels called canaliculi, which collect bile excreted by cells. The bile is carried in the direction opposing blood flow. At the ends of the cords, the canaliculi drain into slightly larger intralobular bile ducts called cholangioles, or ductules. These ductules are usually found within the periportal portion of the parenchyma and perforate the limiting plate to drain into the bile duct. Many hepatic ductules fuse to form the biliary tree (Williams 1802, Netter 9).

Two mesenchymal[14] tracts trace through the liver cell network and around the sinusoids and bile ducts. One is the portal tract, around which the cellular structure assumes the organization of a limiting plate. The limiting plate surrounds the portal tract along its entire length, punctured only where bile ducts enter the tract and blood vessels exit out into the parenchyma. With respect to a cross-section of this plate, all other plates originate from the limiting plate perpendicularly to its circumference.

Glisson's capsule, composed of collagen and elastin, surrounds the liver and continues inward to line the sinusoids and bile ducts. Immediately beneath its surface lies serosal endothelium; while in its deeper layers, lymphatic elements, blood vessels, and nerves may be found.

The parenchyma is surrounded by an intricate network of reticular[15] fibers which are anchored at the portal triads and hepatic vein branches. The network seems to be laid out around the central vein. This has prompted the definition of a liver lobule as being arranged around the central vein, while the portal triads are said to serve as meeting junctions for several lobules. By this observational criteria, the liver lobule is neither sharply defined nor readily distinguishable. Usually in only one case, that of perilobular fibrosis, is lobular delineation observed as obvious. In the absence of the ease of lobular distinction, observers have assumed a more convenient standard: one defined around the portal tracts and their respective bile ducts. In actuality, this seems a better lobular distinction, for the developmental directionality and ultimate orientations

---

[14] Describing "that part of the of unspecialized mesoderm from which the connective tissues, cartilage, bone, blood, heart, and lymphatic vessels are derived," where the mesoderm is "the middle layer of cells of an embryo, from which the skeletal, reproductive, muscular, vascular, connective, etc. tissues develop" (Guralnik 890-891).

[15] "Of or like a net; intricate, entangled" (Guralnik 1214).

of the liver cell plates are dependent on only the gradient of blood flow and pressure within the liver vascular system. (Netter 10)

The vascularization arises from three main vessels: the portal vein, the hepatic artery, and the hepatic vein. These three, in turn, are responsible for the supply and drain, only the supply, and only the drain of blood in the liver. These functions are under partial regulation, for despite the absence of any true muscular sphincters, anatomical features are able to somewhat limit the rate of blood flow.

The portal vein and its branches act as both supplying and draining vessels. After the portal vein enters the liver, it splits into main branches, then again and again into smaller branches until the branch diameter is no more than 0.3 mm, at which point, the branch is termed a distributing vein. The distributing veins both branch off at right angles and finally terminate into smaller inlet venules. The inlet venules exit the main sinusoids to span the limiting plate and extend into the peripheral sinusoids of the different liver lobules, effectively entering the parenchyma. Each inlet venule branches to a group of peripheral sinusoids, and each group of peripheral sinusoids branches into a small radially-organized network centered around what is called a central vein. Within the main sinusoids, portal vein branches that fail to split below the diameter limit of 0.3 mm are called conducting veins. The conducting veins lie parallel to the smaller distributing veins which carry blood in either the same or opposite direction. The conducting veins serve to ensure that the parenchyma in the regions immediately surrounding the main sinusoids have an adequate venous blood supply, since inlet venules branch and branch again to reach further out into the lobules. In this flow hierarchy, the portal vein is seen as a supply source. However, the portal vein branches servicing elements within the portal tract, especially the bile ducts, act as draining vessels. These small branches collect the blood from the capillary plexus within the portal tracts and feed the blood into the inlet venules to join with the blood supplied by the distributing veins. In total, the portal vein ramifications serve to both supply and drain blood. (Netter 11-12)

In contrast, the hepatic artery and its branches only supply blood. The hepatic artery's branches travel parallel alongside the portal vein's tributaries, splitting off to perforate the plate and enter the parenchyma. There, the hepatic arterioles expire at various lengths, feeding the entire liver. Although some arterioles do extend far outward to provide blood to the lobes' outer limits, most of the arterioles do not, instead terminating within the periportal region. The second

venue of the hepatic artery blood supply is within the portal tract. Here, the arterial branches feed the peribiliary plexus, which then drains the blood into the inlet venules of the portal venous system. It is important to realize that this is not a direct route from artery to vein and therefore, is not considered arterioportal anastomosis.[16] Arterioportal anastomosis is not a normal hepatic event, but does occur in cirrhosis. So, the hepatic artery serves only to provide, not to remove, blood. (Netter 12)

The last vascular channel is the hepatic vein and its smaller canals, which all drain blood. The aforementioned groups of parenchymal sinusoids, which carry blood from the inlet venules, each empty into a central vein around which they are oriented. The central veins flow into a sublobular vein, all of which join the inferior vena cava. The hepatic vein and its branches carry blood out of the liver. (Netter 12)

Although the human liver lacks true muscular sphincters, some flow regulation is maintained by other means. The first is through the strategic use of vessel diameter differentials. Smaller veins entering hepatic vein vessels are equipped with a dilation of the diameter immediately before the junction. The reduced diameter of the incoming veins assuages the blood flow. Using the same architectural mechanism, the venules relieve the blood flow that supplies the portal sinusoids. The diameter discrepancy is also employed when blood flows from the sinusoids to the central veins. In all of these cases, the smaller vessel entering the larger vessel is outfitted with a non-muscular sphincter, or an area of reduced diameter, that is able to abate blood flow. The second flow regulation tool is alternating contraction. Arterial blood reaches different levels of the lobules by the alternation of periportal and intralobular arteriole contraction. This nonconstant blood flow ensures that liver functions remain intact by allowing variation in the amount of time a unit of blood is in contact with a specific portion of the liver. (Netter 12)

2.2 Transplantation Surgery

2.2.1 History

Surgery served as a logical and necessary prelude to transplantation development. The first surgical procedures were performed around 8000 BC. Primitive cave paintings from this period show that men began to castrate domesticated animals. These prehistoric surgeries set the

[16] "Interconnection between blood vessels, veins in a leaf, channels of a river, etc." (Guralnik 50).

stage for the first transplantation procedures.

The next definitive acts of surgery occurred in the prehistoric Bronze Age, as evident in skeletal remains from this period of time. In order to relieve intracranial pressure, trephination was often performed. This procedure consisted of removing a circular piece of bone from the calvarium[17] and later reimplanting the same fragment back in its previous position. This surgical procedure was, in effect, transplantation - an orthotopic autograft. Although trephination may have often proved fatal, records imply that many procedures were effective.

Other accounts of concurrent transplantation developments come from recorded myths, legends, and medical notes from Egypt, China, India, and early Christendom, the earliest of these being from Egypt in 2000 BC A Hindu text from 700 BC intricately details the procedure of nasal reconstruction:

> ...the physician takes the leaf of a plant which is the size of the destroyed parts. He places it on the patient's cheek and cuts out of this cheek a piece of skin the same size (but in such a manner that the skin at one end remains attached to the cheek). Then he freshens with his scalpel the edges of the stump of the nose and wraps the piece of skin from the cheek carefully around it, and sews it at the edges. Then he places two thin pipes in the nose where the nostrils should go, to facilitate breathing and to prevent the sewn skin from collapsing. Thereafter, he strews powder of sapan wood, licorice root, and barberry on it and covers it with cotton. As soon as the skin has grown together with the nose, he cuts through the connection with the cheek.

Another account, although mythical, from Rome in the 6th century, evinces the public cognizance of and fascination with transplantation:

> ...a dying man sleeps one night in the church of St. Cosmas and St. Damian. During the night, he sees the saints emerge from the shadows and watches as they examine his cancer-infested leg. One brother removes the diseased leg while the other goes to a local cemetery, exhumes the body of a recently buried Ethiopian

[17] "The upper, domed part of the skull" (Guralnik 202).

> man, amputates and procures one of the cadaver's legs, and returns to the church. The saints join the Ethiopian's leg to the dying man's stump, and the man awakens the next morning, fully recovered from his previously terminal condition.

Teeth transplants, unfortunately largely unsuccessful, began around 1000 AD in Egypt, pre-Columbian North and South America, Greece, Rome, and China. The 15th century heralded a further interest and stronger development in skin grafting, and by the 19th century, accounts show that many tissues had been transplanted: skin, tendons, nerves, cartilage, adipose,[18] corneas, adrenal and thyroid glands, ovaries, partial digestive and urinary tracts, and muscle. Accounts also indicate a large success rate with animal transplantation, but show common failure with human patients. Clearly, transplantation is rooted in prehistoric times and early history with the advent of surgery and subsequently experimentation, both resulting in some success but mostly failure.

As surgical techniques progressed, three developments proved crucial to its increased success. The first was the discovery and use of chemical anesthesia. Ether, the first, was made in 1540 by alchemist Valerius Cordus. Its effects on animals were duly noted, however, ether was not used on human patients until the mid-1800s, then employed by fringe surgeons and dentists. The second important development was the concept of aseptic surgery. In 1865, following Pasteur's investigations in bacteriology, Joseph Lister, an English doctor, designed the first procedural codes for sterile surgeries. Once the medical community adopted his methodologies, the prevalence of infection following surgery lessened greatly. The third essential advance was the introduction of hemostatic procedures during surgery. Although cauterization had been practiced since an early Egyptian surgeon wrote "heat the knife with fire; the bleeding is not great" and ligation had also been in use for some time, the early 1900s brought about a new technique that revolutionized hemostatic methods. At this time a French doctor, Alexis Carrel, invented the arterial clamp, allowing temporary cessation of blood flow. These three developments were harbingers of the time of modern transplantation surgery.

In 1936, a Russian surgeon, V. Voronov, performed the world's first kidney transplant. The outcome was unsuccessful; the patient died two days later. In 1947, Richard Hufnagel, an American doctor practicing in Boston, conducted an effective temporary kidney transplant. His

[18] "Fat in the connective tissue of an animal's body" (Guralnik 17).

pregnant patient was troubled with a uterine infection, so Hufnagel replaced her kidney with that of a dying woman. After three days, before acute rejection set in, Hufnagel switched the kidneys again. Those three days allowed the pregnant woman to recover from her infection. In 1950, Ruth Tucker underwent renal transplantation. Doctors used a donor kidney from a non-related woman who was the same age and blood type as the patient. Results were promising, as Tucker lived for almost a year following the procedure. The cause of her death was chronic rejection. Through working with burn victims during W.W.II, doctor Peter Medawar realized that skin grafts, and probably most transplants, would fare best between identical twin donor and recipient. The validity of this observation become clear when doctors Joseph Murray and John Merrill performed a kidney transplant with a twin donor and recipient, and met with positive results. Neither twin experienced complications, short-term nor long-term. Public awareness of transplantation ascended to a new level when, in 1967, Dr. Christiaan Barnard performed the first cardiac transplant. Unfortunately, the recipient lived a mere three weeks post-transplant. Although milestones had been marked, doctors soon realized that, in order for an operation to be fruitful, the patient's immune system must be suppressed so their body may accept the donor organ.

Hence, the field of immunosuppression was born. So, about thirty years ago, immunosuppressive ideas began to show pertinence within the transplantation community. Matching donors and recipients with respect to histocompatibility was one of the first methods instituted. This involves matching both tissue type, or tissue antigen profile, and ABO blood type. The second approach to immunosuppression involved chemical use. A pioneering technique in this field was total body irradiation. First tried in 1959, it successfully crippled lymphocytes, but also caused unacceptable side effects, such as increased susceptibility to infection and disease. Another chemical technique held promise: the administration of immunosuppressive drugs. However, at the time, doctors were limited to two steroids: cortisone and its derivative, prednisone, both of which had the ability to selectively annihilate only cells of the immune system. The side effects of long-term steroid use were, however, highly undesirable. These included acne and facial hair growth increase, loss of ability to naturally produce steroids, mood changes, blood sugar increase, body fat distribution changes, bone thinning, blood pressure increase, skin thickness decrease, and cataracts. In the early 1960s, another drug emerged: a purine called azathioprine. Synthetically manufactured and able to interrupt the mitosis of non-

self antigens, it proved useful and most beneficial when given in low doses. Side effects exist, but can be tolerated. In 1962, Dr. Thomas Starzl introduced a new drug administration technique: the cocktail approach. This method involved using a combination of immunosuppressive drugs, usually azathioprine and steroids, to treat patients. This method was effective, allowing transplantation survival rates to increase. Then, in 1972, a Swiss biochemist discovered cyclosporine. This drug, able to inhibit both T-cell and B-cell lymphocyte activity, became indispensable in immunosuppressive therapy. Its side effects are many, but like azathioprine, it may be administered in small doses with tolerable results. Today, doctors fit a new drug regiment for each patient, often prescribing different levels of both azathioprine and cyclosporine. (Bergan 2-9) If doctors were able to continuously monitor local immune activity, immunosuppressive use could be limited, resulting in fewer and less severe negative side effects. A local sensor such as is suggested could indicate immune system activity via the measurement of cytokines.

Both liver and kidney transplantation procedures today consist of two parts: donor organ harvest and recipient organ implantation. Thanks to preservation fluids and constant cooling, the two steps may be separated by a great length of time, up to 18 hours for the liver and 72 hours for the kidney. The preservation fluid commonly used is called University of Wisconsin solution (UW), and has the properties of high osmolarity and high concentrations of potassium, calcium, and magnesium, allowing minimum tissue injury during the time preserved on ice. The organ is kept at a temperature between 0-4°C for the duration of storage (Williams 1808, 1834).

The donor patient's liver removal commences with the identification of the organ's arterial supply, the hepatic artery, for it is through this entry that the organ will later be perfused and cooled with solution. Somewhat complicating matters, the hepatic artery reveals itself in textbook configuration only 60-65% of the time, the remaining one-third of cases being variations. A common variation, seen in 20% of cases, is a replaced left hepatic artery from the left gastric artery. Another frequent configuration, comprising about 15% of cases, is a replaced right hepatic artery coming from the superior mesenteric artery. About 5% of the time, both of the aforementioned variations are seen together, or the complete hepatic arterial supply flows from the superior mesenteric artery or from a common coeliacomesenteric trunk. Once the arterial supply has been identified, the surgeon will divide the common bile duct immediately above the pancreas and incise the gallbladder. The bile of the gallbladder will be flushed out

with solution prior to the organ's storage in order to best discourage bile-induced epithelial injury of the tissue. After the gallbladder incision, the aorta must be clamped above the level of the coeliac axis. The liver is then cooled with UW solution by perfusing through the portal vein and hepatic artery. The surgeon then removes the common and external iliac arteries and veins, preserving them in the event that a vascular reconstruction might later be necessary. The liver harvest is then complete.

The liver implantation procedure is a semi-elective procedure and, as such, is usually performed during the daytime. The surgeon first removes the dysfunctional liver. The structures in the porta hepatis are divided close to the liver hilium, the hepatic artery, the common hepatic duct, and the portal vein. The IVC is noted below the liver, the left and right triangular ligaments are split, and the bare area of the liver is then lifted off the diaphragm. The suprahepatic IVC is cut and encircled. The patient's IVC is clamped and the liver removal is finished.

The final step is to replace the diseased liver with the donor liver. After the patient's internal bleeding is under control, the new liver is implanted. First, the surgeon connects the upper IVC, the lower IVC, and the portal vein using a continuous vascular suture. Second, the UW solution is flushed from the organ and the graft is reperfused with blood from the portal vein. Next, the hepatic arteries of the donor organ and patient are joined. If necessary, vascular reconstruction is performed, and the implantation is done. (Williams 1808)

During the donor kidney harvest, the surgeon identifies the vascular anatomy. In most cases, there is a single renal artery, but in 15% of cases, there may be multiple arteries. The arterial twigs which supply the upper third of the ureter must be preserved, as well as a length of the ureter. The implantation procedure involves first arterial and then venous anastomoses and, lastly, the re-establishment of urinary drainage. Because arterial connections to accessory arteries do not occur within the kidney, while venous anastomoses do occur between the main renal vein and accessory veins, the surgeon must take care to connect all accessory arteries to the recipient's vasculature during the implantation, but may ligate accessory veins. The donor ureter is connected to the recipient urinary tract using one of two methods: either implantation of the donor ureter into the recipient bladder or connective suture of both the donor and recipient ureters. The kidney transplantation is then essentially complete. (Williams 1834-1837)

2.2.2 Post-operative Complications

Following transplantation, any number of problems may arise, including vascular occlusion, infection, and rejection. In fact, in one renal transplant study, "rejection was the most frequent cause of transplant nephrectomy (45%), followed by arterial thrombosis (25%), and infection (15%)" (Mora Durban 873).

Occlusion is the blockage of a blood vessel and is usually caused by a blood clot. It may be perceived by qualitative symptoms, for "when a clot lodges in one of the renal arteries, the branches that supply the kidneys, a sudden pain occurs in the side, and the urine becomes bloody" (Berkow 132). Vascular occlusion easily leads to ischemic injury, which occurs within a tissue when its blood supply is stopped. The incidence of ischemic injury is high: each year, more than 1.3 million people are afflicted in the United States alone. A portion of these cases are attributable to organ transplant procedures, during which blood vessels may become cross-clamped ("Ischemia/ Reperfusion Injury").

Vascular occlusion necessarily interrupts aerobic metabolism in the afflicted tissue, since blood is no longer able to deliver or pick up oxygen from the tissue's cells. As a result of the halted aerobic metabolism, metabolites accumulate in the tissue. After a length of time, the ischemic tissue becomes necrotic and unrecoverable. Even if blood flow is restored just prior to this point, more extensive damage will ensue. The oxygen made available through reperfusion stimulates the resumption of aerobic activity, the byproducts of which are free radicals. The abundance of free radicals overwhelms the antioxidant system, causing cellular damage such as lipid peroxidation.[19] Furthermore, cell damage stimulates the synthesis of inflammatory response cytokines, which encourage neutrophil and macrophage attack on the ischemic tissue. The onslaught may not stop with the ischemic tissue, but also affect remote tissues due to the systemic nature of cytokines as soluble regulators. ("Ischemia/ Reperfusion Injury") Ischemic tissue is difficult to repair. Considering that vascular occlusion causes, at best, ischemia and, at worst, necrosis, it is clear that the early detection of occlusion is highly desirable. Fortunately, there exists an early marker: the accumulation of aerobic metabolites. Given a sensor able to detect these metabolites, the early detection of vascular occlusion becomes a viable possibility.

---

[19] "Lipid peroxidation represents the major mechanism of lipid destruction occurring in an organism... Lipid peroxidation is thought to be a major destructive reaction occurring in the plasma components and blood vessel walls leading to the generation of cardiovascular disease" (Assays Currently Available).

Because immunosuppressive therapy is administered in the wake of a transplantation surgery to decrease the possibility of implant rejection, the host's immunity is compromised, increasing susceptibility to infection. Unfortunately, infection is very common: an overall incidence of 70-80% following solid organ transplantation has been reported and infection has been associated with up to 85% of post-transplant deaths (Forsythe 283). Bacterial, fungal, or viral infections may occur. Bacterial wound infections may occur at the surgical wound site and are often marked by fever, redness, swelling, tenderness, or leakage. A common fungal infection is candida, commonly known as yeast, which generally manifests in the mouth or throat but may infect the surgical wound, eyes, respiratory tract, or urinary tract. Common viral infections are cytomegalovirus (CMV), herpes-simplex virus type I and II, and herpes zoster. CMV is one of the most-commonly-occurring infections in transplant recipients; in one study, a CMV infection rate following liver transplantation was 49% (Forsythe 284). The risk of CMV is highest in the first months following transplantation: "infections are rarely seen before 1 month and classically manifest at between 2 and 3 months" (Forsythe 284). Symptoms include fatigue, fever, aching joints, headaches, visual disturbances, and pneumonia. CMV detection is accomplished via the identification of CMV inclusion bodies in biopsy specimens (Forsythe 285). Herpes-simplex virus usually infects the skin, but may attack the eyes or lungs. The first type typically causes cold sores and mouth blisters, while the second type manifests as genital sores. Signs of infection include feeling weak and having painful fluid-filled sores. Although both types are usually transmitted sexually, this is not necessarily the case in transplant recipients. Herpes zoster appears as a rash or small water blisters on the chest, back, or hips. (www.kidneytransplant.org)

Rejection is "any process leading to the destruction or detachment of a graft" (On-Line Medical Dictionary). Three distinguishable patterns of rejection may be described: hyperacute, acute, and chronic, although the investigated application specifically pertains only to acute rejection.

Hyperacute rejection is caused by pre-existing circulating cytotoxic antibodies present in the host serum. In this case, the host body has previously encountered the same antigens present on the donor graft's cells and has produced an immune response against them. Following the immune response, the host body keeps a low-level supply of the generated antibodies in circulation. When the host body detects these antigens again, now on the donor graft, immune

attack is swift. Hyperacute rejection occurs within the first few hours following grafting, often before the surgical operation has even been completed. The reaction consists of the immediate loss of the graft with endothelial cell disruption, platelet margination, complement activation, and thrombosis. (Forsythe 64)

Acute rejection is cell-mediated and most commonly occurs between days 5 and 14 following surgery, though it may occur any time within the first three months, or even longer. It has been suggested that 90% of liver acute rejection cases occur within the first three weeks post-transplant (Lang 776). It may occur after the first month if the host's immunosuppressive therapy is reduced or if prompted by a separate event such as a viral infection. It is recognized by several external symptoms, such as a fever, and may also be described by internal chemical markers, which are thoroughly discussed in Section 2.3.2. (Forsythe 64-65)

Chronic rejection is the least well-characterized form of rejection. It is slow to occur and has several causes. Immunological causes have been suggested in the form of ongoing microvascular endothelial damage by antibody and cell-mediated processes, though other causes must be a factor since typically no significant amount of inflammatory cell infiltrate exists in the organ histology. Although causes remain elusive, specialists agree that chronic rejection may be characterized by the inability to prevent organ failure once a certain stage of deterioration has been reached. (Forsythe 65)

Rejection, infection, and occlusion dysfunctions are positively identified and diagnosed by a biopsy procedure. A biopsy is a procedure in which a small piece of an organ is removed for histological examination. In a needle biopsy, the patient is given a local anesthesia and a needle is inserted through the skin into the organ, often with the guidance of ultrasound[20] or Computed Tomography (CT) scan[21] in order to better locate the abnormal target area. This is usually an outpatient procedure. (Berkow 560, 593)

In an alternate and less common biopsy method, which may be performed to obtain a liver sample, a catheter is introduced to the body through a vein in the patient's neck. It is snaked through the chambers of the heart and positioned in one of the hepatic veins that outlets from the

---

[20] "A diagnostic test that uses sound waves to create images of organs and other areas inside the body" (Newcomer).

[21] "Radiography (using x-rays) in which a three-dimensional image of a body structure is constructed by computer from a series of cross-sectional images made along an axis. Also referred to as CAT scan" (Glossary of HIV/AIDS-Related Terms).

liver. The biopsy needle extends into the liver through the wall of the vein to obtain a sample. Although this procedure may sound more difficult, it is less likely to lacerate the liver. (Berkow 560)

There are many disadvantages to a biopsy procedure. The procedure is non-ideal from a patient care perspective. Following the procedure, the patient must remain hospitalized for at least 3 to 4 hours due to the slight risk of serious complications. The potential problems would most likely stem from organ laceration. In the case of a liver biopsy, for example, laceration may allow blood and/or bile to leak into the abdomen, causing peritonitis, or inflammation of the abdomenal lining. Since bleeding may commence anytime within 15 days post-biopsy, the patient is required to remain within an hour's travelling time of the hospital. Although the risk of complications is small, it is not zero. Complications cause serious problems in 2% of patients, while 1 in 10,000 biopsies prove fatal. The majority of patients experience mild pain in the upper abdomen, sometimes extending to the right shoulder. (Berkow 560) In addition to laceration complications, there is a risk of infection derived from introducing a foreign object into the body. From a clinical viewpoint, a biopsy is flawed because it is used only after external symptoms of ailment manifest and because it requires laboratory processing to yield interpretable results. These two considerations introduce a significant lag time after the event before diagnosis is possible. In this time, the patient's condition may worsen, perhaps irreparably. During organ rejection, once a certain level of deterioration has been reached, no currently available therapeutic manipulation has been able to reverse the inevitable outcome of graft failure (Forsythe 65). A third issue surrounds sampling accuracy. The invasive nature of the procedure limits the number of samples that may be realistically obtained for analysis, a spatial limitation. Perhaps more critically, a temporal limitation also exists. A biopsy analyzes the condition of the tissue at a single moment in time. Because of possible fluctuations in molecular concentrations, this measurement is less useful than a series of measurements taken over a period of time. So, biopsies are an imperfect monitoring method for several reasons: (1) the procedure and follow-up care is time-consuming and spatially-limiting for the patient, in a word, inconvenient, (2) the patient is subjected to residual pain, (3) there is a nonzero risk of serious, potentially fatal, complications, (4) the procedure is only used late in the course of the event, (5) precious time is required to obtain meaningful results, (6) the procedure is spatially-limited, and (7) the procedure is temporally-limited.

A number of other complications can follow a kidney or liver transplant. In the kidney, one complication is anesthesia, or the loss of normal sensation or feeling. Whether or not this is more or less likely to occur depends on patient age. Another possible complication is a myocardial infarction, or a heart attack. This may happen when the blood supply to one area of the heart is interrupted because of narrow or blocked blood vessels. It can cause permanent damage to the heart muscle. Once again, the chance of this depends on the patient's age. A cerebrovascular accident, or a stroke, another age-related event, may also occur. A stroke may be accompanied by hemiplegia, blindness, speech problems, and confusion. Another post-transplant complication is peripheral vascular disease (PVD). It involves the blockage of the large blood vessels of the arms, legs, and feet. Because areas of the arms, legs, and feet do not receive enough blood, these areas experience aching pains and foot sores that heal slowly. Another complication, related to size, is hyperfiltration, in which case kidneys with reduced renal mass progress toward failure due to hypertrophy of the remaining nephrons to meet the excess load, eventually resulting in nephron exhaustion (Forsythe 48). Other complications may reveal themselves quite early after the surgery. These acute problems include drug toxicity (the levels of immunosuppressive medication must be altered), ureteric leak or obstruction, rejection, and lymphocoele (Forsythe 139).

Problems after a liver transplant may include primary poor function or non-function, hemorrhage, rejection, infection, biliary complications, graft ischemia (Forsythe 158). Evidence of rejection is found in 80% of the cases biopsied at the end of the 1st week. Although a biopsy may indicate signs of rejection, if prothrombin time and other liver function tests are improving, there is no need to boost immunosuppressive therapy. If a boost is needed, treatment is usually either intravenous or oral high-dose steroids. If a patient happens to be steroid-resistant, monoclonal (OKT3), or polyclonal antibodies (ATG), or other agents, or switching to tacrolimus may be better. If after experiencing a boost in treatment, the patient still shows signs of ongoing rejection, retransplantation may be necessary, even though severe recurrent rejection in the new graft is a potential risk.

Infection may occur as well, attacking the lungs or biliary tract and presenting itself four to eight weeks post-op with symptoms of fever and leucopenia. The typical treatment is immunosuppression and gancyclovir therapy. Fungal infection is common in patients with chronic liver failure.

Biliary complications include bile leaks, anastomotic strictures, non-anastomotic strictures of the donor bile duct, and sludge formation. The incidence rate is around 10% in adults, but is higher in children. When suspected, the hepatic artery should be analyzed using ultrasound, for hepatic artery thrombosis can cause ischemia and necrosis of the biliary tree. Bile leakage symptoms include presence of bile in the drain fluid, percutaneous aspirate, or fluid found on ultrasound. Biliary obstruction without leakage may be viewed with by ultrasound and confirmed by ERCP (endoscopic retrograde cholangio pancreatography) or PTC (percutaneous transhepatic cholangiography).

Graft ischemia, previously discussed, is also a post-transplant threat. HAT (hepatic arterial thrombosis) occurs most frequently in the first month. It leads to graft necrosis, intrahepatic abscess, or biliary necrosis and bile leakage. Its onset is heralded by spikes in levels of transaminases, particularly in the first few days after grafting. Later, gram negative sepsis or bile leakage may occur. Rates as high as 10% in adults and over 20% in children have been witnessed. (Forsythe 158)

2.3 Immunology

2.3.1 Events in Host Response to Implant

The body's response to an implant is governed by the immune system, a diverse collection of cells that mediate immune responses ranging from mild local inflammation to full-blown systemic rejection (Vander 701). An implant, in this case, is any physical presence in the body that may be recognized as non-self, including for example bacteria and pacemakers. Unfortunately, transplanted organs also qualify. Because a transplanted organ is viewed by the body as a foreign presence, it undergoes an attack by the immune system which sometimes leads to organ rejection.

The rejection process is comprised of two stages: the afferent stage and the efferent stage. In the afferent stage, the host immune system becomes activated. The events of this part of the process may occur in two sites: in the recipient lymphoid tissue after donor cells have infiltrated and/or in the organ graft itself. The efferent stage is characterized by the triggering of the humoral and cellular mechanisms. The humoral system fights primarily foreign material present in body fluids, while the cellular system attacks non-self elements that have already infiltrated host cells (Campbell 854). These mechanisms are responsible for annihilating and removing the

foreign presence. (Lachmann 1687)

The specific events in the two stages are as follows. First, donor antigens are presented by donor and recipient antigen presenting cells (APC) to the helper T cells (Th). The process by which Th cells accept recipient antigens is allorecognition. It is a mechanism that works by the identification of molecular markers. Those most important in transplantation immunology are the major histocompatibility antigens (MHC) and the minor histocompatibility antigens (mH). *In vitro*, MHC-incompatible cells have been shown to induce a severe primary immune response, while *in vivo* they are known to cause rapid graft rejection and/or graft-versus-host disease (GVHD). It is thought that the response is so vicious and speedy because a relatively high number of precursor T cells do exist that are capable of recognizing and responding to foreign MHC presence. (Lachmann 1689-1689)

Once the Th cells are activated, they begin to produce soluble mediators called lymphokines or, more generally, cytokines. A cytokine is "simply a general term for a chemical that is secreted by one cell as a regulator of neighboring cells" (Campbell 866). Cytokines are divided into two categories; type 1 cytokines, such as interleukin-2 (IL-2) and interferon-γ (INF-γ), promote cellular immunity and protect the host, whereas type 2 cytokines, including IL-4 and IL-10, suppress cellular immunity and enhance the progression of infection (Xu 1504). The cytokines produced in Th cell activation include IL-2, IL-4, INF-γ, and others. In fact, different subsets of Th cells produce different cytokines. Th1 cells produce IL-2, IFN-γ, and tumor necrosis factor-β (TNF-β), while Th2 cells generate IL-4, IL-5, and IL-6. The two subsets yield the cellular and humoral responses, respectively. (Lang 776)

Next, activated Th cells trigger the effector part of the rejection process by either direct contact or lymphokine mediation. T cell cytotoxic precursors (Tcp) mature into effector cytotoxic cells (Tc) that attack and kill organ graft cells. Th cells and lymphokines stimulate the growth and differentiation of B cells, which are responsible for the production of graft-reactive antibody. In the effector portion of the process, macrophages are activated, developing cytocidal capability. The lytic activity of natural killer cells (NK) is increased. Other leukocytes are attracted to the rejection site, amplifying the response. Tissue cells in the vicinity of the attack increase their expression of major histocompatibility complex (MHC) antigens through the increased release of INF-γ which further amplifies the immune response. (Lachmann 1688) Eventually, enough donor tissue destruction may occur as to render the organ dysfunctional,

rejected. Organ failure ensues, and, barring intervention, is followed by systemic failure. Patient death may occur.

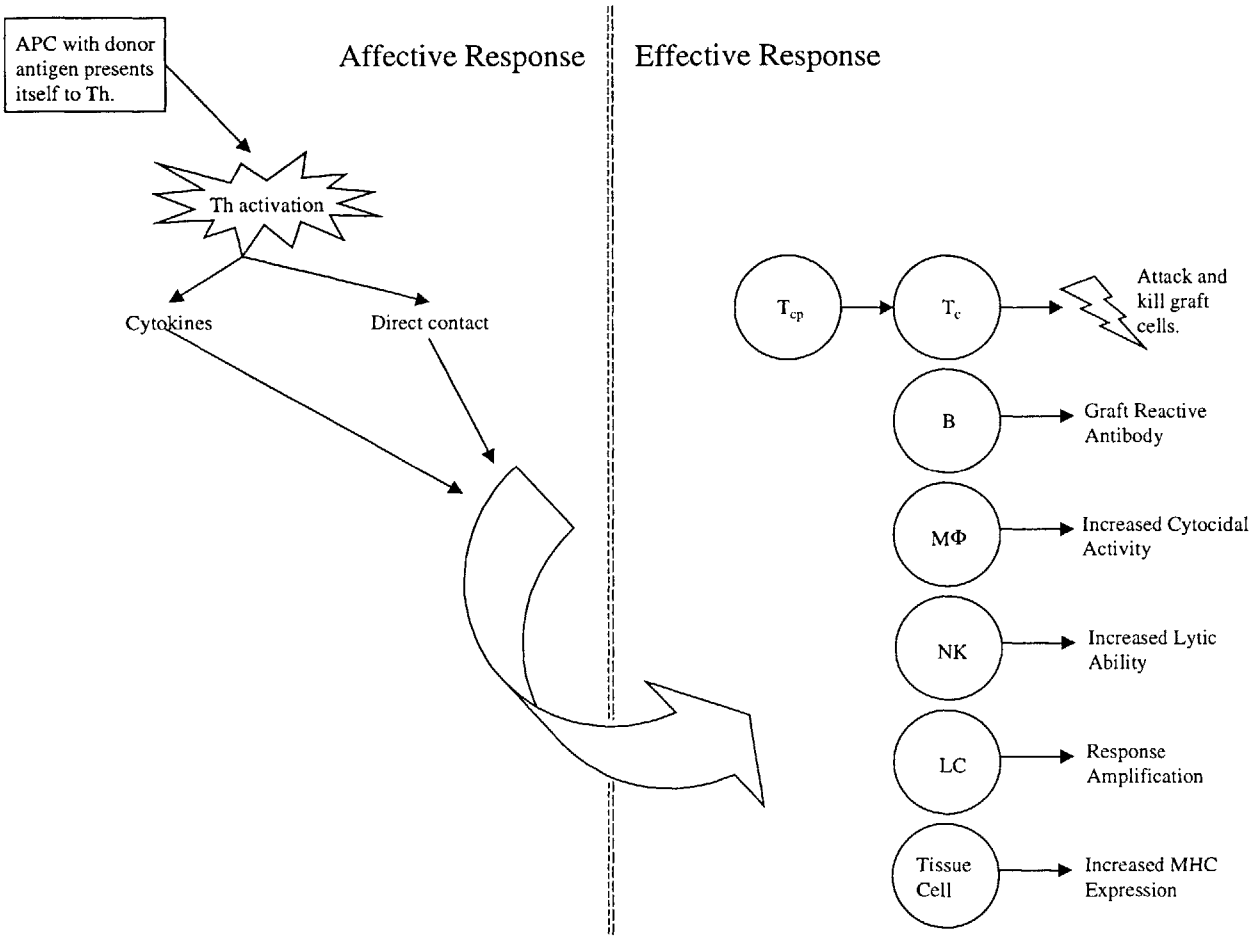

Figure 4: The Rejection Process

2.3.2 Target Marker Literature Review

As a testament to the current understanding of the origin and progression of bodily ailments as a group of fundamentally chemically-based phenomena, an ever-growing body of recent research suggests that physiological ailments may be identified and distinguished from other ailments by specific chemical markers. In other words, a physical ailment is the result of a series of complicated, interconnected inner body chemical reactions. Oversimplified, each reaction yields a product and that species serves as the a reactant in the next step in the pathway.

$$R_1 + R_2 \rightarrow P_1 \quad (1)$$

$$P_1 + R_3 \rightarrow P_2 \quad (2)$$

$$P_2 + R_4 \rightarrow P_3 \tag{3}$$

Although real reactions are much more complicated, the idea of a pathway producing a chemical species is intact. If the next reaction produced not only a chemical product, but also a macroscale physiological ailment, as in

$$\ell(t)P_3 + m(t)R_5 \rightarrow n(t)P_4 + \text{ailment} , \tag{4}$$

then P_4 could be referred to as a chemical marker of the ailment. P_4 could be called a specific chemical marker if each and every time P_4 is produced in quantity n, or quantity profile over time n(t), the ailment exists, and if each and every time the ailment exists, then P_4 is produced in quantity n, or quantity profile n(t). In the same way, P_3 and R_5 could be named early chemical markers. If their quantity profiles always match the ailment and the ailment always matches $\ell(t)$ and m(t), then they are specific early chemical markers. The same would hold for any species in the chemical pathway upstream of the product and ailment of interest.

Any specific chemical markers, whether early or not, would aid in the detection and identification of acute immunorejection, infection, and vascular occlusion following kidney or liver transplant since current methods of testing are invasive, inconvenient, and untimely. A noninvasive, painless, and real-time detection of these markers would be ideal. Fortunately, current research studies indicate that these markers do exist. Although many studies imply marker existence, there is a paucity of published data on quantified kinetic profiles over time. The sensor being designed will give researchers a tool with which to create detailed profiles. These profiles will later aid in ailment detection when the sensor is used in the clinical arena.

There are many chemical markers of acute kidney rejection cited in the body of published research. The most prevalent is interleukin-2 (IL-2), but others are also highly noticed. These include IL-1, IL-3, IL-4, IL-6, IL-7, IL-10, IL-15, IL-17, ENA-78, interferon γ (IFN-γ), tumor necrosis factor β (TNF-β), granzyme B, Fas ligand, and sIL-2R. These are all cytokines released by T helper cells, with the exception of ENA-78, a chemotactic and neutrophil-activating peptide (Schmouder 118), granzyme B and Fas ligand, cytotoxic attack molecules (Sharma 2364), and sIL-2R, soluble interleukin-2 receptor (Lee 844). Many researchers have looked for these markers in different forms, including levels in the circulating blood serum, in

the transplanted kidney itself, and in mRNA form.[22] Their relevant results are summarized here.

Researchers from Hopital Paul Brousse in Villejuif, France decided to study the activity of IL-1, IL-2, and IL-3 in renal grafts during phases of rejection and tolerance in 1987. Patients included those with and without cyclosporine A immunosuppressive treatment. Seventeen patients were included in the study, which found that "acute rejection is associated with high release of cytokines (IL-1, IL-2, and IL-3)." (Charpentier 1573)

At the University of Helsinki in Finland, researchers Maury and Teppo measured serum IL-1 levels in 12 patients. They report:

> From 10-fold to 20-fold elevations of interleukin 1 occurred in association with 10 of 12 graft rejection episodes. The interleukin 1 elevation preceded the clinical rejection diagnosis by an average of one day in transplant recipients with initially functioning grafts, and by two days in recipients with delayed onset of graft function. The results show that the release of interleukin 1 into the circulation is an early event in renal allograft rejection and demonstrate the potential utility of interleukin 1 antigenic assays in the early diagnosis of rejection.

This study found IL-1 to be a valuable early marker for acute rejection. (Maury 143)

In 1991, Catherine Vanderbroecke and other researchers at Hopital Necker in Paris, France and Charing Cross and Westminster Medical School in London, England studied the expression of IL-6, TNF-α, and IFN-γ in normal and acutely rejecting kidney grafts. In the normal grafts, no detectable levels of IL-6, TNF-α, or IFN-γ were measured. They also found that significantly elevated levels of only IL-6 were found in renal biopsies from six of the eight patients exhibiting acute rejection. (Vanderbroecke 602)

Po-Huang Lee and other investigators in Taiwan measured IL-2 and sIL-2R levels in serum samples from 32 renal allograft patients. Their findings document markedly increased levels of sIL-2R in patients with acute rejection episodes, as compared to levels in stable patients. The rise in sIL-2R occurred one to four days earlier than the clinical diagnosis of acute rejection. However, different elevated levels of sIL-2R were also found in patients experiencing

[22] Levels of mRNA would indicate levels of the chemical species itself, as mRNA formation is a step in the direct process of chemical production from the cell's genome.

acute tubular necrosis or infection. Lee asserts that monitoring sIL-2R levels could be "particularly helpful in differentiating the allograft dysfunctions of rejection and cyclosporine nephrotoxicity." Although levels of IL-2 differed between patients experiencing acute rejection and normal patients, they were not significantly different between patients with cases of acute rejection, cyclosporine nephrotoxicity, or acute tubular necrosis. (Lee 844)

At the Cornell Medical Center in New York, NY, and the Hennepin County Medical Center in Minneapolis, MN, researchers Guo-Ping Xu and others researched levels of mRNA expression of type I and type II cytokines in acutely rejecting kidney allografts. Ninety-eight biopsies were tested, and the results indicated that "...intragraft expression of IL-10 mRNA and IL-2 mRNA are significant correlates of acute rejection." They also discovered that IL-4, IL-7, IFN-γ, and TGF-β_1 mRNA levels are not indicative of acute rejection. The researchers advocate strategies of constraining intragraft IL-10 expression in order to possibly avert acute rejection. These findings were published in 1995. (Xu 1504)

Also that year, findings were presented by Kutukculer and others from the University of Newcastle upon Tyne in England that show that detectable plasma[23] IL-2 levels predict impending graft rejection. Although IL-2 levels are an early marker, IL-4 and IL-6 levels were found to be more reliable in the process of differentiating rejection from other ailments, particularly toward the end of week 1 post-transplant. IL-3, IL-8, and soluble CD23 were not indicative of rejection, as many patients with high levels of these species did not show any evidence of acute rejection. (Kutukculer 334)

Robert Schmouder and others, in 1995 at the University of Michigan Medical School in Ann Arbor, Michigan, looked into the possible role that epithelial-derived neutrophil-activating factor-78 (ENA-78) may play in renal allograft rejection. ENA-78 is a 78-amino acid peptide with chemotactic properties. It also activates neutrophils during inflammation. The role of ENA-78 in rejection seems a likely possibility, as biopsy tissue from acutely rejecting human renal allografts had higher levels of ENA-78 mRNA compared with control cases. The findings speculate that, within the rejecting graft, IL-1β produced by both host and donor cells may encourage ENA-78 production by allograft tubule cells. (Schmouder 118)

---

[23] Plasma is the aqueous medium of blood. It is comprised of many substances, including electrolytes, proteins, lipids, carbohydrates (notably glucose), amino acids, vitamins, hormones, nitrogenous products of metabolism (for example urea and uric acid), gaseous oxygen, carbon dioxide, and nitrogen. (Berne 359)

In 1987, Adam McLean and researchers investigated the chemical milieu of the acutely rejecting kidney by taking fine needle aspirates during the first ten days following transplantation. Detection of IL-2, IL-4, IL-6, IL-10, and IFN-γ mRNA was analyzed. During the first four days, all of the grafts produced a cell infiltrate rich in monocytes, an event accompanied by a rise in IL-10 expression. Following day four, all grafts showed either stable or increasing infiltrate. Of the grafts exhibiting dense infiltrate, roughly half developed acute rejection. Cytokine mRNA analysis led to the conclusion that "IL-2 and IFN-γ gene expression are necessary, but not sufficient, for the development of acute cellular rejection in the first 10 days of kidney transplantation, and are more closely associated with the period leading up to rejection than with the period of graft dysfunction." (McLean 374)

In 1998, Xian Chang Li and others at Harvard Medical School and the Children's Hospital in Boston, MA researched the effects of IL-9 gene expression in murine and human renal rejection. They failed to show IL-9 mRNA expression during islet allograft rejection in IL-$2^{-/-}$ and IL-$4^{-/-}$ double knockout (DKO) mice. None of the human renal allograft biopsies showed IL-9 expression either, regardless of the presence or absence of rejection. Despite the findings, the investigators did exclaim "vigorous expression of IL-2, IL-4, IL-7, and IL-15 genes during acute allograft rejection." (Li 265)

Also in 1998, at the Centro de Histocompatibilidade do Norte in Porto, Portugal and Brigham and Women's Hospital in Boston, MA, fine-needle aspiration biopsy was performed to test cytokine levels among T helper cell subsets. The findings showed that "IL-2 synthesis on day 7 post-transplantation reliably predicted the risk of impending acute rejection during the first weeks." (Oliveira 417)

A histological study by Lipman and others conducted at McGill University in Montreal, Canada and the University of Manitoba in Winnipeg, Canada examined the correlation between TNF-α, IL-1β, transforming growth factor β (TGF-β), IFN-γ, IL-2, IL-4, IL-10, IL-15, granzyme B, perforin, and Fas ligand transcripts and clinical acute rejection diagnoses based on histology. The findings report that "histological features of rejection are often accompanied by enhanced expression of pro-inflammatory gene transcripts, despite the absence of clinically overt graft dysfunction." In other words, histological evidence of acute rejection is present despite the fact that the graft does not yet show overall ailment and the patient does not yet exhibit external symptoms of acute rejection. (Lipman 1673)

Reverse transcriptase-polymerase chain reaction (RT-PCR) was used by researchers at Cornell Medical School in New York, NY to investigate the intragraft expression of mRNA encoding for granzyme B and Fas ligand, as well as for cytokines IL-2, IL-4, IL-10, IFN-γ, and TGF-β_1 in human renal allografts. One hundred and twenty-seven core tissue samples were taken from 107 patients and tested. Their findings show that granzyme B mRNA, Fas ligand mRNA, IL-2 mRNA, and IL-10 mRNA are molecular correlates of acute rejection. (Sharma 2364-2365)

Cees Van Kooten and others at Leiden University Hospital in the Netherlands and Schering Plough in France have examined the possibility of IL-17 relevance in the acute rejection of renal allografts. The paper relays the results of the first demonstration of IL-17 protein expression in pathological conditions and examines the idea that IL-17 may be a critical element in the regulation of local inflammatory responses responsible for acute rejection. (Van Kooten 1526)

These studies all investigate the possible role of different chemical species as markers of acute rejection in the kidney. While some studies may present contradictory findings, it is clear that there exists some chemical profile of acute renal rejection. No one study, however, completely defines the profile, although together as a group, they define the players. These investigations reveal a very good possibility of a profile consisting of some or all of the species' individual profiles in time. The species involved are most likely: IL-1, IL-2, IL-3, IL-4, IL-6, IL-7, IL-10, IL-15, IL-17, ENA-78, interferon γ (IFN-γ), tumor necrosis factor β (TNF-β), granzyme B, Fas ligand, and sIL-2R. There are surely even others yet unknown. However, a profile consisting of information regarding how each of these named targets varies with time in a normal healing mode of post-transplantation and in an acute rejection mode should be more than adequate to characterize a rejection episode.

The studies also rule out some chemical species as markers of acute renal rejection. For example, IL-3, IL-8, IL-9, IFN-γ, TGF-β_1, and soluble CD23 are reported to not be correlates of rejection. Other studies back up these findings and present other non-appropriate markers. Serum IL-8 is confirmed to not be a good marker: "Serum IL-8 measurements were of no value in predicting rejection due to low sensitivity (24%)" (Budde 871). Soluble E-selectin has been shown to not be an early unequivocal indication of rejection (Weston 50).

Although the body of research conducted concerning chemical markers of acute liver

rejection is not as large as for the kidney, some studies shed light on the key constituents of a potential profile. One study even presents chemical species kinetic profile information.

Researchers Carlos Cosenza and others, at the Cedars-Sinai Medical Center in CA, investigated levels of cytokine mRNA expression in 36 liver biopsy specimens taken from 20 recipients of primary orthotopic liver allografts. Species measured were: IL-1β, IL-2, IL-4, IL-6, IL-10, IFN-γ, TNF-α, and β-actin. IL-1β, IL-6, and IFN-γ were consistently detected in rejecting allograft biopsies. TNF-α and IL-2 were also detected, but only during the early phases of the rejection. IL-4 was detected in both normal and rejecting biopsy specimens. (Cosenza 16)

At the California Pacific Medical Center in San Francisco, California, researchers Thomas Lang, Sheri Krams, and Olivia Martinez analyzed both bile and serum samples taken from 18 post-transplant livers at 2-3 day intervals for the first 26 days. Researchers measured levels of IL-2, IL-4, IL-10, and IFN-γ. Levels of IL-4 and IL-10 rose significantly at the site of graft rejection, while IL-2, IL-4, and IFN-γ levels increased in the circulation. The study concludes that "...acute rejection of human [liver] allografts can proceed in the presence of minimal levels of the Th1 cytokines IL-2 and IFN-γ and high levels of IL-4 and IL-10." This study also presents cytokine profiles over time. These profiles were constructed using IL-2, IL-4, IL-10, and IFN-γ levels in the bile of eighteen patients following liver transplantation. Corresponding graphs showing the profile trends are shown below. (Lang 776)

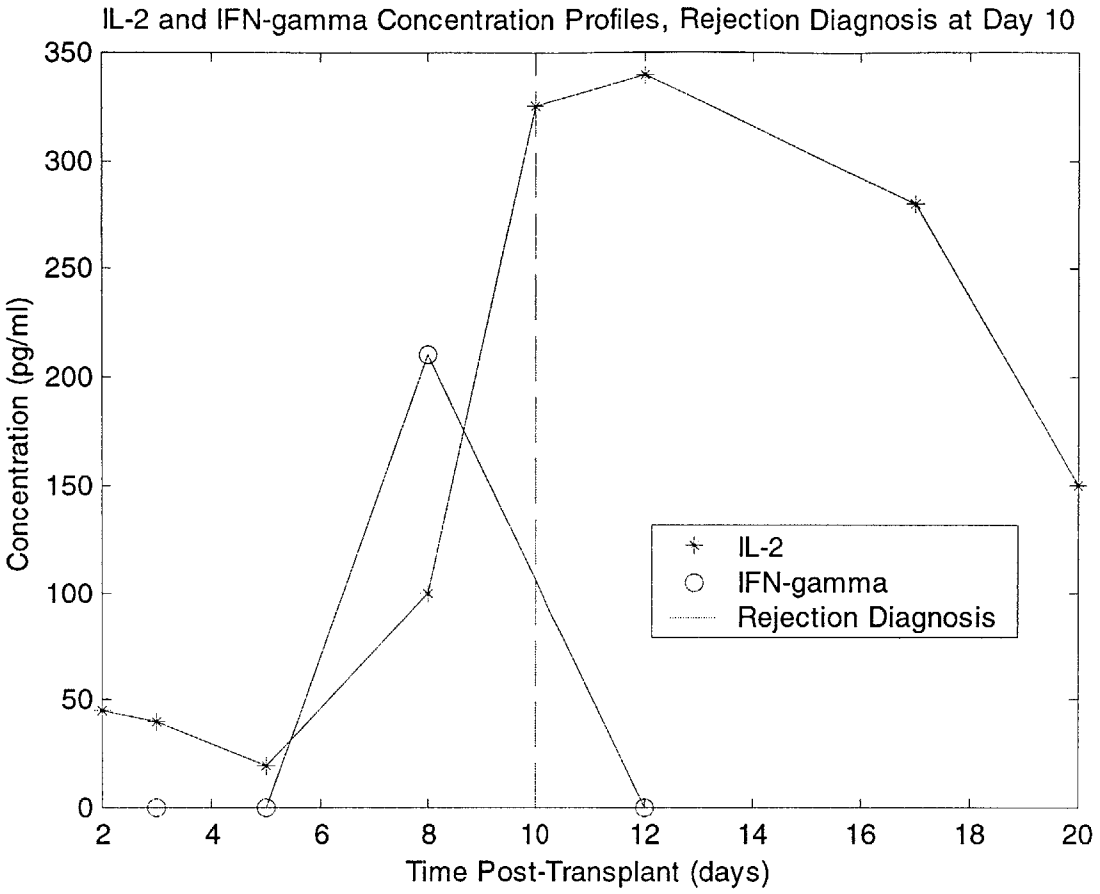

Figure 5: IL-2 and IFN-γ Concentration Profiles, Rejection Diagnosis at Day 10

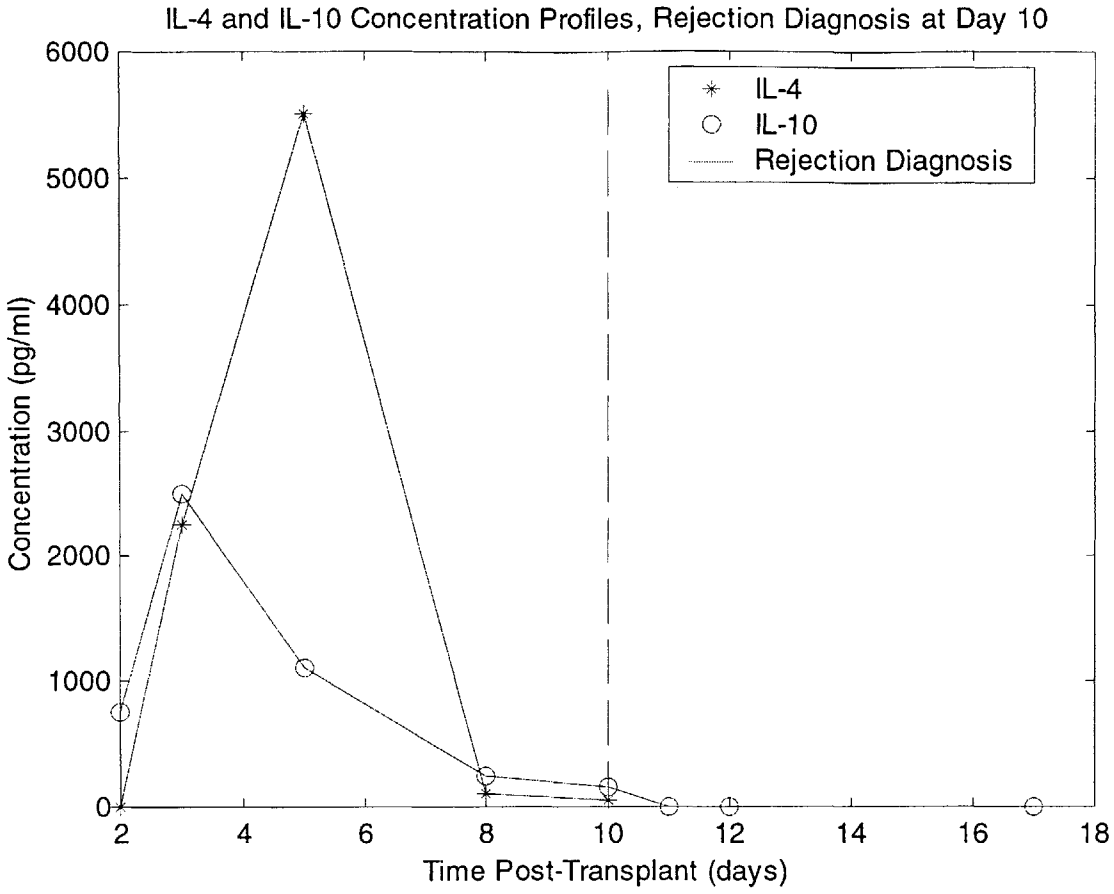

Figure 6: IL-4 and IL-10 Concentration Profiles, Rejection Diagnosis at Day 10

So, as in kidney transplantation, liver transplantation normal and rejection cases may also be characterized by chemical marker profiles. The representative graphs above, although pertaining to measurements extracted from bile samples, are most likely very similar in shape to the profiles of the chemical markers within the organ extracellular milieu. Such profiles, once generated, could be used to identify an impending acute rejection episode within a transplanted liver.

Acute rejection is not the only ailment that is related to chemical markers. Vascular occlusion, as mentioned in Section 2.2.2, is marked by a surge in aerobic metabolites, oxygen radicals ("Ischemia/ Reperfusion Injury"). Oxygen radicals are produced when cells reduce molecular oxygen (O_2) to water. This reaction is catalyzed by cytochrome c oxidase and involves the transfer of four electrons to oxygen. This reaction proceeds through intermediates of partially-reduced oxygen species. A transfer of one electron yields a superoxide anion radical (O_2^-). This can produce hydrogen peroxide ($H_2O_2 + O_2^-$). When another electron is removed

from oxygen, a hydroxyl radical is formed (OH^-). This chemical is extremely reactive; it spontaneously reacts with any molecule from which it can strip a hydrogen atom. Both of these intermediates are reactive with oxygen species; in particular the hydroxyl radical can react with all biological macromolecules, such as lipids and proteins. The first reaction produces a second free radical, which then reacts with another macromolecule to continue the leapfrog process. ("Free Radicals and Oxidative Stress") These intermediate oxygen species could serve as chemical markers of vascular occlusion.

Because an infection attacks the immune system, it is frequently marked by a reduction in the number of leukocytes, white blood cells. While leukocytes themselves are too large to adhere to the sensing element of the flexural plate-wave gravimetric sensor, perhaps leukocyte byproducts could be sensed. Even if this is not readily possible, the non-identification of the problem as either rejection or occlusion suggests infection as the culprit.

Table 1: Possible Targets

ACUTE REJECTION • Kidney ➢ IL-1, IL-2, IL-3, IL-4, IL-6, IL-7, IL-10, IL-15, IL-17, ENA-78, IFN-γ, TNF-β, granzyme B, Fas ligand, sIL-2R • Liver ➢ IL-1β, IL-2, IL-4, IL-6, IL-10, IFN-γ, TNF-α
VASCULAR OCCLUSION • Oxygen Radicals
INFECTION • Leukocyte Products

2.4 Biomaterial-Tissue Interaction

2.4.1 Events in Host Response to Sensor

In order to elucidate the events and their consequences involved in the implantation of a biomaterial, it is first helpful to describe the control case: wound healing in the absence of an implant. Healing maybe defined as "the process of restoration of injured tissue," and generally[24] may only occur in vascularized tissue. Healing by first intention, also referred to as primary or direct healing, is the restoration of continuity of injured tissue without the intervention of

[24] There has, in fact, been a limited success with encouraging articular cartilage, an avascular tissue, to regenerate. *In vivo*, the most successful experiments have yielded tissue which is histologically similar to cartilage, but which unfortunately does not fully integrate with the surrounding tissue. (Shortkroff 152-153)

granulation tissue,[25] for example, the healing of a scalpel incision in soft tissue. Healing by second intention, on the other hand, involves granulation tissue which fills the defect in the injured tissue. (Rubin & Farber 86) An illustration of this type of healing is a full thickness[26] wound in dermis, the healing of which results in scar tissue (Ferdman & Yannas 712). The first phase of healing, acute inflammation, consists of five chronological steps, the features of which may significantly overlap: (1) vascular response, (2) clotting, (3) phagocytosis, (4) neovascularization, and (5) new collagen synthesis. Acute inflammation tends to be short-lived; depending on the extent of the injury, this phase will last from a few minutes to a few days (Fraser 146). The second phase, chronic inflammation, may or may not ever occur, depending on whether or not the tissue heals by regeneration or repair. Inflammation is defined as "the reaction of the vascularised living tissue to the local injury which serves to destroy or dilute the injurious agent/medical device and the injured tissue" (Fraser 145). The kinetics and extent of inflammation depend on several factors, among them age, sex, health, and immunological and pharmacological status (Fraser 142).

The first stage of healing, the vascular response, involves three processes in response to the cutting of blood vessels during wound formation. First, the diameter of the surrounding blood vessels decreases due to soluble regulator action on the controlling smooth muscle cells. This constriction attempts to lessen the blood flow, or implement hemostasis[27] (Vander 741). Secondly, the surrounding vessels become increasingly permeable to fluid and cells as regulators influence vessel endothelial cells. A main affector is histamine, which causes contraction of endothelial cells lining the vessels. Cell contraction yields gaps between cell junctions, thereby increasing the permeability of the vessel. The unit cell process[28] for this reaction is characterized by:

---

[25] Granulation tissue is "highly vascularised tissue that replaces the initial fibrin clot in a wound. Vascularisation is by ingrowth of capillary endothelium from the surrounding vasculature. The tissue is also rich in fibroblasts (that will eventually produce the fibrous tissue) and leucocytes" (On-Line Medical Dictionary).

[26] Full thickness refers to a dermal wound extending down through the epidermis and most of the dermis, with appreciable width. In dermal regeneration/repair experiments, this type of wound is necessary in order to ensure that results are not due to any contributing effects of the neighboring epithelial cells of the remaining dermis. In contrast, partial thickness wounds leave an appreciable portion of the dermis intact.

[27] "Elimination of bleeding" (Vander 741).

[28] The unit cell process concept and notation is a unique and useful method by which complex biological processes may be decomposed and better understood. It was pioneered by Myron Spector, Ph.D. and Ioannis V. Yannas, Ph.D.

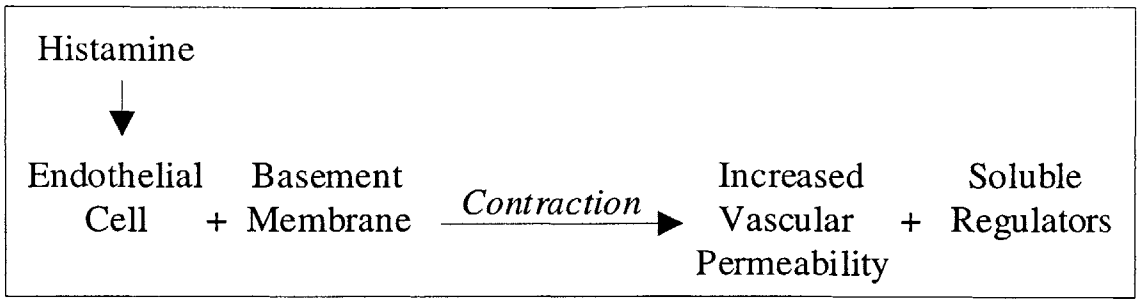

Figure 7: Unit Cell Process

Increased vascular permeability leads to leukocyte margination.[29] The third event is leukocyte migration through the gaps in the vessel wall. This occurs in three steps: leukocyte adhesion to the endothelial cell, emigration through the gap, and migration through the tissue extracellular matrix. Each step may be characterized by a unit cell process influenced by soluble regulators and aided by cellular adhesion molecules (CAMs).

The second step in the wound healing process is clotting. Following injury in a vessel wall, platelets circulating in the blood adhere to the wound site and accumulate. Platelet adhesion to collagen at the wound site is via von Willebrand factor (vWF), a protein released by the endothelial cells and the platelets. This protein attaches to the collagen and to the platelets, uniting the two. Once a platelet has adhered, it releases the contents of its secretory vesicles, including adenosine diphosphate (ADP) and serotonin. These chemicals stimulate platelet surface characteristic changes, which in turn help more platelets to adhere to the existing platelets. Thromboxane A_2, an eicosanoid, is also released, encouraging local platelet aggregation. Fibrinogen, a plasma protein, also aids by forming connections between adjacent platelets. This positive-feedback process quickly produces a platelet plug within the injured vessel. Because surrounding endothelial cells produce the inhibitory eicosanoid prostacyclin (PGI_2) and a vasodilator and inhibitor nitric oxide, platelet aggregation does not uncontrollably continue to grow beyond the injured area. (Vander 742-743) Blood coagulation, or clotting, also occurs, transforming the blood into a solid gel called a clot, or thrombus. Thrombin, an enzyme formed by a series of activation cascades in the vicinity of the wound, catalyzes a reaction that splits fibrinogen into several large portions that then form fibrin. The loose strands

[29] Margination refers to the movement of the leukocytes from their normal position, the vessel center, to the inner circumference.

of fibrin are mechanically stabilized by enzymatic cross-linkages, and then trap erythrocytes and other cells in their meshwork. The result is a blood clot. (Vander 743-744)

Phagocytosis follows blood clotting. In this process, polymorphonuclear neutrophils (PMNs), macrophages, and multinucleated foreign body giant cells are attracted to the wound site via stimuli, including chemotactic means. Chemotaxis may be stimulated by chemotactic peptides, leukotriene B_4, lymphokines,[30] growth factors such as PDGF and TGF-β, and fragments of collagen, fibronectin, or complement molecules. Once the phagocytic cells arrive in the wound area, they contact and bind via membrane receptor binding. The formation of a phagosome occurs, in which the phagocytic cell membrane portion containing the debris invaginates. Once the debris has been engulfed, an internal lysosome packet fuses with the debris and degrades it. Degradative agents include lysosomal enzymes and free radicals of oxygen. The entire process is regulated by different eicosanoids and cytokines. The different types of phagocytic cells have different active lifetimes. While PMNs survive for only a few days, macrophage precursors may circulate in the blood for 24 to 72 hours, macrophages can live in tissue for weeks, and multinucleated foreign body giant cells can exist in the tissue for months.

As phagocytic cells clean away wound debris, neovascularization takes place. The formation of a new blood vessel starts with the enzymatic degradation of the basement membrane of the wounded vessel. Following is endothelial cell migration and proliferation. As endothelial lining matures, a new capillary tube is formed. Even though damage usually occurs to more than one vessel, endothelial cells organize to form new vessels.

The last part of normal wound healing is the synthesis of new collagen to replace tissue loss. These last steps, the formulation of new vascular tissue and fibrous tissue, determine whether or not the wound healing is categorized as regeneration or repair. If the ratio of the mass of the vascular tissue to the mass of the collagenous tissue is approximately equal to one, then the mode of healing produces granulation tissue, which usually leads to regeneration of the wounded tissue. If the ratio is much less than one, then healing yields scar, indicative of a repair process.

Depending on the healing modality, chronic inflammation may or may not ensue. Chronic inflammation refers to a late-stage condition characterized by the persistence of macrophages and fibroblasts in a synovium-like layer surrounding the original wound and/or the

[30] Lymphokines are cytokines from lymphocytes.

formation of a granuloma. A granuloma consists of a concentrated area of epithelioid cells, which are macrophages whose appearance is altered to resemble epithelial cells, and multinucleated foreign body giant cells. It may also be an aggregation of lymphocytes surrounding by fibrous tissue. Such persistent inflammation can cause problems or may remain stable.

The relevant events provoking a bodily response to the introduction of an implant are inflammation, wound healing and/or regeneration of the affected tissue, and the foreign body response (Fraser 143).

The surgical introduction of an implant into the tissue environment involves the severing of blood vessels. Thus, the first contact medium between the biomaterial surface and the host is usually blood (Fraser 143). Blood is comprised of platelets, serum, and many proteins. In fact, the main solutes present are a variety of macromolecular proteins, occurring in high concentrations in all biological fluids, around 80 g/l in blood (Fraser 144). Besides blood, extracellular fluid is often present. Fraser writes:

> Although it is convenient to consider blood-material interactions separately from tissue-material interactions, it should be kept in mind that many of the cells and the mechanisms involved are closely related. Regardless of the tissue or organ into which a biomaterial is implanted, initial inflammatory response is activated by the injury to vascularised connective tissue, and therefore blood and its components are involved primarily (143).

Within minutes, sometimes within seconds, proteins adsorb to the biomaterial surface (Fraser 144). Although any number of proteins may attach, the most prevalent are albumin, immunoglobulins, and fibrinogen. Other absorbing proteins include kininogen, Hageman factor, von Willebrand factor, fibronectin, and complement components (Fraser 144). Current evidence suggests that the first step in the inflammatory response may be the adherence of fibrinogen (Fraser 148). Protein adsorption depends on several factors. Surface topography, charge density, distribution and mobility, surface groups, structural ordering, and the extent of hydration all greatly effect the outcome (Fraser 144). Over time, these proteins undergo conformational

changes[31] and exchanges with other proteins in the extracellular milieu (Fraser 144).

In studying protein absorption, two questions are especially relevant: how many interactions exist and how meaningful are these interactions? The answers to these questions come by analyzing the number of binding sites on the biomaterial surface and the protein strength of binding to those sites. In many biomaterial applications, it is desirable to attempt to maximize both of these variables to ensure tissue adherence. In this specific application, however, protein adsorption around the inflow and outflow openings threatens to block fluid passage, essential to the viability of sensor results. In these regions, it is necessary to minimize the number of binding sites and the binding strength. While this is true for the areas surrounding the fluid pathway, it is not applicable for the remaining surface area of the sensor housing. In other areas, the number of binding sites and the strength of binding should be increased to allow device fixation within the surrounding extracellular matrix and tissue cells. This will discourage sensor movement within the organ space, which otherwise could produce biomaterial particulate debris. The presence of particulate debris encourages macrophage recruitment and leads to chronic inflammation.

A model has been proposed to quantify protein adsorption characteristics (Andrade 36). This model assumes non-interacting binding sites. The ligand A binds to a site on the biomaterial P and forms a new species, the bound product PA:

$$P + A \rightarrow PA. \tag{5}$$

The association rate of the reaction may be quantified by an association constant, k_A:

$$[P][A] \Rightarrow k_A[P][A]. \tag{6}$$

Similarly, the dissociation rate of the bound product is characterized by a dissociation constant k_D:

$$[PA] \Rightarrow k_D[PA]. \tag{7}$$

Reaction equilibrium dictates that

$$k_A[P][A] = k_D[PA]. \tag{8}$$

Thus, the equilibrium constant k of the reaction is defined as

[31] "If the protein is adsorbed such that its three-dimensional shape of secondary structure is changed, then we say that the protein has undergone a change in conformation. A conformational change is often called 'denaturation,' because many of the 'normal' characteristics of the protein can be expected to be altered" (Andrade 7).

$$k = \frac{k_A}{k_D} = \frac{[PA]}{[P][A]}. \tag{9}$$

The experimental data for binding are typically expressed as a ratio $\bar{\nu}$:

$$\bar{\nu} = \frac{[PA]}{[P_T]}, \tag{10}$$

where P_T represents the moles of total protein, equal to

$$[P_T] = [P] + [PA]. \tag{11}$$

Combining Equations 9, 10, and 11 yields

$$\bar{\nu} = \frac{k[A]}{1 + k[A]}. \tag{12}$$

If the biomaterial happens to have n identical, non-interacting binding sites for the ligand A, then the equation becomes

$$\bar{\nu} = \frac{nk[A]}{1 + k[A]}. \tag{13}$$

Then, a binding isotherm plot may be generated. The binding isotherm reveals how avidly the ligand A is bound to the biomaterial through the value of k, the constant slope at low concentrations of A. As k increases, so does the binding strength. If k is less that 10^4 liters/mol, then the reaction is said to be nonspecific. The graph also shows the number of binding sites, n, as the value of $\bar{\nu}$ corresponding to the asymptote of large concentrations of A. Equation 9 may be rewritten to the form:

$$\frac{\bar{\nu}}{[A]} = nk - k\bar{\nu}, \tag{14}$$

which is associated with a plot form called the Scatchard plot. This type of plot more readily allows one to determine the number of binding sites n and the strength of binding given by k. The point where the line intersects the x-axis is n and the slope of the line is -k. Further work might investigate these parameters and utilize binding isotherm and Scatchard plots of experimentally-obtained data in order to better characterize the housing coating.

Following protein adsorption, acute inflammation ensues. Protein conformational changes, constantly ongoing, alter the protein identity from self to non-self (Fraser 145). Platelets and immune cells adhere to the proteins on the surface of the implant (Fraser 147). Both cellular and humoral responses of the immune system are activated. In the following four

days, white blood cells, or neutrophils, monocytes, or macrophage precursor cells, and phagocytic macrophages are recruited to the implant site. Macrophages then secrete their chemical degradative enzymes in what is termed a "respiratory burst." As macrophages digest debris and clean the site surrounding the implant, tissue reconstruction begins around day three. Between days four to nine, fibroblasts synthesize new collagen fibrils. Depending on tissue adherence to the implant and the extent of vascularization, an avascular fibrous capsule may form, surrounding the implant. Chronic inflammation may later occur. It may be provoked by sensor leakage of internal chemicals or by the formulation of particulate debris from friction between the implant and the tissue. As long as neither of these two events occur, chronic inflammation is not likely (Fraser 27-28), although "the individual immune response to a biomaterial shows a broad variability and depends on the age and health of an individual" (Fraser 151).

2.4.2 Biomaterial Literature Review

The definition of a biomaterial is a systematically and pharmacologically inert substance designed for implantation or incorporation within the human body (Fraser 140). Biomaterials include both synthetic and natural polymers, metals, ceramics, and different combinations of these materials (Fraser 140). A biomaterial is the interface between a medical implant and the living tissue in which it resides. As such, it should not cause any adverse effects, such as a direct injury to the living tissue, a hostile immune response, other adverse systemic effects, or delayed-onset negative effects (Fraser 140). In order to determine the likelihood of *in vivo* responses, biomaterials are first tested outside of the body, *in vitro*. Properties that may be quantified include molecular weight and molecular weight distribution, specific gravity, hardness and tensile properties, metal content, thermal properties, and surface characteristics visualized via scanning electron microscopy (Fraser 155). Any adverse effects may be described as cytotoxic, irritant, sensitizing, systemic, genotoxic, or carcinogenic (Fraser 159). Although material science advances continue to yield better materials, precious few materials, perhaps none, have "proved to be both safe and effective over a long time. Materials that initially seemed to be appropriate and successful became dangerous after a long implantation time and further, more detailed scientific investigation" (Fraser 140). Nevertheless, the biomaterial research community continues to strive to attain a material worthy of the optimistic definition of a biomaterial given

above. Promising new techniques attempt to create these materials in different ways.

Materials analyzed include glass, polystyrene, titanium and associated alloys, Nafion, chitin, and polyethylene. An experiment analyzing the protein adsorptive properties of glass and polystyrene searched for links between adsorption rates and the ionic and hydrophilic or hydrophobic properties of the two materials. In different cases, it was found that albumin, complement C3 (C3), fibronectin (FN), and vitronectin (VN) competitively adsorbed to the surfaces, while immunoglobulin G (IgG) adsorption was just the opposite. Hydrophilic glass and polystyrene surfaces fared better than the hydrophobic surfaces with respect to adhesion protein (C3, FN, and VN) adsorption, but worse with albumin and IgG adsorption. Although protein adsorption in itself is a potential problem for implantable sensors, the study determined that it did not necessarily correlate to monocyte and foreign body giant cell adhesion, which can cause chronic inflammation problems. (Collier 178) From a manufacturing standpoint, MacKay bemoans that, while glass and ceramic are excellent coverings for biomaterials, they are difficult to form (104).

Titanium has long been considered a relatively stable biomaterial. Vascular staple clips (VCS), pioneered in the 1980s, are permanent titanium implants commonly used for cerebral revascularization anastomosis and microvascular anastomosis (Pikoulis 494). In fact, "titanium alloys are well known for their superior mechanical properties as well as for their good biocompatibility, making them desirable as surgical implant materials" (Bordji 929). While this is true, material analysis has shown that titanium behaves poorly in response to friction (Bordji 929). To elaborate, friction of implants may cause the generation of particulate debris in the tissue space over time. Particulate debris presence is troubling, since it activates the recruitment of macrophages and the chronic inflammatory response.

While titanium may illicit inflammatory reactions, studies have shown that polytetrafluoroethylene (PTFE), a biomaterial candidate, implants cause "a more pronounced, persistent inflammation" (Rosengren 1779). Chronic inflammation is less likely to occur if the surrounding tissue cells integrate more closely with the biomaterial. Lessening the physical space between the implant and the tissue cells discourages implant movement. Since implant movement causes friction and, thus, particulate debris formation, macrophage stimulation is less likely to occur. In a study comparing the adherence of epithelial cells to titanium and hydroxyapatite (HA), the cells adhered three times more frequently to HA than to titanium,

titanium alloy, or plasma-sprayed titanium (Meffert 105). While HA, then, appears to be an attractive biomaterial, results of another study are not as optimistic. Ogiso and others analyzed the physical weakening and dissolution of HA-coated implants, noting that "crystallization of super-fine HA crystals occurred in the amorphous phase of the HA coating and progressed over time" (1426). The crystallization causes weakening by making the amorphous phase brittle. Brittleness allows stress accumulation within the HA coat, which results in a decrease in binding strength between the HA coat and any substrate. While these results pertain to bone experiments, the group also showed that "the HA coating dissolved in soft tissue," starting again with super-fine HA crystals. (Ogiso 1426)

Nafion is a polymer whose early test results suggested that it showed "sufficient biocompatibility to make it a viable candidate for some implantable biosensor applications" (Turner 361). In fact, rigorous testing of subcutaneously, intraperitoneally, and transvenously-implanted Nafion membranes in rats was conducted. These tests used scanning electron microscopy and histological examination of the explanted membranes and surrounding tissue samples to "reveal little, if any, evidence of acute or chronic foreign body inflammatory response" (Turner 361). Despite these encouraging findings, material tests performed *in vitro*, by thermal annealing at 150 °C, and *in vivo*, after four weeks of subcutaneous implantation in rats, showed extensive cracking. The mineralization may or may not have been due to calcium phosphates present in the membranes after implantation. (Mercado & Moussy 133) Regardless of the mechanism, it is clear that Nafion is a non-ideal biomaterial.

Other potential biomaterials are chitin and its derivative, chitosan, or deacetylated chitin, which have been "well recognized as a biocompatible material due to properties such as no antigenicity, relative inertness, biodegradability and non toxicity" (Ohashi & Karube 13). Chitin has often been utilized in the biomedical community; research has reported on several medical applications including absorbable sutures, drug carriers, and veterinary practice uses. In addition, it has been shown to accelerate the process of wound healing, which may be of advantage in implant applications. Although chitin shows extraordinary promise as a biomaterial, its use is not recommended for long-term studies, as it is biodegradable. (Ohashi & Karube 13)

Polyethylene has been successfully used in both acute and chronic implantation studies. An implantable system for continuous extracellular glucose concentration measurement housed

its sensor components within a two-part polyethylene shell with polycarbonate cap. The system was implanted in dogs and operated for over a year without issue. Of the systems that did fail, pre-existing manufacturing defects were discovered in the sensor bodies. (Shults 940-941)

From the studies discussed above, some conclusions may be drawn. Glass and polystyrene may both be appropriate materials, although their surface modifications concerning hydrophobicity will most likely affect macrophage and foreign body giant cell stimulation, which may in turn encourage chronic inflammation initiation or escalation. For this reason, it may be best to avoid used glass and polystyrene as principal biomaterial constituents. Titanium should be avoided as well, due to its similar effect to encourage inflammation in certain cases. HA should also not be used as a main biomaterial, since evidence has shown that it undergoes crystallization and resultant weakening in its amorphous phase. Likewise, Nafion is not an ideal candidate due to its propensity for cracking. While chitin and chitosan would otherwise be ideal, they are biodegradable and, therefore, unsuitable for permanent implant applications. Considering the successful use of polyethylene and polycarbonate in chronic implantation research, these materials seem to be the best candidates for the proposed application.

Many factors govern the host response to a biomaterial. While the literature is quick to admit that these factors are not completely understood currently, several factors have been correlated to different body reactions. One factor, as briefly mentioned above, is the relative porosity versus smoothness of the material surface. Significant differences in both cellular response and material stability have been noted when comparing the effects of very smooth surfaces to very rough, or highly porous, surfaces. This has led researchers to agree that surface topography contributes to controlling the biocompatibility of a biomaterial. (Fraser 142)

This factor is related to the events of the body's healing process. Following the first week of healing after implantation, a fluid-filled space appears between the surface of a material and the surrounding tissue interface. This fluid is comprised of a myriad of proteins as well as a low concentration of inflammatory cells. (Gretzer 851) Over time, this space reduces as tissue cells establish adhesion to a porous material and commence ingrowth. In contrast, the fluid-filled space often remains stable or increases its concentration of macrophages and foreign body giant cells over time in the case of a smooth implant. Then, in many cases of smooth implants, fibrous tissue surrounding the fluid layer thickens and contracts to form a fluid-filled sac. (Van Kooten 1) This capsule often impairs implant function, and may, in fact, be very painful for the patient,

as is often the case in breast implant difficulties. Clearly, according to surface topography effects on inflammation, a biomaterial with a high porosity is desired.

Capsule formation may not only encourage inflammation, an adverse body reaction, but may also inhibit sensor function, an adverse effect on the sensor inflicted by the host. Fraser notes the problem:

> Smooth solid structures apparently become surrounded by a fibrous capsule, whereas spongy surfaces continue to be supplied by vascular tissue. The fibrous capsule surrounding the sensor presents a structurally distinct barrier of collagen fibrils, which might have an effect on the substrate mass transport, resulting in a delay in sensor response and an underestimation of analytes (153).

Essentially, the fibrous capsule may inhibit the analytes of interest from perfusing the tissue immediately surrounding the sensing element of the implant. So, a highly-porous biomaterial is also desirable, considering optimum sensor performance.

However, the principal biomaterial does not have to be the biomaterial which contacts the living tissue. In many applications, one material is used as the main form of the implant, while another covers or coats its surface. For example, in the previously mentioned subcutaneously-implanted glucose sensor, the polyethylene housing and polycarbonate cap are subsequently fitted with a surgical-grade polyester velour jacket in order to encourage sensor fixation within the tissue (Fraser 124). Expanded Teflon has also been used for this purpose, and it has been noted that fibroblast capsule tissue "tends to grow aggressively into such materials and form a strong mechanical bond" (Fraser 121). A simpler method than jacketing is "creating particular chemical functionalities on the existing surface, for example, hydroxyl, carboxyl, amine, sulphonate or phosphate group" (Fraser 30). This is accomplished with the use of derivatizing chemicals or by exposing the material surface to reactive ions or ionising radiation (Fraser 30). In such a way, adsorption of one type of protein may be lessened or slowed by covering the surface with a specific chemical group (Fraser 30).

Some materials may be effectively used as encapsulants and sealants, as well as protective coatings to minimize fluid leakage into the sensor package. Biomedical polymers such as epoxy resins, silicones, polyurethanes, PTFE, and polyamides have often been used for this purpose. Unfortunately, these materials are not always ideal coatings, but in at least one

research project involving implantable microchemical sensors, a common polyamide, Kapton, was successfully used (Cosofret 2).

Other materials commonly used as outer membrane coatings include cellulose, cellulose acetate, various polyurethanes, polyvinylalcohol, alginate-polylysine-alginate, PVC, polyethylene glycol (PEG, PEO), and PEG-containing copolymers (Fraser 155). Heparinized plastic has also been used (MacKay 108). Fairly unsuccessful attempts have been documented using Dacron, Teflon, silicone rubber, polypropylene, polyethylene, polyvinyl, nylon, polyurethane, and orlon (MacKay 108).

In searching to find biocompatible coatings, researchers often take one of three approaches. The coating is often chosen to have some specific biological activity, to be inert, and therefore biocompatible because it does not react with the body at all, or to be masked, so that the body does not recognize the material as foreign. Learning more about how material surfaces interact with the body enables researchers to design a customized surface which will react with its environment in the desired specific fashion. Indeed, one researcher recommends, "Sensor membranes containing polymers functionalised with biological motifs, such as sequences from adhesion proteins or growth promoters, may be worth investigation" (Fraser 42). Heparinized surfaces are an example of this methodology. Heparin is a polysaccharide that prevents blood clotting by suppressing the coagulation system. When affixed to a biomaterial surface, heparin has retained anticoagulation activity for up to four months *in vivo*. Whether or not heparinized surfaces can continue their activity for longer periods of time remains to be seen. (Fraser 157) Coating biomaterial surfaces with heparin attempts to form a biocompatible surface by producing a specific biological effect.

The second methodology, of using a material which has close to no interaction whatsoever, is apparent in the use of diamond-like carbon. These surfaces have shown "no cytotoxic effects" as well as a "reduced material-tissue interface" (Fraser 159). While these surfaces are indeed inert, they are not more biocompatible than other surfaces, as they do not truly interact with the body, but are simply ignored by it.

The third approach is constructing a biomaterial surface that looks like it is a part of the body itself. In this method, the surface mimics the makeup of host-resident surfaces. The best example is phospholipid-based surfaces. Cell membranes are a phospholipid bilayer with negatively-charged phospholipids such as phosphatidylserine residing next to the cytoplasm and

neutral phosphorlcholine (PC) molecules next to the extracellular matrix. PC-head groups typically comprise about 90% of the lipid components of the outer layer. They show "low interaction and binding with plasma proteins such as factor XII, complement, fibrinogen, immunoglobulins, and albumin" (Campbell 229). Based on these facts, biomaterial surfaces have been constructed with a covering of PC-heads in order to mimic the cell membrane. This appears to work. PC-sheathed surfaces have been shown to be highly hydrophilic, and therefore resistant to protein adhesion because of the adsorbed layer of water molecules surrounding the surface. In one study of PC-coated PVC, platelet adhesion and activation *in vitro* was drastically reduced by 99%. In other polymer studies, fibrinogen adsorption was reduced by 90%. (Fraser 158) One researcher lauds, "A PC-coated surface should...be an ideal starting point for developing tissue-inducing biomaterials" (Campbell 229). Mimicry using PC-heads is an effective method of producing a biocompatible material.

In the biomaterial application of implantable sensor design, it is important to consider the material's or coating's ability to act as an effective moisture barrier, as water vapor diffusion may cause sensor drift and other problems (MacKay 101). It is known that plastics do "slowly pass moisture" (MacKay 101). Water soak testing of several typical coatings reveal that paraffin results are best, even after 2 years. However, paraffin does not adhere well to other materials and is brittle and easily cracks. Using a mixture of half paraffin and half beeswax may yield better results, although this combination was not soak-tested. (MacKay 104)

2.4.3 Biocompatibility

Biocompatibility is "the ability of a material to perform with an appropriate host response in a specific application" (Fraser 140). This definition arises from the fact that every material currently known affects the body in an adverse fashion to some degree. That given, it is most desirable that a material elicit a minimum negative influence.

When determining biocompatibility, one must consider both the actions of the material on the body and the effects of the body upon the material; in other words, the host response and the material response (Fraser 142). While both must be analyzed, the more complicated response by far is the effect of the cell-mediated actions imposed by the local inflammatory cells (Fraser 141).

More specifically, biocompatibility pertains to the "energetics and kinetics of all physical,

chemical, and biochemical processes at the interface between the biomaterial and the biological system," the reactions at the biomaterial surface. It is this surface which directly aggravates any processes, including changes in the physical and chemical properties of the material, such as surface composition, corrosion, biodegradation, and surface free energy. Processes also include changes of the biological system that are initiated by the material surface interaction, such as toxic or immune reactions and cancer. (Fraser 140-141)

Materials are deemed biocompatible in the U.S. by the FDA on a case by case basis. The FDA keeps no list of materials termed biocompatible, as the definition itself implies application dependency. This is because the reactions between a specific material and specific tissue are highly interactive and must be considered together. The FDA evaluates on the basis of biocompatibility, effects of manufacturing techniques on implant features, intended use of the device, and the physiological exposure environment. (Bronzino 2802-2818)

2.5 *In vivo* Biosensor Technology

2.5.1 Definition

A biosensor may be defined as "a device incorporating a biological sensing element connected to a transducer," where a transducer "converts an observed change (physical or chemical) into a measurable signal, usually an electronic signal whose magnitude is proportional to the concentration of a specific chemical or set of chemicals" (Eggins 2). Biosensors may be classified according to several criteria, among them analyte, biological component, methods of biological component immobilization, transducer, and performance factors.

The analyte is the substance for which measurement is desired. Essentially any substance "that is consumed or produced in a biochemical process can in principle be analysed" (Eggins 7). The biological component refers to the substance which reacts in a highly specific manner with the analyte. It may be an enzyme which catalyzes the reaction or an antibody which binds the substrate. Other examples include microorganisms, like yeast and bacteria, tissue material, and nucleic acids (Eggins 8). Methods of fixing the biological component to the sensing element vary. Adsorption to the sensing surface is the most simple. Microencapsulation consists of containing the component between two membranes. Entrapment refers to trapping the component in a gel or matrix. Covalent attachment or cross-linkage may also be employed.

Types of transducers used to quantify the signal include electrochemical, field effect

transistor (FET), optical, piezoelectric, surface acoustic waves, and thermal transducers (Eggins 8-9). Electrochemical means include potentiometric, voltammetric, and conductimetric. Potentiometric devices involve the potential measurement of a cell at zero current, the potential being proportional to the logarithm of the analyte concentration. Voltammetric sensors apply an increasing or decreasing potential to a cell until oxidation or reduction of the analyte occurs. At that time, a sharp current spike height reveals the concentration of the analyte. If the oxidation or reduction potential is known, then that potential may be applied and the current level may be observed. This is called amperometric sensing. Conductimetric transducers take advantage of the fact that ionic properties of a solution change with a biochemical reaction. The relationship between the conductance and the concentration of analyte depends on the nature of the reaction. FET transducers utilize electrochemical transducer methods on a miniaturized chip. Optical devices employ fiber optics in absorption spectroscopy, fluorescence spectroscopy, luminescence spectroscopy, internal reflection spectroscopy, surface plasmon resonance and light scattering. Piezoelectric transducers use current-generating vibrating crystals and measure their frequency changes due to particle adsorption to their surfaces. Surface acoustic wave devices use the same concept of frequency variation. Thermal transducers measure the heat produced or absorbed by a biochemical reaction. (Eggins 8-9)

Some significant performance factors are selectivity, sensitivity, accuracy, response time, recovery time, and working lifetime. Selectivity is the sensor's ability to distinguish between different analytes, mainly dependent on the biological component. Sensitivity range refers to the concentration levels of analyte which may be measured. Typical values are sub-millimolar, but may go down to femtomolar range. Typical accuracy should be in the range of $\pm$ 5%. Response time is the time lag between the measurement event and the signal reading, usually 30 s or more. The recovery time refers to the time it takes for a biosensor to be ready to analyze the next sample. Normal range of recovery times is a few minutes. The amount of time it takes for the biological component to be exhausted is the working lifetime. This value commonly varies from a few days to a few months or even longer. (Eggins 9-10)

2.5.2 Benchmarking Information

Sensor benchmarking is conducted in order to obtain a working knowledge of reasonable design parameters. Because of this motivation, information gleaned usually pertains to the

design parameters relevant to the current application. As such, the material presented is not meant to summarize the designs, but to merely reflect the relevant parameters.

Sensor benchmarking data may be logically organized according to (1) the analyte or physical parameter being measured, (2) the site of measurement, or (3) the means of measurement. Biosensor information is presented here in terms of the analyte or physical parameter being measured. A biosensor is "a deliberate and intimate combination of a biomolecule and a man-made transducer" (Fraser 10). A biosensor, by this definition, excludes devices which measure non-molecular parameters, such as blood pressure, as such measurements do not involve a biomolecule. Such devices fall under the definition of bioprobe "because although they measure in a biological system, they probe a purely physical parameter like temperature, pressure, nuclear relaxation time or the emission of nuclear radiation" (Fraser 11). The following benchmarking study includes both types of sensors, although the former type is more representative of the current application exploration. Furthermore, only implantable sensors are discussed.

Glucose sensing is, by a large margin, the most popular and abundant research and development implantable sensor application. Such sensors are perfectly targeted for use in diabetes mellitus therapy. Diabetes mellitus is a distressingly common, life-threatening disease which affects glucose metabolism. As the incidence rate continues to rise, due to people's relatively recent tendency to consume more sugar-rich diets, this type of *in vivo* sensing appears to be most commercially-attractive. (Fraser 3, 8)

The concept of *in vivo* glucose sensing began over 30 years ago, when Clark envisioned an enzyme electrode that would oxidize glucose with the enzyme glucose oxidase (Reach & Wilson 383A). The ideas of a fuel cell and an automated insulin injection system based on sensor feedback control were introduced by Chang in 1973 (352).

In 1982, an affinity sensor based on optical measurement was designed. The idea was based on the competitive binding of a specific metabolite and a flourescein-labeled analogue to a receptor site. In this design, concanavalin A, a protein with a particular binding to glucose, was bound to the inside of a hollow dialysis filter. A single optical fiber was inserted into the tube in order to measure the unbound analyte. Preliminary feasibility tests were conducted successfully. (Schultz 245)

A needle-type glucose sensor with a telemetry system was developed in 1986. The size

of the sensor was 4 cm x 6 cm x 2 cm and it weighed 50 g. The sensor transmitted by converting current signals to high-frequency audio. The noise range of the monitoring record was 0.3 ± 0.04%, which was significantly smaller than with a wire-connected system, 2.5 ±0.3%. Sensor time lag was five minutes. (Shichiri 298)

A telemetry-instrumentation system for glucose and oxygen sensing was designed in 1988. The potentiostat system transmitted via frequency modulation for up to 3 months using a single lithium power cell. The data collection capabilities of the device were comparable to bench-top instrumentation. Final device measurements were 5.0 cm x 5.5 cm x 1.1 cm and the weight was 70 g. (McKean & Gough 526-532)

In 1992, a thoughtful review article by Reach and Wilson attempted to define many of the parameters necessary for successful glucose sensor development. The linear range was suggested up to 15-20 mM, while the sensitivity was suggested to be high enough, around 0.3 to 3 nA/mA, to produce a reasonable signal-to-noise ratio. (384A)

Another needle type electrode sensor was designed with a flexible 0.29 mm diameter. The electrode contained four layers, which were serially deposited within a 0.125 mm recess on the tip of a 0.25 mm gold wire. The recess held a mass of less than 5 μg, containing no leachable chemicals. The outermost biocompatible layer of the sensor was constructed by photo-crosslinking polyethylene oxide. Seven hours following implantation, a severe drop in sensitivity was noticed. Because the sensitivity was regained upon electrode placement in buffer solution, the loss might have been due to protein adhesion upon the sensing surface. This design was formulated in 1994. (Csoregi 3131)

Also in 1994, a telemetry-instrumentation system was developed in order to monitor several multiple subcutaneously implanted glucose sensors within a given area. The potentiostatic sensor measured glucose concentrations via an enzyme electrode and translated these to current levels, which were converted to frequencies. These frequencies were transmitted at programmable intervals of 4, 32, and 256 s to an externally-located receiver. The unit could track ten sensors in the same 10 m radius for up to 1.5 years. The implantable device measured approximately 1.2 cm x 3.2 cm x 7.0 cm and weighed about 27 g. (Shults 937-941)

The next year, a microchip glucose sensor fabricating method was introduced, showing excellent standardization and reproducibility. The chips sensed electrochemically. It was noted that chips constructed with titanium underlayment were more sensitive to glucose fluctuations

than were those with chromium underlayment. (Patzer M409)

Also in 1995, glucose sensor concept validation was conducted experimentally. Results showed that the concentration of glucose present subcutaneously is very nearly identical to the concentration in the bloodstream. Secondly, it was demonstrated that electrodes residing in the subcutaneous space do, in fact, yield accurate blood glucose level readings under hypo-, normo-, and hyperglycemic conditions. Thirdly, the experiments revealed that an automated insulin pump utilizing feedback control would be a relevant possibility. Lastly, subcutaneous glucose sensor function was shown between intervals of one to ten days. (Fischer 21)

The same year, the kinetics of glucose delivery to the subcutaneous tissue was examined in rats. The sensor used was a 0.3 mm amperometric electrode. Glucose masses of 100, 200, and 400 mg/kg of body weight were injected and times to peak current were measured at 7.5 ± 3.9, 9.8 ± 5.5, and 10.0 ± 4.4 minutes. These times represent the total sensor lag times for each quantity. (Quinn E155)

Again that year, a glucose sensor review covered the different glucose sensing technologies under investigation. These included hydrogen peroxide based enzyme electrode sensors, oxygen based enzyme electrode sensors, mediator based enzyme electrode sensors, continuous microdialysis sensors, membrane-covered catalytic electrode sensors, and optical sensors. Other concepts were also discussed. (Gough & Armour 1005-1009)

In 1997, another needle-type glucose sensor was developed. This sensor utilized an electrochemically-coated heparin electrode surface in order to discourage platelet and protein adhesion. A sensitivity of 3 nA/mM and a linear range from 40 to 400 mg/dL was accomplished when the device was tested in whole blood. Storage capability in buffer was 12 weeks. (Yang 54)

That year, a refillable glucose sensing telemetry system was invented. The sensor contained a mini-potentiostat, a frequency modulation signal transmitter, and a power supply. The whole device measured 5.0 cm x 7.0 cm x 1.5 cm. It was able to measure an upper bound of 25 mM of glucose with a sensitivity of 0.5 μA/mM. The delay time of readings ranged between 3 to 7 minutes. The device was tested subcutaneously in dogs. (Atanasov 669)

In 1999, the U.S. Food and Drug Administration (FDA) approved the application for a subcutaneous glucose monitoring system developed by MiniMed. The sensor is not fully implantable; its transcutaneous wire link attaches to its pager-style monitor. Each sensor is

designed to remain in the body for up to 3 days and records glucose averages over 5 minute intervals. The sensing element is a 1 mm wide electrode. This is the first glucose sensor now available on the market. (Subcutaneous Glucose Monitoring System: Fact Sheet)

Implantable biosensors designed to measure other parameters are less common, but do exist. A pressure-balanced unit measuring intracranial pressure was introduced in 1977, complete with an on-board telemetry system. The sensor applied a known external pressure to a patient's scalp a small distance above the implanted sensor. The sensor was able to detect the zero-point of the external apparatus by radio telemetry, calculate the pressure balance, and send a signal output. The internal system's telemetry was realized by a resonant circuit and the external system detected the resonant frequency. Intermittent or continuous data could be recorded. Test results claim negligible temperature drift, no calibration ambiguities, and a fast dynamic response. The sensor implantation was successful both short and long-term. (Zervas 899)

A review article written in 1986 commented on the advances of *in vivo* sensors. Sensor types discussed included implants for general hospital use, transient-use probes to replace blood tests, short-term implantable probes, and long-term implantable probes. The authors suggested evaluation of sensors based on performance criteria of selectivity, sensitivity, fast response, site-reversible, small, rugged, inexpensive, biocompatible, calibratible, facile use by non-experts, and ease of telemetry. (Thompson & Vanderberg 255)

A novel solution to blood flow monitoring during and after surgery was proposed in 1990. The implantable pressure sensor was secured to a blood vessel by a releasable tie. It was designed to be used with vessels 2.5 to 5 mm in diameter. Attachment does not require any tissue-puncturing techniques, although lead wires are exteriorized through the chest wall, a non-ideal situation with infection possibilities. The sensor remains in place for several days, after which it is pulled out of the body through the transcutaneous opening. This approach was tested in dogs for up to 16 days. (Rabinovitz 148)

Another sensor which connected transcutaneously was developed in 1995. The application was the continuous measurement of lactate within the bloodstream or tissues. The sensor utilized an electrode similar to the electrode developed for glucose sensing, but based on fixed L-lactate oxidase. The sensor remained stable *in vitro* for up to 1 week. During this time, it responded specifically to lactate over a broad range of concentrations. The sensor was also tested *in vivo* in the canine left atrium with lead wires exteriorized. (Baker & Gough 1538)

In 1997, an optical sensor to determine the levels of critical gases and electrolytes in blood was developed. This was a six-channel unit using superblue lights as light sources and photodiodes. Performance characteristics evaluated included dynamic response, linearity, channel reproducibility, reversibility, long-term drifts, photobleaching of indicator, cross-talk, ionic strength, and selectivity of pH measurements. (Bruno 507)

The next year heralded the design of an externally-powered, multichannel, implantable stimulator-telemeter for the control of paralyzed muscle. The system used biopotential sensing and telemetry to control movements of the wrist. It included a command control structure, an inductive radiofrequency link to provide power and bi-directional transcutaneous communication, a command decoder, and modular circuitry. The system was also designed with biocompatible hermetic packaging, lead systems, and in-line connectors to be used in chronic implantation. A prototype was constructed and underwent animal testing. (Smith 463)

2.5.3 Regulation and Controls

The FDA medical device regulatory program consists of four parts. The first is manufacturer registration. The second is product listing. The third is pre-market evaluation of newly emerging devices and review of clinical testing that produces data that supports pre-market applications. The last part covers post-market requirements, including product tracking, performance studies, fabrication controls, and manufacturing site inspections. (Bronzino 2802 - 2818)

Biomedical devices are categorized into three headings by the FDA according to the level of risk involved in their use. Class I devices are those for which the safety and effectiveness may be controlled with a minimum level of regulation. Such general controls include manufacturing site registration, device listing, pre-market notification, and adherence to good manufacturing practices (GMP). An example of a Class I device is a tongue depressor. Class II devices must meet general and special controls. Such special management consists of performance standards, post-market overview, patient registry, guidance documentation, and other controls. A stainless steel bone plate implant is considered a Class II device. Class III medical devices pose the most risk to the patient, yet are those devices used in supporting or sustaining life or significantly improving the quality of life. General and special requirements must be met, as well as other, more stringent controls. A good example of such a device is a heart valve. (Bronzino 2802-

2818) The proposed sensor would most likely be categorized as a Class II or III device, due to its implantable nature of operation. Future design efforts should therefore be conducted in a manner adhering to the applicable FDA regulations.

Standards do exist, providing guidance to any medical device design and manufacturing venture. In Europe, biocompatibility testing is per standards known as the Medical Device Directive (MDD) and the Active Implantable Medical Device Directive (AIMDD) issued by the European Commission (Fraser 159). International standards for medical devices have been set by the International Standards Organization (ISO) Technical Committee 150, comprised of 20 countries, including the U.S. Each year, committee members meet to develop new standards that gain international recognition and acceptance. The committee generates standards pertaining to both materials and devices, setting their property and performance criteria, and specifies test methodologies to ensure consistent material and device evaluation. Subcommittees exist on the subjects of materials, cardiovascular implants, neurosurgical implants, bone and joint replacements, osteosynthesis, terminology, certification, and retrieval and analysis of implants. Such wide coverage yields standards in every area of biomedical development. In the U.S., material biocompatibility is addressed by ISO 10993, entitled Biocompatibility of Materials (Fraser 150). Other standards may be obtained through the U.S. office, the American National Standards Institute (ANSI) based in New York. (Bronzino 2802-2818)

3 Design

3.1 Methodology

The design process allows an innovative idea to develop to fruition. It changes an elusive thought into reality. It answers the question "how?," fleshes a concept into substance, and allows it to come to market as a tangible product. A good design methodology ensures that nothing is lost on the journey from idea to prototype, that the customer's needs are kept paramount, and that as many options as possible are considered. A methodology such as this yields the best product possible. One such methodology is presented in Product Design and Development by Karl Ulrich and Steven Eppinger. The first five parts of their design process guided this product design: (1) identifying customer needs, (2) establishing target specifications, (3) analysis of competitive products, (4) concept generation, and (5) concept selection (Ulrich & Eppinger 18-19).

3.1.1 Identify Customer Needs

The first part of the design process is the identification of the customer's needs. This is important because the product must meet or exceed these needs in order to ensure the customer's satisfaction. This part may be split into six steps: (1) define the scope of the effort, (2) gather raw data from customers, (3) interpret the raw data in terms of customer needs, (4) organize the customer needs, (5) establish the relative importance of the customer needs, and (6) reflect on the results and the process (Ulrich & Eppinger 35).

In the first step, the effort may be defined through the creation of a mission statement. The mission statement often includes information such as a brief product description, key business goals, target markets, any constraining assumptions, and stakeholders (Ulrich & Eppinger 36-37). For the design task at hand, the mission statement is as follows:

Table 2: Mission Statement

Product Description	• An implantable sensor capable of detecting and distinguishing between liver and renal graft acute immunorejection, vascular occlusion, and infection, occurring within the first month following transplantation
Primary Market	• Research facilities • Educational institutions
Secondary Markets	• Pharmaceutical industry • Medical care facilities at which liver and renal transplantation occur
Stakeholders	• Patient • Transplantation surgeon • The Charles Stark Draper Laboratory, Inc. • MIT (Massachusetts Institute of Technology) • CIMIT (Center for Innovative Minimally Invasive Therapy), a consortium whose members include Draper Laboratory, MIT, Brigham and Women's Hospital, and Massachusetts General Hospital (MGH)

The second step, gathering raw data from the customer, was completed through an informative interview with a lead user, defined as a customer who experiences needs months or years ahead of the majority of the marketplace and stands to benefit substantially from product innovations (Ulrich & Eppinger 39). Such a customer is a particularly good source of information for two reasons. First, because the customer has had to cope with the inadequacies of existing products or methods, he or she can often more readily explain his or her specific needs. Secondly, the customer may already have envisioned solutions to meet those needs

(Ulrich & Eppinger 39-40). Brian Cunningham, Ph.D.,[32] who worked on sensing element development at Draper Laboratory, and the author met with Joseph P. Vacanti, M.D.[33] of Harvard Medical School, who practices transplantation surgery and conducts groundbreaking tissue engineering research. We met at MGH on November 2nd, 1998 in order to discuss application-specific issues pertaining to the development of the implantable biosensor. Notes of the interview proceedings were taken by hand (Appendix A).

In order to interpret this raw data in terms of the customer's needs, the third step, each customer statement must be translated into a need. During this process, it is helpful to keep several points in mind. The need should be expressed in terms of what the product has to do, not in terms of how it might do it. The need should be expressed just as specifically as the customer statement. Positive, not negative, phrasing should be used. The need is best expressed as an attribute of the product. The words "must" and "should" are to be avoided, as they confer unintentional importance levels to the needs. The customer statements from one lead user, while invariably instructive, do not address every pertinent issue, as would theoretically occur if a large number of customers were interviewed. Because this was prohibited by accessibility and time demands, additional statements were generated by the author. These additional statements address issues unmentioned by the lead user which the author feels warrant attention. With the guidelines in mind, the following need statements were derived from the customer's statements and the developer's augmenting statements. The italicized statements are derived from the interview with the lead user, while the remaining statements are of the author's origin.

---

[32] Cunningham is a task leader and project engineer at Draper Laboratory, where he is responsible for new product development using MEMS process technology. In this capacity, Dr. Cunningham has demonstrated new process technology for on-chip vacuum packaging of micromechanical resonators, novel thin film microphones, micromirror displays, and high performance micromachined inertial instruments. His focus on these projects involves identification of system requirements, selection of appropriate technology, analytical modeling of performance, and process development/prototype demonstration of micromechanical sensors and actuators. His background is primarily in the areas of semiconductor process technology, micromachining, applied physics, and material science. Dr. Cunningham has two patents and 23 technical journal publications. (CIMIT Staff)

[33] Vacanti is the John Homans Professor of Surgery at Harvard Medical School, a visiting surgeon at Massachusetts General Hospital (MGH), director of the Wellman 6 Surgical Laboratories, director of the Laboratory of Tissue Engineering and Organ Fabrication, and director of pediatric transplantation at MGH. Dr. Vacanti's major research interests are tissue engineering, liver transplantation, biliary atresia, and congenital diaphragmatic hernia and lung development. Together with fellow tissue engineering pioneer Robert Langer, Ph.D., Dr. Vacanti developed a biodegradable and implantable system, which generates new tissue as permanent replacement structures, aiming to solve the lack of donor organs and tissue. Dr. Vacanti has authored more than 120 original reports, 30 book chapters, and nearly 200 abstracts. He has more than 25 patents or patents pending in the United States, Europe, and Japan. (CIMIT Staff)

Table 3: Statements and Functional Requirements

STATEMENT	FUNCTIONAL REQUIREMENT (INTERPRETED NEED)
• *Detects acute rejection.*	• Detects acute rejection markers. • Distinguishes acute rejection markers from markers for infection and vascular occlusion.
• *Detects infection.*	• Detects infection markers. • Distinguishes infection markers from markers for acute rejection and vascular occlusion.
• *Detects vascular occlusion.*	• Detects vascular occlusion markers. • Distinguishes vascular occlusion markers from markers for acute rejection and infection.
• *Works throughout critical period.*	• Device lifetime exceeds the critical period.
• *Implanted within the site of potential problems.*	• Resides on or in organ of interest.
• *Could have removable leads.*	• Could have removable leads.
• *Only one attachment mechanism design is necessary for different organs; tissue is similar.*	• One attachment mechanism design will suit both liver and kidney.
• *Interval monitoring is acceptable; continuous not necessary.*	• Gives information at time intervals.
• *One sensor per organ is sufficient.*	• System includes one sensor per organ.
• *Size is not critical.*	• Final size is within a range.
• Not necessary to cut open body to remove.	• Remains biocompatible indefinitely.
• Attachment does not harm organ.	• Attaches such that organ continues to function normally.
• Presence does not harm bodily system.	• Is biocompatible.
• Does not interfere with other testing.	• External connecting apparatus is light and maneuverable. • Internal device located such that other tests may be performed in a normal fashion.
• Works.	• Robust. • Minimum number of misses. • Failsafe in place.
• Gives correct values.	• Accurate. • Minimum number of false alarms.
• Fits well into body.	• Final size is within a range. • Shape is unobtrusive.
• Stays in place within body.	• Attachment is firm.
• Detects problems early.	• Detects early indicator markers.
• Can read concentrations off quickly and easily.	• Display unit is easy to read and operate.

STATEMENT	FUNCTIONAL REQUIREMENT (INTERPRETED NEED)
• Gives easily detectable, attention-alerting warning signs.	• Visual and audio signals alert ailment detection.
• Easily and quickly implantable.	• May be easily placed within the body during surgery. • May be quickly implanted during surgery.

In the fourth step, the need statements were organized categorically as given below. This logical arrangement later allows facile analysis toward the construction of a list of critical subproblems.

Table 4: Categorical List of Functional Requirements

DETECTION • Device detects ailment markers. ➢ Detects acute rejection markers. ➢ Detects infection markers. ➢ Detects vascular occlusion markers. • Device distinguishes ailment markers. ➢ Distinguishes acute rejection markers for infection and vascular occlusion. ➢ Distinguishes infection markers from markers for acute rejection and vascular occlusion. ➢ Distinguishes vascular occlusion markers from markers for acute rejection and infection.
ATTACHMENT • One attachment mechanism design will suit both liver and kidney. • Resides on or in organ of interest. • Attaches such that organ continues to function normally. • May be easily placed within the body during surgery. • May be quickly implanted during surgery. • Attachment is firm.
BIOCOMPATIBILITY • Is biocompatible. • Remains biocompatible indefinitely. • Final size is within a range. • Shape is unobtrusive.
PERFORMANCE • Device lifetime exceeds the critical period. • Robust. • Minimum number of misses. • Failsafe in place. • Accurate. • Minimum number of false alarms.

LOGISTICS
• External connecting apparatus is light and maneuverable. • Internal device located such that other tests may be performed in a normal fashion. • Could have removable leads. • Gives information at time intervals. • System includes one sensor per organ. • Display unit is easy to read and operate. • Visual and audio signals alert ailment detection. • May be easily placed within the body during surgery. • May be quickly implanted during surgery.

The fifth step is the assignment of relative importance values. This is undertaken in order to be equipped to make tradeoff decisions pertaining to conflicting customer needs later in the design process. These values were assigned by the developer on the basis of her impressions of the customer's needs.

Table 5: Relative Importance Assignment for Functional Requirements

1 = Feature is critical. 2 = Feature is highly desirable, but the product could work without it. 3 = Feature would be nice to have, but is not necessary. 4 = Feature is not important, but is fine if it is included in the product. 5 = Feature is undesirable.

FUNCTIONAL REQUIREMENT	RELATIVE IMPORTANCE
• Detects acute rejection markers. • Distinguishes acute rejection markers from markers for infection and vascular occlusion.	• 1 • 1
• Detects infection markers. • Distinguishes infection markers from markers for acute rejection and vascular occlusion.	• 1 • 1
• Detects vascular occlusion markers. • Distinguishes vascular occlusion markers from markers for acute rejection and infection.	• 1 • 1
• Device lifetime exceeds the critical period.	• 1
• Resides on or in organ of interest.	• 1
• Could have removable leads.	• 5
• One attachment mechanism design will suit both liver and kidney.	• 2
• Gives information at time intervals.	• 2
• System includes one sensor per organ.	• 1
• Final size is within a range.	• 1

FUNCTIONAL REQUIREMENT	RELATIVE IMPORTANCE
• Remains biocompatible indefinitely.	• 1
• Attaches such that organ continues to function normally.	• 1
• Is biocompatible.	• 1
• External connecting apparatus is light and maneuverable. • Internal device located such that other tests may be performed in a normal fashion.	• 3 • 3
• Robust. • Minimum number of misses. • Failsafe in place.	• 1 • 2 • 1
• Accurate. • Minimum number of false alarms.	• 1 • 2
• Shape is unobtrusive.	• 2
• Attachment is firm.	• 3
• Detects early indicator markers.	• 3
• Display unit is easy to read and operate.	• 3
• Visual and audio signals alert ailment detection.	• 3
• May be easily placed within the body during surgery. • May be quickly implanted during surgery.	• 2 • 2

The sixth, and last, step in the first part of the design process is reflection. During this step, it is important to ask whether or not the results are consistent with what is expected from the developer's knowledge of the customer. Unexpected results should be challenged and re-examined. Reflection of this case leads to the conclusion that the results are aligned with the developer's knowledge of the customer's and developer's needs.

3.1.2 Establish Product Specifications

After careful reflection, the second part of the design process, establishing target specifications, is undertaken. Specifications are translated from customer needs and describe exactly what a product must do. Target specifications represent the idealistic goals of the development effort. Following concept selection, target specifications are refined to take into account tradeoff factors. This results in more realistic product specifications. However, it is important to establish goal specifications early, in order to guide the rest of the design process (Ulrich & Eppinger 18). There are four steps to this activity: (1) prepare a list of metrics, (2) collect competitive benchmarking information, (3) set ideal and marginally acceptable target values for each metric, and (4) reflect on the results and the process.

A specification is comprised of two elements, a metric and a value (Ulrich & Eppinger 55). The metric is a phrase that should "reflect as directly as possible the degree to which the product satisfies the customer needs" (Ulrich & Eppinger 57), while the value quantifies the level necessary for the customer's satisfaction. For example, "average time to implant" is a metric, while "less than 5 minutes" is a corresponding value. Since the metrics are derived from the customer needs, there should be at least one metric for each need statement. In order to easily view the needs-metrics relationship, a table is shown. In this case, each need is met by one and only one metric. Due to time restriction, many metrics remain unspecified. Although some of the given metrics are unspecified, they effectively convey the type of information that must be sought in future design efforts. Identification, alone, of the relevant types of metrics is a valuable asset to a more in-depth design effort.

Table 6: Functional Requirements and Metrics

#	FUNCTIONAL REQUIREMENT	METRIC
1	Detects acute rejection markers.	Sensitive to □ ppm of rejection marker.
2	Distinguishes acute rejection markers from markers for infection and vascular occlusion.	Selectively measures rejection marker = misbind error is not greater than 5%.
3	Detects infection markers.	Sensitive to □ ppm of infection marker.
4	Distinguishes infection markers from markers for acute rejection and vascular occlusion.	Selectively measures infection marker = misbind error is not greater than 5%.
5	Detects vascular occlusion markers.	Sensitive to □ ppm of vascular occlusion marker.
6	Distinguishes vascular occlusion markers from markers for acute rejection and infection.	Selectively measures vascular occlusion marker = misbind error is not greater than 5%.
7	Device lifetime exceeds the critical period.	Sensing element does not saturate before 4 weeks.
8	Resides on or in organ of interest.	Located □ m away from organ surface.
9	Could have removable leads.	Could have removable leads.
10	One attachment mechanism design will suit both liver and kidney.	Number of attachment designs is 1.
11	Gives information at time intervals.	Gives information at read-out every □ seconds.
12	System includes one sensor per organ.	Number of sensors per organ is 1.
13	Final size is within a range.	Overall size is within □ by □ by □ m.
14	Remains biocompatible indefinitely.	Illicits < detectable immune response in a chronic sense, over □ years.

#	FUNCTIONAL REQUIREMENT	METRIC
15	Attaches such that organ continues to function normally.	All organ products and functions remain normal.
16	Is biocompatible.	Illicits < detectable immune response in a acute sense, over □ years.
17	External connecting apparatus is light.	External connecting apparatus has minimum weight, at most □ pounds.
18	External connecting apparatus is maneuverable.	External connecting apparatus moves vertically and horizontally, and rotates 360 degrees.
19	Internal device located such that other tests may be performed in a normal fashion.	Sensor is □ m away from other test equipment and does not interfere with their results.
20	Robust.	Vibration testing yields □ cycles at □ Hz to housing failure.
21	Minimum number of misses.	Number of misses is < 5%.
22	Failsafe in place.	Frequent data read-out to minimize a miss.
23	Accurate.	Target marker measurement is accurate to □ ppm.
24	Minimum number of false alarms.	Number of false alarms is less than 5 per month of sensor use.
25	Shape is unobtrusive.	Corner radii > 0.
26	Attachment is firm.	Vibration testing yields □ cycles at □ Hz to attachment mechanism failure.
27	Detects early indicator markers.	Detects markers > 1 day average prior to ailment diagnosis.
28	Display unit is easy to read.	Marker levels may be read in < 1 minute.
29	Display unit is easy to operate.	Number of display screens is < 5.
30	Visual signals alert ailment detection.	Visual signal is □ lux, vibrant color.
31	Audio signals alert ailment detection.	Audio signal is □ decibels and □ Hz.
32	May be easily placed within the body during surgery.	Surgeon makes < 5 movements to attach sensor.
33	May be quickly implanted during surgery.	Surgeon attaches sensor in < 3 minutes.

The second step in establishing the target specifications is competitive benchmarking. Benchmarking is the critical analysis of competing products. Exploring the competition's strengths and weaknesses allows the development of a better product, one that incorporates the known advantages while providing solutions to the disadvantages. Although there is no directly comparable product in existence today, similar implantable devices are on the market and can provide guidance. A thorough presentation of benchmarking information was previously given in Section 2.5.2, and from this information, the following conclusions have been drawn. It

should be possible to make the sensor chronically implantable, as others have been. Multi-channel telemetry may be preferable considering the possibility that multiple sensors may be used in the same area. Size, material, and power requirements vary according to application. Other specific conclusions may be drawn and will be made as the design progresses.

The given benchmarking conclusions aid in the third step, setting the target and marginally acceptable values for each metric. These values will not be set here; it is suggested that future design efforts strive to specify these values. The last step, reflection, is undertaken to ensure that both metrics and values are set at reasonable goals. The target specifications are then complete.

3.1.3 Generate Concepts

Concept generation is a crucial part of the design process. In this step, critical subproblems are identified and examined. Once mulled over, solutions are mentally fabricated; these numerous solutions are called concepts. Each concept solves a subproblem of the large problem at hand. The overall problem is the design of an implantable biosensor, while the subproblems may be elaborated.

The relevant critical subproblems arise from functional decomposition of the paramount problem: design an implantable device capable of detecting and distinguishing acute rejection, infection, and vascular occlusion in the kidney or liver throughout the critical period, up to four weeks post-transplant. First, ask: what are the functions that the device must perform in order to solve the larger problem? The answer may be most simply stated as three tasks: (1) obtain information, (2) transfer information, and (3) remain biocompatible.

Second, ask: how are these functions fulfilled? Each of the three tasks is achieved through a set of actions. The first task, obtaining information, is accomplished through four basic events. The first condition is that the target exists in the device environment; this statement is associated with the choice of device placement. The second event is that the sample is filtered. Filtration of the environment must occur to obtain a measurable sample. Third, the sample must contact the sensing element. Contact gives the possibility of target binding. Fourth, the sample minus the bound target should return to the environment. The unbound sample returns to the environment in order to allow the next sample assay.

The second task, transferring information, happens through three actions. First, the

relevant target binding information is packaged in the form of a signal. Next, the signal is transferred through the host body. Lastly, the signal is received outside of the host.

Biocompatibility, the third condition, is comprised of two requirements: (1) the device does not harm the host and (2) the host does not harm the device. Each of these subtasks is associated with its own set of actions necessary for acceptable performance. In order for the device to remain benign to the host, the device must elicit a minimum immunological host response. This depends on four conditions: (1) the device material in contact with the host, characterized by biomaterial-tissue interactions, (2) the device form, determined by the overall shape, (3) amount of fluid leakage out of the device, and (4) the fixation firmness of the device within the surrounding tissue. Host harm to the device is governed by two conditions: (1) the amount fluid leakage into the device and (2) the extent of fibrous tissue capsule formation surrounding the device, which determines the level of measurable analyte.

So, the set of critical subproblems is comprised of these conditions necessary for functional fulfillment. These are given in italics in the organizational chart below.

Table 7: Organizational Chart of Critical Subproblems

OBTAIN INFORMATION • The target exists in the environment = device placement. • The sample is filtered. • The sample contacts the sensing element. • The sample minus the bound target returns to the environment.
CONVEY INFORMATION • The signal is generated within the device. • The signal is transferred through the host. • The signal is received outside the host. • The signal is displayed outside the host.
REMAIN BIOCOMPATIBLE • Device does not harm the host = minimum immunological host response. ➢ Material ➢ Shape ➢ Device fixation in the surrounding tissue ➢ Fluid leakage out of the device • The host does not harm the device = minimum obstruction of device performance. ➢ Fibrous tissue capsule formation ➢ Fluid leakage into the device

The critical subproblems are individually solved by feasible solution concept generation, evaluation, and best-concept decision. Concepts have been generated for each subproblem. In

most cases, concepts are merely that, first-pass ideas. Once a concept is selected, it is further developed. The concepts proposed and chosen are described in the next section.

3.1.4 Select Concepts

Although the design process thus far has proceeded with a systematic and almost scientific degree of clarity, this next step often introduces a slight feeling of constructive hocus-pocus. Concept selection methods range from the highly logical lists of pros and cons to the almost detached method of an external customer decision. Some other methods include ruling by intuition, prototyping and testing several concepts, and constructing decision matrices (Ulrich & Eppinger 107). In this case, selecting one concept sometimes necessitates a certain concept selection for another subproblem. An example of such constraint is seen in choosing a sensor shape; the sizes of all of the constituent components of the device dictate the housing size, a part of the shape description. Such design parameter interdependence is elaborated in the following diagram.

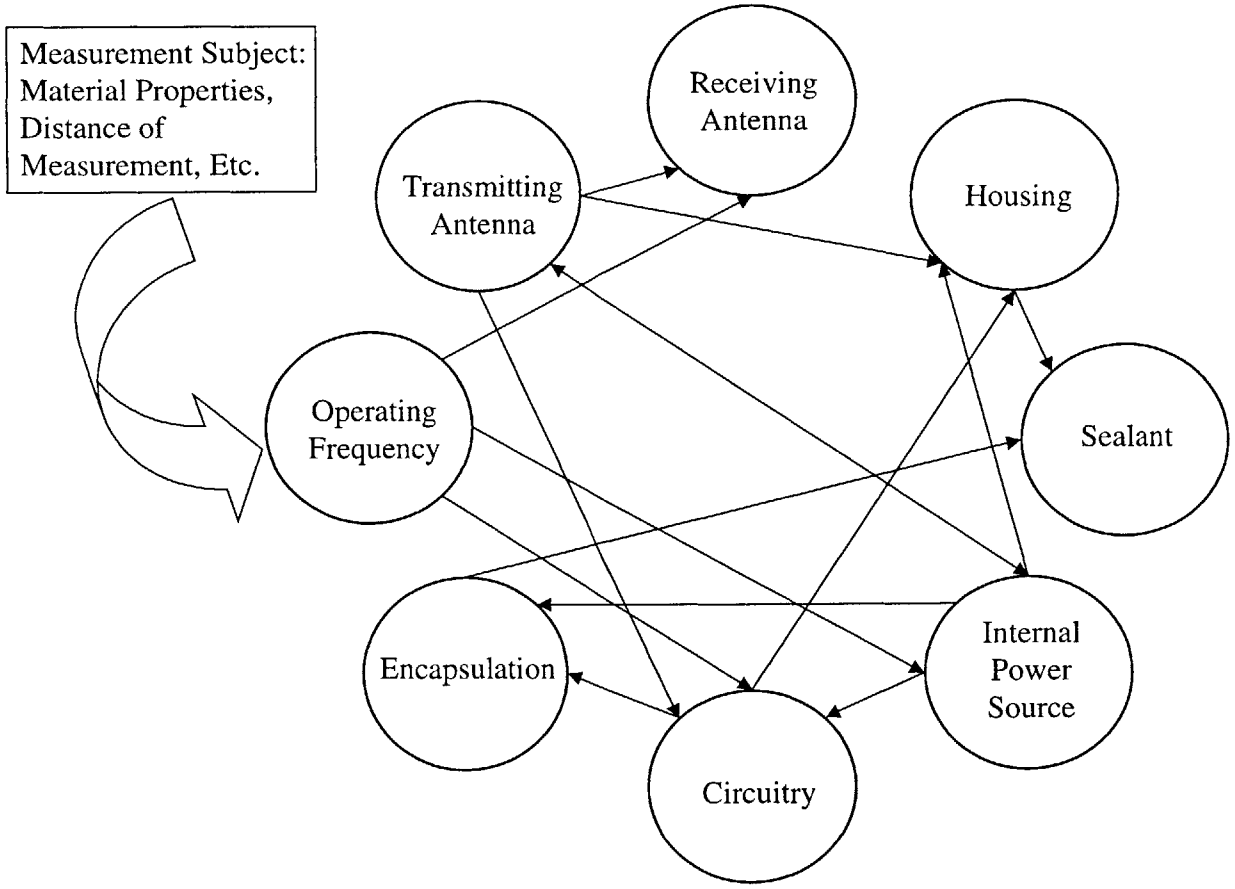

Figure 8: Design Parameter Interdependence

In this scenario, almost every design parameter affects at least one other. The operating frequency directly impacts calculation of attenuation, and hence, the power necessary to run the transmitter. The operating frequency must be in the frequency range of the receiver and the circuitry is also certainly designed with the operating frequency in mind. The transmitting antenna design decides the design of the receiving antenna, since they should be similar in geometry. Its size and shape affect the size and shape of the housing and the circuitry must be designed to drive the antenna. The housing affects the sealant choice, as the sealant must adhere well to the housing material. The size and shape of the power source influence the size and shape of the housing. The encapsulant, or potting, must be chosen so that its temperature in liquid form does not exceed the battery's thermal requirements. The circuitry size and shape affects the size and shape of the housing and the sealant is chosen to adhere to the encapsulant used. Other interdependencies exist within the system that are not mentioned here due to their complexity, for example, the interaction between the housing and the living tissue. Now, solutions to critical subproblems are discussed.

In order to obtain pertinent information from the tissue environment, the sought targets must exist in the environment. This criteria yields definition of device placement position. According to Steve Dawson, M.D. and C. B. Carpenter, M.D., the cytokines and other analytes of interest reside in highest concentrations within the organ itself, not in the circulatory system. Dawson also revealed that a graft rejection, infection, or occlusion episode would result in comparable levels of targets throughout the organ body, suggesting that one point within the organ would most likely yield essentially identical target concentration readings as another arbitrary site within the organ. Another source gives:

> Systemic cytokine levels are difficult to interpret because their importance lies in the local microenvironment so that systemic levels may not accurately reflect what is occurring locally (Forsythe 80).

Another author agrees:

> A sensor that is used to provide information to help control a device surgically placed in the body to replace or assist a failing organ should be implanted, since this is the best way to communicate... (Bronzino 725-727).

This given, the site of implantation is narrowed from the entire host to the organ of interest. In order to maximize ease of surgical implantation, functional requirements numbers 32 and 33, and minimize the extent of tissue damage due to the implantation procedure, functional requirements numbers 14, 15, and 16, the optimal placement position is just between the organ capsule and the organ body, a tissue space roughly a few cm in width. So that the device may best measure the analytes in question, the sample should be filtered. Filtration will disallow clumping of larger and smaller scale molecules within the device at the sensing element surface. Concept generation resulted in the following: a dialysis sheet membrane, dialysis tubing, a mechanical scaffolding structure, an electrochemical filter, a sifter-type grid, and a cage structure with bars. A dialysis membrane selectively-permeable to chemical species of molecular sizes in the range of those of the desired targets will efficiently exclude larger and smaller molecules from analysis. As the sizes of the targets range from around 115 amino acids for IL-1 to 184 amino acids for IL-6, for example, a dialysis membrane rejecting flow to molecules outside of that range is ideal (Lachmann 269, 300). The third requirement for information gathering is that the targets contact the sensing element surface. Because the sensing element works by selectively binding the analyte, physical contact is necessary. Several concepts were generated, including a simple diffusion model, a miniature pump mechanism, a polarity-pull scheme, utilizing a suction-pressure method, and a chamber system with moving mechanisms. Simple diffusion into and out of the fluid chamber of the sensing element is the simplest solution to bring the analyte to the sensing surface. The fourth requirement, of allowing an exit path for the sensed sample, is also accomplished through simple diffusion.

To allow the transfer of information outside of the body, first the information must be translated into a signal within the body. This may be accomplished through electrical means, whereby the sensing element detects the change in mass of the sensing surface as a shift in the frequency of the surface, and the frequency shift is quantified in electrical terms by an electric circuit. The electrical signal may be transferred through the body by many methods, including ultrasound, radio, or optics. For this application, radio transmission is chosen because of the distance that the signal must propagate in order to exit the tissue. The circuit outputs the electrical signal as a current, with a certain magnitude and amplitude, which is fed into an a magnetic coil. The current in the coil generates a magnetic dipole field which transmits the signal from the device through the tissue. Signal reception occurs outside of the host body.

Another magnetic coil is used to pick up the signal present in the field, and the signal is thereafter processed by external circuitry to yield a measured target concentration value. As measurements are made, values are stored and displayed as a concentration profile with time. The details pertaining to these design decisions are discussed in following sections.

The last necessary condition for solution of the problem is biocompatibility of the device with the host. The device will harm the host in a minimal fashion as long as the immunological response is minimized. A minimal response depends on the material, shape, fixation, and leakage of the device. The material chosen to construct the device housing is polyethylene. This material has previously proven positive results in chronic biomaterial studies, as was referred to in Section 2.4.2. The shape of the device also contributes to the immunological response. Less angular shapes reduce the host response, so smooth transitions between surfaces should be utilized; large radii should be applied to all surface meeting planes. Device fixation plays an important role as well, as loose coupling between the device and the surrounding tissue allows more movement and increased friction, which may result in particulate debris formation from the biomaterial surface. As previously explained, the presence of particulate debris leads to macrophage and foreign body giant cell activation. Possibilities examined for fixation include a porous coating, a clamp-like device, a stake-like device, a hook-like device, a tether, electrochemical attraction, hydrostatic/hydrophilic reaction, disulfide bridges, and covalent/ionic bonding. Using a coating of porous material on the main body of the housing will allow device fixation through tissue ingrowth and resulting mechanical interdigitation. Coating the porous layer itself with a chemical which encourages tissue ingrowth, such as fibronectin, will further increase adherence. Any fluids which may leak out of the device are potentially hazardous as well. Foreign fluid in the extracellular milieu will, like debris, result in the recruitment of immune cells. In order to minimize fluid leakage, reliable gasketing is introduced. So that the host does not impair the device function, the formation of a fibrous tissue capsule should be discouraged. To this end, it is suggested, again, that the main housing body be coated with a porous material in order to allow tissue ingrowth and mechanical stabilization. So that fluid may diffuse in and out of the semi-permeable membrane freely without obstruction from proteins adhered on the device surface surrounding the opening, these areas should be coated with PC-heads, as was discussed in Section 2.4.2. The cell membrane-like coating will discourage protein adsorption around the area of diffusion. The host system may also interfere with sensing if body

fluid leaks into the housing. The gasketing mentioned above will also serve to protect against this possibility.

The system design presentation is logically organized according to the purposes the solution fulfills, the critical subproblems solved, namely: (1) obtain information, (2) convey information, and (3) remain biocompatible. The first requirement is met by the actual sensing element and its associated supporting components. The second subproblem is solved by the biotelemetry system and the data display. The third decree is answered by the housing, the encapsulant, and the gasketing. Design choices pertaining to one component may affect the effectiveness of another subproblem solution. For example, in order to best obtain information, the fluid sample must be filtered to discourage interference of larger particles and thus increase the fluid chamber diffusion rate. If particles of length in the extracellular milieu adhere to the edges of the housing surrounding the filtering membrane surface, target molecule passage is impeded. In order to ensure that adhesion does not occur, a specific coating is applied to the housing local to the edges surrounding the filter. This coating, while aiding in the first purpose, obtain information, is a design constraint of the third purpose, remain biocompatible, as it is a specification of the housing. This is one example of previously-discussed design component interrelation.

3.2 Presentation

3.2.1 Obtain Information

3.2.1.1 Sensing Element

The sensing element chosen to detect concentration of target molecules is the flexural plate-wave gravimetric sensor. This sensor is particularly well-suited to biological sensing, "offer[ing] advantages over existing ultrasonic bulk- and surface-wave sensors" (Wenzel & White 700). It is advantageous compared to bulk- and surface-wave gravimetric sensors because it is more sensitive to added mass while operating at significantly lower frequencies. A second advantage is its electronics isolation from the sensing environment, while a third is its low-loss liquid-phase operation. (Wenzel & White 700)

The device consists of thin composite plates of zinc oxide, aluminum, and silicon nitride. Interdigital transducers in the ZnO layer emit and receive plate waves. Coupled to an amplifier, they form a feedback oscillator whose frequency f depends on the mass per unit area M of the

plate. The mass consists of the plate mass, the mass of a chemical coating, and the mass of any molecular targets which have adsorbed to the coating. In the application investigated, the coating consists of chemical species able to irreversibly bind the target species. Thus, once a target is bound, its normalized mass per unit area Δm contributes to the initial mass per unit area M_0, such that

$$M = M_0 + \Delta m . \tag{15}$$

The change in mass changes the oscillator frequency f in a specified manner. The phase velocity of the flexural waves travelling through the plates is a function of the wavelength of the waves launched from the interdigital transducers λ and is given as

$$v(\lambda) = \left[\frac{T + \left(\frac{2\pi}{\lambda} \right)^2 D}{M} \right]^{\frac{1}{2}}, \tag{16}$$

where T is the in-plane tension in the direction of propogation per unit width perpendicular and D is the flexural rigidity of the composite plate and coating. This tension component may be related to the sensor fabrication process. The flexural rigidity may be calculated as

$$D = \frac{Ed^3}{12(1-\sigma^2)}, \tag{17}$$

where E is Young's modulus of the material, d is the thickness of the plate, and σ is Poisson's ratio. The wavelength is dependent on the interdigital transducer spacing, described by period P. The transducers launch waves at

$$\lambda = \frac{P}{n}, \; n = 1, 2, 3, \ldots \tag{18}$$

When $n = 1$, $\lambda = P$, and the oscillator frequency may then be described as

$$f = \frac{v(P)}{P}. \tag{19}$$

So, changes in mass due to chemical binding are detectable through shifts in oscillator frequency.

In order to analyze the level of this detectability, sensor sensitivity[34] is analyzed. The

[34] Sensitivity is equal to (TP/(TP+FN)), where TP is true positive and FN is false negative. A true positive reading is characterized by sensor detection when the stimulus is present; a false negative reading is characterized by no sensor detection when the stimulus is present, a miss.

gravimetric sensitivity of the sensor is

$$S_m = \lim_{\Delta m \to 0} \frac{1}{f} \frac{\Delta f}{\Delta m}, \tag{20}$$

where Δf is the frequency shift. For small fractional shifts,

$$\frac{\Delta f}{f} = S_m \Delta m. \tag{21}$$

For the simple case of an isotropic plate, its mass per unit area M is equal to its density times its thickness:

$$M = \rho d, \tag{22}$$

and sensitivity may be calculated using the equations above. Thus, the sensitivity of the sensor is

$$S_m = -\frac{1}{2\rho d}. \tag{23}$$

It is apparent from this result that as the thickness of the plate decreases, the sensitivity of the sensing element increases, a highly desirable result if the objective is to maximize the number of true positive readings. (Wenzel & White 700-701)

The flexural plate-wave gravimetric sensor was developed by Stuart Wenzel and Richard White at the University of California, Berkeley, in 1990. It was constructed and tested, detecting vapors of toluene 1,1,1-trichloroethane and carbon tetrachloride in the parts per million (ppm) concentration range, running at an operating frequency of 4.4 MHz. The device has been further developed and tested at the Charles Stark Draper Laboratory, Inc. in Massachusetts, although no published data is currently available.

The size scale of the technology is such that a sensor chip capable of detecting a single type of target molecule is merely 1 mm x 1 mm in surface area and of minute thickness value. A grid chip capable of detecting levels of 100 different targets may be fabricated within an area of 10 mm x 10 mm; each 1 mm x 1 mm surface area is selectively coated with a membrane sensitive to the target of interest. The flexibility to simultaneously assay 100 different chemical targets in real-time is a powerful asset that may be advantageously exploited by the current application. The flexural plate-wave gravimetric sensor is ideally suited to obtain information in the current application.

3.2.1.2 Sensor Response Time vs. Sensing Element Lifetime

Sensor response time and sensing element lifetime are mutually exclusive performance metrics; the optimization of one comes at the cost of the other. Both are linked to the target diffusion through the semi-permeable membrane and the fluid chamber space and attachment to the detector surface. The specifics of the way in which these two aspects are interrelated is explained through the use of a simple fluid sampling model and analysis.

The sensor response time refers to the time it takes for a change in target concentration within the extracellular environment to result in an indication of this event at the system output, the data display. As any event may be assumed to share an essentially identical transmission lag time, the response time may from here on be considered to refer to the time it takes for the change in concentration within the body to result in a change in concentration in a fluid layer of infinite thinness just above the coating surface of the sensing element. It is also assumed that once a target molecule is present within this boundary layer, it instantaneously binds to an available site on the coating. This is a valid assumption, as in reality this reaction is extremely rapid.

In order to ensure that the sensing element coating will remain viable throughout the product lifetime L_P, it is essential to quantify the coating lifetime L_C in the context of typical target molecule concentration levels. The coating lifetime must equal or exceed the product lifetime:

$$L_C \geq L_P . \tag{24}$$

Although a sensing surface will be comprised of multiple sections having coatings for multiple targets, it is assumed that this discussion pertains to the limiting coating and target. This target must be identified experimentally. Because this target is present in the highest concentrations in the extracellular environment, its coating binding sites are most quickly exhausted.

In order to best explain the design tradeoff between the response time and lifetime, a simple model approximating the physical system is derived. The model consists of six sections: (1) the ambient environment of the patient, (2) the semi-permeable membrane through which the target passes, (3) the first boundary layer of the fluid chamber inside the sensor body, (4) the central layer of the fluid chamber, (5) the second boundary layer of the fluid chamber, and (6) the detector surface. There are four target concentration levels: (1) that of the ambient environment C_P, (2) that of the first boundary layer C_M, (3) that of the central layer C_S, and (4)

that of the second boundary layer C_D. The thickness of the semi-permeable membrane is given as ℓ, and that of the fluid chamber is d. The distance through the semi-permeable membrane and fluid chamber is measured in the x-coordinate as is illustrated in the diagram below. The model includes target concentration fluxes F_P, F_S, and F_D, also shown below. It assumes that the outer boundary of the membrane is kept at steady-state concentration C_P and that the inner boundary is kept at C_M. The initial concentration of the inner boundary is C_0.

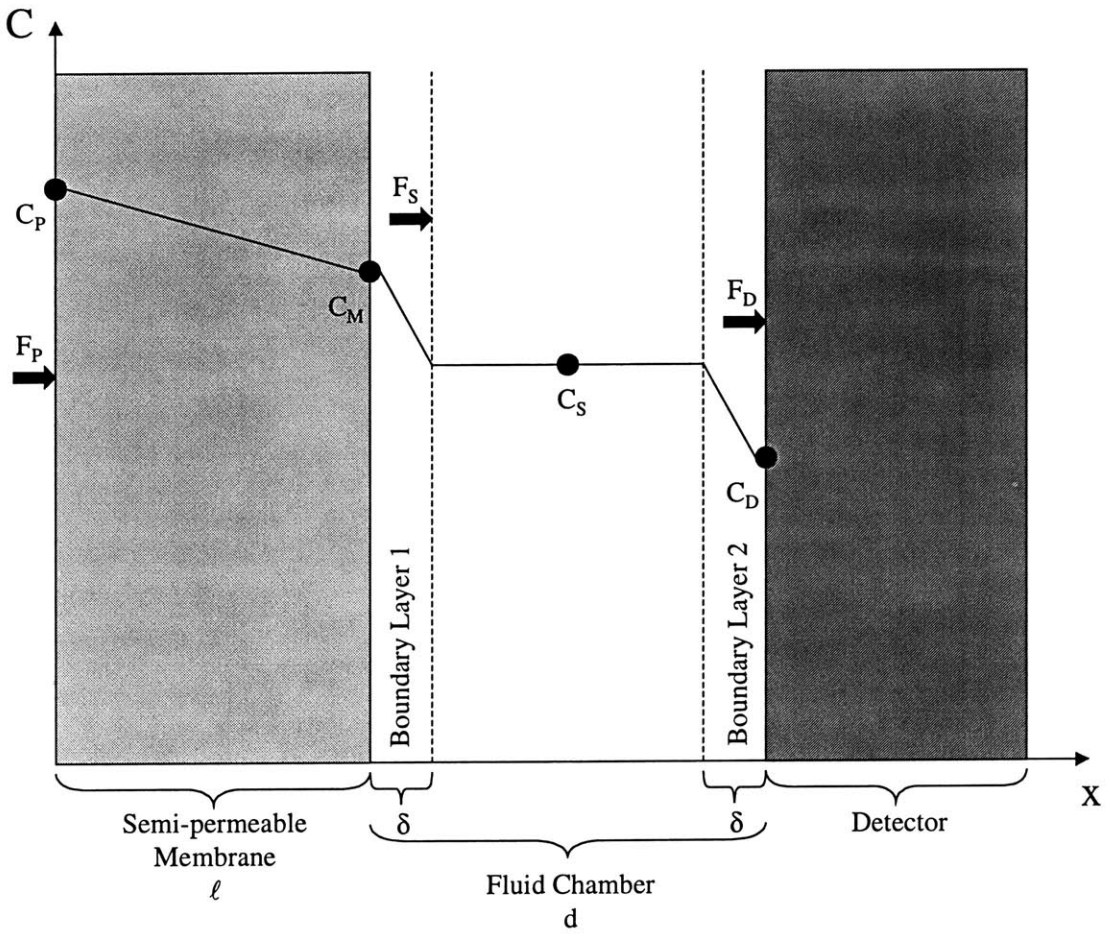

Figure 9: Fluid Path Model

The following variables are used in the model.

N ≡ Number of sensing element binding sites

m_A ≡ Number of attached targets

m ≡ Number of targets in layer of infinite thinness directly above sensing element membrane surface

M_∞ ≡ Total amount of target which enters the semi-permeable membrane in the time from initial to steady-state

M_t ≡ Total amount of target which enters the semi-permeable membrane during time t

A ≡ Area of a single sensing element binding site

A_T ≡ Total area of all sensing element binding sites

C_0 ≡ Initial target concentration.

C_P ≡ Concentration of target in the ambient environment

C_M ≡ Concentration of target in the first boundary layer

C_S ≡ Concentration of target in the fluid chamber

C_D ≡ Concentration of target in the second boundary layer

F_P ≡ Concentration flux out of the ambient environment and into the semi-permeable membrane

F_S ≡ Concentration flux out of the semi-permeable membrane and into the fluid chamber

F_D ≡ Concentration flux out of the fluid chamber and onto the sensing element

D_D ≡ Diffusion constant at the sensing element surface

D_M ≡ Diffusion constant at the semi-permeable membrane

D ≡ Diffusion constant of the fluid

Three distinct transport phenomena control target attachment at the detector, and hence, the response time and the lifetime. These are: (1) the diffusion of molecules through the semi-permeable membrane, (2) the diffusion of molecules through changing concentrations in the fluid chamber, and (3) the attachment of molecules to the detector surface. The first event is likely the rate limiter; its effects on the rate of binding are greater than the effects of the diffusion in the fluid chamber or attachment to the detector under normal operating circumstances. The equations pertaining to the first event will be discussed shortly. The second and third events are now characterized. As was previously stated, it is assumed that once a target exists in the concentration C_D, it immediately binds to an available site. Then, the flux out of the secondary boundary layer and onto the coating may be described by the change in concentration through the second layer over the distance between these concentrations, multiplied by some diffusion constant for the fluid:

$$F_D = -D\frac{\partial C}{\partial x} \cong -D\frac{C_D - C_S}{\delta}, \tag{25}$$

where D is the diffusion constant and δ is the thickness of both the first and second boundary layers. Likewise, the flux out of the first boundary layer and into the central layer is calculated using

$$F_S = -D\frac{\partial C}{\partial x} \cong -D\frac{C_S - C_M}{\delta}. \tag{26}$$

The concentration in the central cavity of the fluid chamber is given as an initial concentration C_0 plus the change in fluxes at the boundary layers over the distance times time :

$$C_S = C_0 + \left(\frac{F_S - F_D}{d}\right)t. \tag{27}$$

Using this type of approach, it would be possible, if desired, to deconstruct the fluid chamber into infinite layers of differing concentrations, each with its own flux governed by the differential equation $-D(\partial C/\partial x)$. In addition, the concentration of each layer might be linked to its neighboring layers as above. In this fashion, a more realistic model might be constructed. However, for the present purposes, it is sufficient to work with the simple model described.

Assuming that F_D is limited by the action of the membrane, it becomes useful to describe the target transport through this membrane. This may be accomplished by using the following mathematical equations. In the following formulation, since the dominant element is assumed to be the membrane, the fluid chamber thickness is assumed to be minimized to a infinitely thin section, so as to not affect the target flux onto the detector. This assumption leads to the approximation that the concentration within the first boundary layer C_M is one and the same as the concentration within the second boundary layer C_D. Although some variable values are estimated, there is insufficient information with which to guess others. Using the formulations set herein, a numerical solution might be obtained through the use of variable values revealed through experimentation with a physical system. However, such experimentation is beyond the scope of this thesis and is therefore suggested as further work.

Assuming that the coating consists of a monolayer of N target binding sites, the coating lifetime refers to the time it takes to fill every available site. This amount of time may be deduced from the rate at which targets attach to the coating, the concentration flux F_D. The concentration flux is a rate of transfer per unit area, a value of number of things per area per

time. Thus, if the area it takes for a target to attach A is known, plus the total available area A_T is known, the amount of time it takes to fill the area is able to be derived, as the "frequency of attachment" is

$$f_a = \frac{\#\,\text{targets}}{(\text{area})(\text{time})} \bullet \frac{\text{total area}}{\#\,\text{targets}} = \frac{1}{\text{time}}. \tag{28}$$

Its inverse is the amount of time it takes to fill the coating, or the coating lifetime, hence

$$L_C = \frac{1}{f_a}. \tag{29}$$

So, in order to calculate the coating lifetime, F_D, A, and A_T must be estimated.

In order to find the area it takes for a target to attach, consider the size of a representative target. IL-6 may be taken as an example. This molecule is composed of 184 amino acids. Although a specific number of amino acids does not directly correlate to a given path length or area due to highly specific interactions that are the nature of tertiary molecular structure, an upper bound length may certainly be given by the generous assumption that the molecule does not fold and its entire length must contact the coating surface. In order to transform this length into an area per molecule, another extremely generous assumption is made that the width is equal to the length. Amino acids are attached to one another by peptide bonds, carbon to nitrogen single bond interactions, for which the length of the bond is 0.132 nm (Brabson & Enfield). The path length of IL-6 is then 24.288 nm, yielding an estimated area of about 6 x 10^{-16} m^2 per molecule. This may be considered a representative A.

The total area available for molecular binding is given as the sensing element surface, which is the surface area of the flexural plate wave gravimetric sensor that is exposed to coating. This area, A_T, is approximately 1 mm x 1 mm, or 1 x 10^{-6} m^2.

Thus, given A and A_T, it is possible to determine N, the number of molecules that can attach to the coating, or the number of binding sites. N is equal to

$$N = \frac{1\ \text{molecule}}{6\times10^{-16}\ \text{m}^2} \bullet 1\times10^{-6}\ \text{m}^2 = 1.7\times10^{9}\ \text{molecules}. \tag{30}$$

First, the target concentration within the semi-permeable membrane as a function of distance and time is solved for the time period between its initial and steady-state values. The concentration at a distance x within the semi-permeable membrane at time t is approximated with a two-term expansion to

$$C(x,t) = C_P + (C_D - C_P)\frac{x}{\ell} +$$
$$\frac{2}{\pi}\left[(C_D\cos\pi - C_P)\sin\left(\frac{\pi x}{\ell}e^{\frac{-D_M\pi^2 t}{\ell^2}}\right) + \left(\frac{C_D\cos 2\pi - C_P}{2}\right)\sin\left(\frac{2\pi x}{\ell}e^{\frac{-4D_M\pi^2 t}{\ell^2}}\right)\right] + \quad (31)$$
$$\frac{4C_0}{\pi}\left[\left(\sin\frac{\pi x}{\ell}e^{\frac{-D_M\pi^2 t}{\ell^2}}\right) + \left(\frac{1}{2}\sin\frac{3\pi x}{\ell}e^{\frac{-9D_M\pi^2 t}{\ell^2}}\right)\right]$$

(Crank 50). Second, the total amount of target which enters the membrane may be quantified. The amount of the target which enters the semi-permeable membrane during the time from the initial time to steady-state is

$$M_\infty = \ell\left[\frac{1}{2}(C_P + C_D) - C_0\right] \quad (32)$$

(Crank 50). The two-term expansion approximate amount of the target which enters the semi-permeable membrane following steady-state during the time t is

$$\frac{M_t}{M_\infty} = 1 - \frac{8}{\pi^2}\left[e^{\frac{-D_M\pi^2 t}{\ell^2}} + \left(\frac{1}{4}e^{\frac{-9D_M\pi^2 t}{\ell^2}}\right)\right] \quad (33)$$

(Crank 50). The total target content within the membrane at any time t is given as $M_t + \ell C_0$

(Crank 51). Thirdly, the amount of target leaving the membrane may be described. The rate at which the target leaves the membrane is $-D(\partial C/\partial x)_{x=\ell}$, using the concentration equation above. This equation is integrated with respect to time to yield the total amount of target passing through membrane in time t to two terms:

$$Q_t = D_M(C_P - C_D)\frac{t}{\ell} + \left(\frac{2\ell}{\pi^2}\right)\left[(C_P\cos\pi - C_D)\left(1 - e^{\frac{-D_M\pi^2 t}{\ell^2}}\right) + \left(\frac{C_P\cos 2\pi - C_D}{4}\right)\left(1 - e^{\frac{-4D_M\pi^2 t}{\ell^2}}\right)\right]$$
$$+ \left(\frac{4C_0\ell}{\pi^2}\right)\left[\left(1 - e^{\frac{-D_M\pi^2 t}{\ell^2}}\right) + \left(\frac{1}{9}\left(1 - e^{\frac{-9D_M\pi^2 t}{\ell^2}}\right)\right)\right] \quad (34)$$

(Crank 51). If the sheet $-\ell < x < \ell$ is initially at C_0 and the target enters at constant flux $F_P = F_S$ over unit area of surface, in other words, $D(\partial C/\partial x) = F_P$, $x = \ell$, then the difference in concentration is given by the two-term expansion approximation:

$$C - C_0 = \frac{F_P \ell}{D_M}\left[\frac{D_M t}{\ell^2} + \frac{3x^2 - \ell^2}{6\ell^2} - \frac{2}{\pi^2}\left[\left(-e^{\frac{-D_M \pi^2 t}{\ell^2}} \cos\frac{\pi x}{\ell}\right) + \left(\frac{1}{4} e^{\frac{-4D_M \pi^2 t}{\ell^2}} \cos\frac{2\pi x}{\ell}\right)\right]\right] \quad (35)$$

Defining these relationships allows variable calculation once an expression for F_D is elucidated.

To that end, the rate at which target molecules attach to the coating may be described as a function of the target concentration just above the coating, the total number of binding sites, the number of molecules already attached, and some diffusion constant:

$$\frac{dm_A}{dt} = C_D\left(\frac{N - m_A}{N}\right)D_D . \quad (36)$$

The concentration C_D may be estimated as the number of molecules in the layer as a function of time divided by the number of binding sites times the area of a single site:

$$C_D = \frac{m(t)}{NA} . \quad (37)$$

This concentration may also be calculated from the equation above, given the knowledge of the initial concentration at the inner boundary of the membrane C_0. This may be assumed to be zero.

The sensor response time and the coating lifetime are directly related to the flux F_D. A high flux rate results in rapid depletion of available binding sites and, hence, a short lifetime. Since the flux F_D may be described, through use of interrelating equations such as are derived above, as a function of the flux into the sensor F_P, a high F_D also indicates a fast response time. A low flux, on the other hand, implies a long coating lifetime and a slow response time. The flux F_D is linked to the diffusion gradient that exists through the semi-permeable membrane and fluid chamber space. The larger the gradient, the higher the flux, and vice versa. This diffusion gradient is dependent upon two variables. The first is the difference in concentration value between the external environment and the boundary layer neighboring the detector, C_P - C_D. The second variable is the distance separating these concentrations, $\ell + \delta$. The gradient is given as a particular relationship between the two, $\partial C/\partial x$. The largest gradient is produced with a large difference in concentration over a small distance, whereas the smallest gradient is yielded by a small change in concentration over a large distance. These relationships are shown in the following diagram.

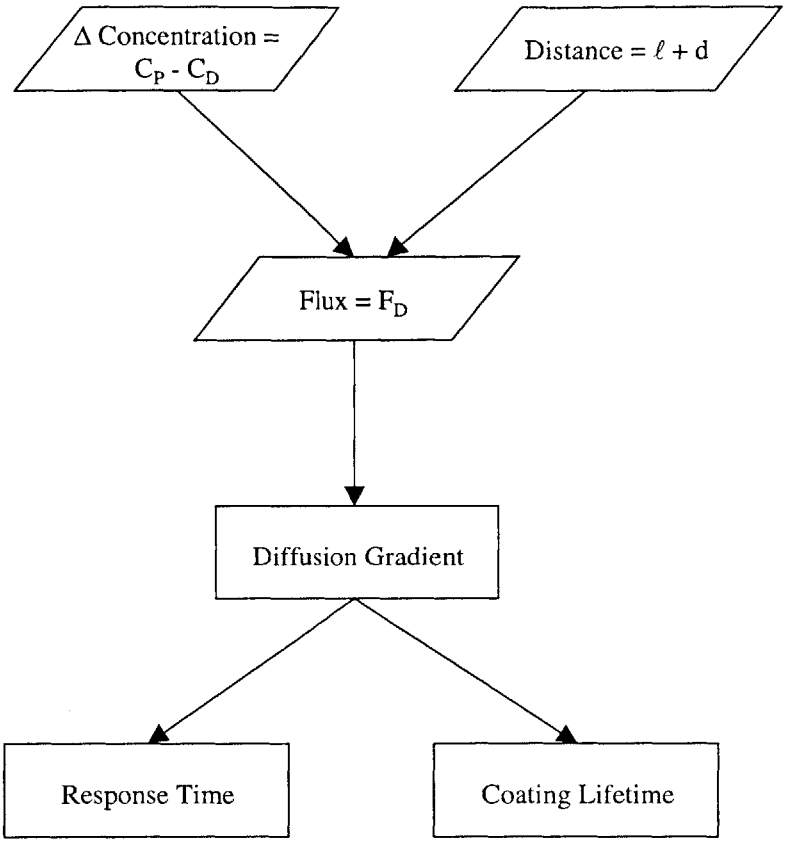

Figure 10: Fluid Path Model Parameter Interrelationships

This linkage, of concentration and distance to the diffusion gradient to the flux into the detector, has specific implications for the process of sensor design with the purpose of response time and lifetime optimization. In order to optimize the response time and the coating lifetime, without increasing the area of the detector or of the semi-permeable membrane, the concentration gradient and the distance over which the fluid travels should be set accordingly. While the concentration in the patient C_P is an independent variable, the porosity of the membrane is a design specification which may be altered to effectively increase of decrease the ratio between C_P and C_D existing at any given C_P. In this way, the concentration gradient at different values of C_P may be somewhat controlled. Another factor relevant to the concentration desired at the detector is the sensing element sensitivity. This is a measure of how much target must bind to the surface in order to yield a detectable response. If the detector has high sensitivity, less target need attach in order to produce a sensor response, and hence, C_D need not be large. In this case,

it might perhaps be advantageous to keep the difference in concentration low so as to not extinguish the binding sites too quickly. A lower porosity will decrease C_D, and increases the detector lifetime, yet also decreases the response time. The distance is a variable directly set by the design. The thickness of the semi-permeable membrane ℓ, as well as the height of the fluid chamber δ, may be specified. Reducing both decreases the response time, but also decreases the coating lifetime. Once preliminary experimental measurements are obtained, a compromise between sensor response time and detector lifetime may be established, and then these metrics may be set.

As an additional note, although the lifetime of the current sensor coating is anticipated to well exceed the product lifetime, future work may investigate clever design concepts for increasing sensor response time and sensor lifetime without an appreciable increase in overall device size or power requirements. Such concepts might be applied toward chronic sensor projects. One possibility may be to incorporate several layers of detector surfaces with some cascading deployment mechanism. Such a technique might be implemented through the imposition and timely removal of any one of different types of target barriers, whether they be related to target size, charge, hydrophobicity, et cetera. It is envisioned that the overlying semi-permeable membrane specific to each wave of detector surface in a cascade might do double duty as acting barrier. Using this elegant approach, sensor lifetime is greatly increased at minimal spatial cost.

3.2.2 Convey Information

3.2.2.1 BIOTELEMETRY SYSTEM

3.2.2.1.1 DEFINITION

Telemetry may be defined as the method by which information in one location may be transferred to another location, usually wirelessly (Carden 1). Biotelemetry is the transfer of data from a transmitter within a living animal to a receiver located externally. It is the method by which target molecule concentration information gathered at the sensor within the body will be transmitted to a receiver outside the body, so that it may then be processed and displayed. Some factors to be optimized are given by Fraser: small package size, adequate battery lifetime, low-noise transmission range, low electrical interference, ease of data collection and processing, and reasonable cost. He adds that, "telemetry links in research environments have the added

requirements of ability to track simultaneously multiple sensors, flexibility in data transmission intervals, minimal cross-talk between transmitters, and transmitter recyclability" (128). While not all of these topics are broached in this thesis, it is noted that those not discussed should be examined in further work culminating in a final design for prototype construction.

3.2.2.1.2 TYPE

There are different ways in which telemetry may be accomplished, including optical, ultrasound, and radio methods, all three of which utilize electromagnetic energy. Within the body, the depth of signal penetration is directly related to the frequency of transmission. Electromagnetic behavior differs according to frequency. In the high-frequency regime, electromagnetic energy observably displays particle behavior, while in the low-frequency range, the detectable behavior is more classically wavelike (Hecht 33). The electromagnetic spectrum is divided according to wave frequency, although the categories do overlap. Shown below is a table of the electromagnetic radiation spectrum. Gamma rays are the highest energy, longest wavelength and highest frequency category. This radiation is emitted from particles in transition within the nuclei of atoms. X-rays are less energized and may be created by the rapid deceleration of highly-charges particles. Ultraviolet light is next on the spectrum. An example of ultraviolet radiation is UV rays released by the Sun, which ionize atoms in the Earth's atmosphere, creating the ionosphere. Visible light is a narrow band on the electromagnetic spectrum, from about 3.84×10^{14} Hz to 7.69×10^{14} Hz. It is usually created by outer-shell electron rearrangement in atoms and molecules. Infrared light is at a lower frequency than visible light, and, even lower are microwaves. The lowest frequency and lowest energy waves are radio waves. Radio waves range in frequency from around a few Hz to 10^9 Hz. They are generally created by electronic circuitry. In this frequency range, the particle nature of electromagnetic radiation is not apparent; the radiation displays only smooth wave-like behavior. (Hecht 68-75)

Table 8: The Electromagnetic-Photon Spectrum

EM WAVES	FREQUENCY (HZ)	WAVELENGTH (M)	PHOTON ENERGY (J)
γ-Rays	$\approx 5 \times 10^{19}$ - 1×10^{23}	$\approx 6 \times 10^{-12}$ - 3×10^{-15}	$\approx 3 \times 10^{-14}$ - 7×10^{-11}
X-Rays	$\approx 3 \times 10^{16}$ - 5×10^{19}	$\approx 9 \times 10^{-9}$ - 6×10^{-12}	$\approx 2 \times 10^{-17}$ - 3×10^{-14}

EM WAVES	FREQUENCY (HZ)	WAVELENGTH (M)	PHOTON ENERGY (J)
Ultraviolet	$\approx 8 \times 10^{14}$ - 3×10^{16}	$\approx 4 \times 10^{-7}$ - 9×10^{-9}	$\approx 5 \times 10^{-19}$ - 2×10^{-17}
Light	$\approx 4 \times 10^{14}$ - 8×10^{14}	$\approx 8 \times 10^{-7}$ - 4×10^{-7}	$\approx 3 \times 10^{-19}$ - 5×10^{-19}
Infrared	$\approx 3 \times 10^{11}$ - 4×10^{14}	$\approx 1 \times 10^{-3}$ - 8×10^{-7}	$\approx 2 \times 10^{-22}$ - 3×10^{-19}
Microwaves	$\approx 1 \times 10^{9}$ - 3×10^{11}	$\approx 3 \times 10^{-1}$ - 1×10^{-3}	$\approx 7 \times 10^{-25}$ - 2×10^{-22}
Radiofrequency	$\approx 1 \times 10^{2}$ - 1×10^{9}	$\approx 3 \times 10^{6}$ - 3×10^{-1}	$\approx 7 \times 10^{-32}$ - 7×10^{-25}

Optical and ultrasound wavelengths fail to penetrate the depth necessary in the current application. Due to the internal depth of the transmitter placement, telemetry at radio frequency is the optimal choice.

3.2.2.1.3 NEAR-FIELD VS. FAR-FIELD

Biotelemetry system design depends on the distance of observation. A radio field is comprised of an alternating electric and magnetic field, which may be considered as the sum of two superimposed fields, one which starts off with a strong amplitude but which quickly decreases in amplitude with distance and one which is weaker in strength but changes more slowly over distance. Within distances close to the source of transmission, then, the first field, called the near-field, will dominate, while at distances far from the source, the second field, the far-field, will be prominent. If the receiver is within one-sixth of a wavelength, then the design follows near-field assumptions, whereas if the receiver is farther away, then the design investigates far-field constraints. (MacKay 225-226)

Signal behavior differs greatly in the near and far-fields, so it is important to decide within which the telemetry system operates. This depends on the distance from the transmitter to the receiver, $z_1 + z_2$, and the wavelength λ of the signal. The wavelength is specified by the operating frequency f, per the equation

$$v = \frac{1}{\sqrt{\varepsilon\mu}} = f\lambda, \tag{38}$$

where v is the velocity of the signal in the medium, ε is the material electric permittivity, and μ is the material magnetic permeability. While the permittivity varies greatly in different mediums,

the permeability does not usually change appreciably from the permeability of free space.[35] Then, if

$$z_1 + z_2 < \frac{1}{6}\lambda, \tag{39}$$

where z_1 is the distance from the transmitter to the skin-air interface and z_2 is the distance from this interface to the receiver, then the telemetry system operates in the near-field. If

$$z_1 + z_2 > \frac{1}{6}\lambda, \tag{40}$$

then it is in the far-field. Most biological telemetering experiments involving operating frequencies less than 25 MHz are conducted in the near-field (MacKay 230). Benchmarking of similarly implanted devices shows near-field operation; the designer therefore preliminarily assumes near-field operation (MacKay 255). After an operating frequency has been defined, this assumption will be revisited and verified.

3.2.2.1.4 Magnetic Dipole vs. Electric Dipole

In near-field telemetry, electromagnetic radiation is negligible; the signal is conveyed either by a transmitter electric or a magnetic dipole, which couples to another respective dipole, which acts as a receiver. In the ideal case, the magnetic method is visualized by a voltage transducer comprised of two parallel coils, while the electric configuration is conceptualized as a capacitor of two charged plates. In far-field telemetry, the signal is in the form of electromagnetic radiation and may be described in terms of energy waves.

An electric dipole field may be characterized by lines of force connecting a positive and negative charge separated by a short distance. This is the same as when electric current flows from a positive to a negative electrode. Both share a similar solution. The magnetic field induced by a steady current in a loop of wire also shares this non-constant solution. (MacKay 227) The shape is described:

> At a given distance the field strength along the axis is just twice that to the side. There is some field at all points near a steady dipole, with the direction being along the lines of force. ... A number of the transmitting antennas used in or on animals effectively

[35] Given by $\mu_0 = 4\pi \times 10^{-7}\ Ns^2C^{-2}$ (Hecht 37).

are dipoles, and their near-field components can be visualized as having this form (MacKay 228).

Thus, an electric dipole is formed from a current element of magnitude I and length ℓ and its strength is proportional to the product $I\ell$, while a magnetic dipole consists of a current loop and its effectiveness is proportional to the area A, the number of turns N, and the current I (MacKay 228).

It seems as though the choice of electric or magnetic antenna for the telemetry system could be arbitrary since their near-field solutions are essentially identical, however, this is not the case. In fact, a magnetic coil is a far superior choice for the particular application for the following reason. Although body tissue is more like a semiconductor than a conductor, the resistance is low enough so that the tissue acts like a short circuit between the ends of an electric dipole antenna. In contrast, a magnetic coil is negligibly affected by the tissue conductivity, except at relatively high frequencies. (Welkowitz 316) This makes a magnetic loop antenna an attractive choice as a transmitter. In fact, "many of the small transmitters which have been described" send out "their signals from a small coil" (MacKay 249).

The receiver should also be a magnetic coil. In the near-field of a magnetic dipole, most of the field energy is in the magnetic field, whereas in the near-field of an electric dipole, most of the energy is in the electric field. Appropriately, in the near-field, a magnetic field antenna should be used to receive from a magnetic dipole and an antenna sensitive to an electric field should be used with an electric dipole. (MacKay 229) The secondary coil should be oriented such that it is in a plane parallel to the plane of the transmitter a distance $z_1 + z_2$ directly above the transmitter. This is explained by MacKay:

> If we orient a receiving loop in such a way as to receive a maximum signal, then the axis of the loop will point along the lines of force. By analogy, consider a compass placed near a bar magnet. If the axis of the magnet passes through the compass, then the compass will point directly at the magnet. If the axis of the magnet is then turned 90 degrees without otherwise moving compass or magnet, then the compass needle will turn 90 degrees until it is parallel with the axis of the magnet. Thus location of the transmitter is not found by direction finding, but rather by moving the antenna until a position

of strongest signal is obtained, whereupon the transmitter is almost below the antenna (232).

It is easy to visualize a handheld or clip-on receiver device poised directly above the liver or kidney, resting upon the prone patient's abdomen. In this way, the distance from the skin-air interface to the receiver antenna, z_2, is minimized. The distance may be considered essentially zero. MacKay also describes a special relationship between the radius of the receiving loop and the distance from the transmitter to the receiver: "On the basis of several mathematical arguments, it can be shown that there is an optimum diameter receiving loop for the signal emitted by the tiny loop in a typical endoradiosonde" (231). The criteria suggest that the radius of the receiver antenna loop r_s should be about equal to the distance from the transmitter to the receiver, equal to z_1, the distance from the transmitter to the skin-air interface, added to z_2 (MacKay 231). However, the distance may now be considered as just z_1, due to the above assumption. Therefore, the antenna diameter is equal to twice z_1. For reasons to be elucidated in Section 3.2.2.1.9, this is estimated as equal to 0.508 m. While this seems to be a large diameter, it is the minimum required in order to obtain signals from halfway through an average human body. These statements help set some of the specifications for the receiver antenna loop.

3.2.2.1.5 PHYSICAL DESCRIPTION

Given the decision that both transmitter and receiver will be magnetic coils, the understanding of the basic concept of near-field magnetic telemetry is crucial. The principal ideas are fairly simple. A transmitter within the body contains a coil and a capacitor in parallel. The coil current oscillates at a natural frequency, and its oscillations are maintained by an associated tuned circuit. A battery provides the power necessary to cause the current oscillations. A second capacitor is connected to the circuit and feeds the signal, which becomes changes in the oscillation pattern. The current oscillations in the coil result in a time-varying magnetic dipole field. External to the body, a second coil in a receiver detects the magnetic field and current is induced. (MacKay 3-4) In the system designed, two sensing elements will be present; one is a reference. The signal sent to the receiver alternates between the two sensing elements according to a timing circuit. A basic diagram elucidates this concept.

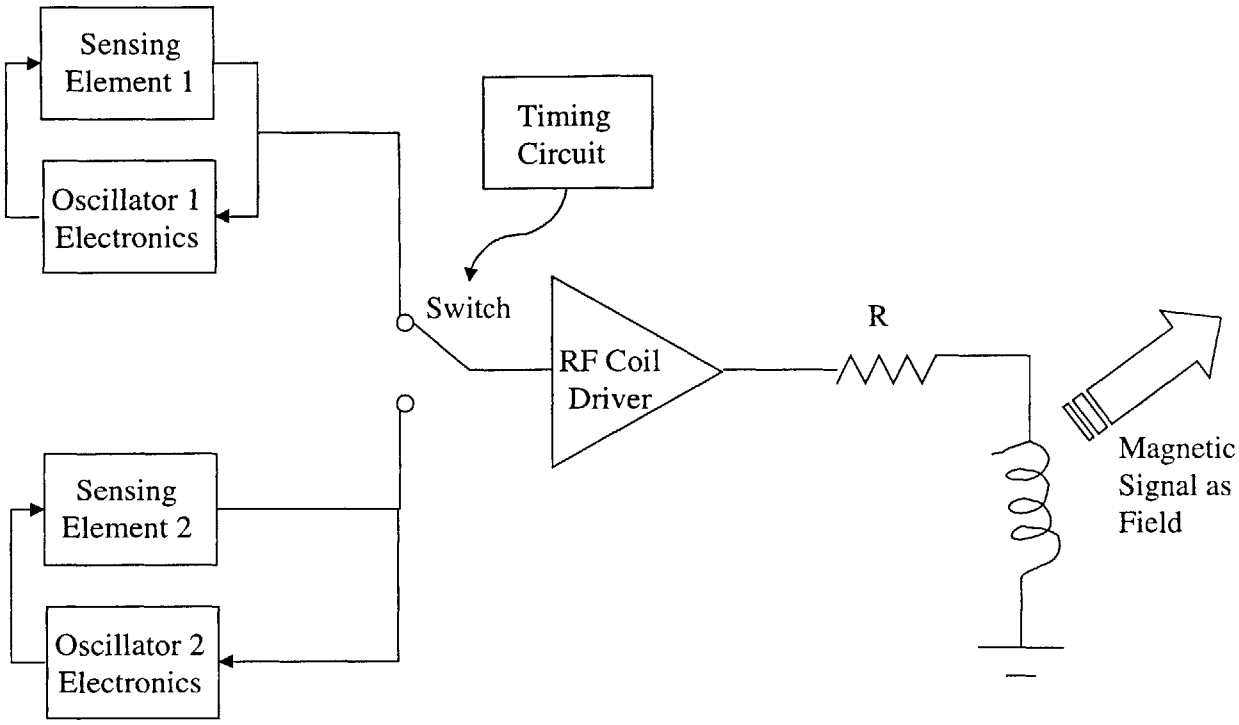

Figure 11: Basic Telemetry Concept

3.2.2.1.6 FM vs. AM

The coils can modulate either the frequency or the amplitude of the electromagnetic wave. In frequency modulation (FM), the amplitude is unchanged, and the information is transferred via altering the frequency, whereas in amplitude modulation (AM), the converse applies. Amplitude modulation is useful for sending data characterized by frequency, but frequency modulation is sometimes more appropriate in the transmission of data quantifying absolute values of a variable (MacKay 81). For example, in the case of an ingested pill-type transmitter using amplitude modulation, every time the transmitter changes its orientation with respect to the stationary receiver or moves behind a different thickness of tissue, the amplitude will be changed. This amplitude modulation does not reflect a change in the physiological variable of interest, its purpose as designed, but rather reflects a change in orientation or attenuation. To make matters more confused, the physiological variable may also be changing,

modulating the amplitude, so that it is impossible to discern what is changing: the orientation, the attenuation, the variable of interest, one of the three, or some combination. Frequency modulation should be used in such an application, as a given number of cycles per second at the transmitter will equal a given number of cycles per second at the receiver; frequency does not change with orientation and attenuation (MacKay 4-5). In the specific application at hand, the transmitter orientation and attenuation will remain constant, as will the receiver orientation, so that either amplitude or frequency modulation is acceptable.

3.2.2.1.7 IDEAL VOLTAGE TRANSFORMER

It is possible then, using an implanted magnetic dipole antenna, to design a communication link with a device external to the body; the telemetry link is conceptualized as a non-ideal voltage transformer. Elucidation requires a description of an ideal transformer. An ideal transformer is comprised of two wire coils tightly wound on a core material of infinite permeability, such that all the flux of one coil links with the other. The currents flowing in each coil, i_1 and i_2 respectively, may be defined such that when both are positive, the fluxes are in opposition. With this configuration, the total flux at the core is then given by

$$\Phi = \frac{N_1 i_1 - N_2 i_2}{R}, \tag{41}$$

where N is the number of turns of the respective coil, and R is the reactance of the core described by

$$R = \frac{\ell}{\mu A}, \tag{42}$$

where ℓ is the average length of the core and A is the cross-sectional area of each coil. From these expressions, it is possible to describe the flux linked by each coil, λ_1 and λ_2:

$$\lambda_1 = N_1 \Phi = \frac{\mu A}{\ell}\left(N_1^2 i_1 - N_1 N_2 i_2\right) \tag{43}$$

$$\lambda_2 = N_2 \Phi = \frac{\mu A}{\ell}\left(N_1 N_2 i_1 - N_2^2 i_2\right), \tag{44}$$

which may also be written as

$$\lambda_1 = L_1 i_1 - M i_2 \tag{45}$$

$$\lambda_2 = -M i_1 + L_2 i_2, \tag{46}$$

where L is the self-inductance of each coil and M is the mutual inductance between the coils. These variables are given as

$$L_1 = N_1^2 L_0 \tag{47}$$

$$L_2 = N_2^2 L_0 \tag{48}$$

$$M = N_1 N_2 L_0, \tag{49}$$

where L_0 is the inductance computed as

$$L_0 = \frac{\mu A}{\ell}. \tag{50}$$

From the rewritten expressions of the flux linked in each coil, the voltage across each coil is made known according to

$$v_1 = \frac{d\lambda_1}{dt} = L_1 \frac{di_1}{dt} - M \frac{di_2}{dt} \tag{51}$$

$$v_2 = \frac{d\lambda_2}{dt} = -M \frac{di_1}{dt} + L_2 \frac{di_2}{dt}. \tag{52}$$

The mutual inductances follow the relation

$$M = k\sqrt{L_1 L_2}, \qquad 0 \le k \le 1, \tag{53}$$

where k is the coefficient of coupling, which depends on the permeability characteristics of the core. For an infinite permeability material, there is no flux leakage, and k is equal to unity. Then, the mutual inductance may be related to the self-inductance by

$$M = \frac{N_2}{N_1} L_1 = \frac{N_1}{N_2} L_2. \tag{54}$$

Because of this relationship, the ratio of the coil voltages is exactly equal to the turns ratio:

$$\frac{v_1}{v_2} = \frac{d\lambda_1 / dt}{d\lambda_2 / dt} = \frac{N_1}{N_2}. \tag{55}$$

In the ideal transformer, the inductances are infinite, which means that in order for the voltages and fluxes to remain finite, the currents must exist in the inverse turns ratio given by

$$\frac{i_1}{i_2} = \frac{N_2}{N_1}. \tag{56}$$

From the prior two equations, it is apparent then that the power delivered by a source to the first

coil (primary winding) is exactly equal to the power delivered to the load across the second coil (secondary winding):

$$v_1 i_1 = v_2 i_2 . \tag{57}$$

In an ideal transformer, there is no loss of power; power is conserved. (Zahn 413-416)

3.2.2.1.8 Shape of Magnetic Field

While a primitive description of either an electric or magnetic dipole field has been given, the near-field of a magnetic dipole may be further described. The primary winding is considered to be an elemental magnetic dipole. The near-field of an oscillating, time-varying magnetic dipole may be described as a quasi-static field. This refers to the assumption made when the charge distribution ρ and the current density J vary slowly with time at a very low frequency and the range of interest R is small compared with the wavelength λ (Cheng 284). Radiation is negligible and coupling between the primary and secondary is through the magnetic field only. The quasi-static assumptions yield an approximate solution for the electric and magnetic components of the field which is only valid under the conditions enumerated. It neglects the time-retardation effects coupled to the finite velocity of propagation of time-varying fields (Cheng 284). In other words, the solution assumes changes occur instantaneously and utilize equations applicable to static fields. This is an acceptable assumption in the near-field.

The electric and magnetic components of the near-field due to a magnetic dipole antenna may be found by considering a small loop of radius b which carries a uniform, time-harmonic current i(t), given as

$$i(t) = I\cos(\omega t). \tag{58}$$

This scenario is shown in the following diagram. It is possible to derive the electric and magnetic near-field components as:

$$E_\phi \approx \frac{-j\omega\mu_0 Ib^2}{4R^2}\sin\theta \tag{59}$$

$$H_R \approx \frac{Ib^2}{2R^3}\cos\theta \tag{60}$$

$$H_\theta \approx \frac{Ib^2}{4R^3}\sin\theta, \tag{61}$$

where ω is the angular frequency, R is the radius of observation measured from the center of the

loop, and j is the imaginary number arising from utilization of phasor notation and is indicative of a phase shift. These equations govern the electromagnetic field intensity at any point in the near-field. (Cheng 502-506)

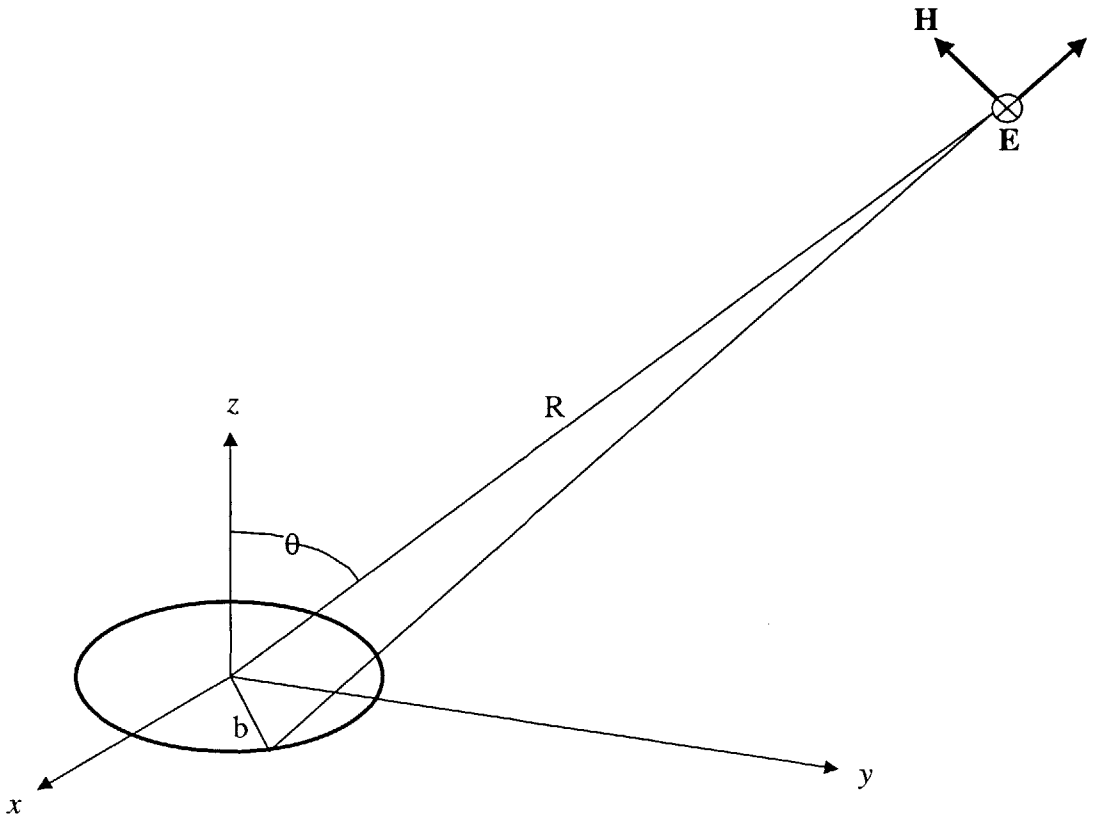

Figure 12: Magnetic Dipole Antenna

3.2.2.1.9 OPERATING FREQUENCY

The near-field of a magnetic dipole is attenuated due to the dielectric properties of the material in which it exists. Because these properties vary with frequency, the operating frequency has profound effects on the signal transmission. These properties cause signal loss, called attenuation, which is the loss associated with the permeability and conductivity of the medium. Because it is such a universal phenomena in studies of signal transmission, a design guideline has been established based on its effects. A first-pass frequency choice may be made according to this criteria.

Although attenuation is the most crucial consideration in the choice of operating frequency, other factors do exist. From these factors, it becomes apparent that frequency choice

involves many tradeoffs. It is a well-known fact that at high frequencies, telemetry system antennas operate more efficiently (Welkowitz 317). Although this compromise must generally be considered, it may be neglected in the near-field case:

> ...antenna or propagation effectiveness requires a frequency as high as possible, whereas attenuation effects require use of the lowest possible frequency. This suggests an optimum compromise. In some near-field cases, an increase in frequency does not increase the antenna signal. Then the lowest possible frequency is desired, at least to the degree that the skin depth is several times the desired range (MacKay 254).

A second factor that encourages a high operating frequency is atmospheric noise. Although a receiver may have very little inherent noise, extra noise, due to the atmosphere, appears once an antenna is connected. Atmospheric noise levels depend on the time of day, weather conditions, and latitude. The noise level falls below the receiver noise range at frequencies of approximately 30 MHz and above (MacKay 253). A third consideration is that low frequency circuitry components tend to be larger than high frequency components, which can affect overall size of the device (MacKay 253). If this is a limitation, however, changing circuit design type may alleviate this restriction (MacKay 253). While these facts may suggest using a high frequency, others indicate a low frequency is better. A telemetry system operating at a low frequency is more stable to environmental interference, such as stray capacitances since circuit capacitance is already large (MacKay 253). While this is true, units have been made to function at higher and lower frequencies, so this is not a severe handicap (MacKay 253). At low frequency, the oscillator Q can be made relatively high, which can improve the reliability and stability of the oscillator.[36] Q is relatively high when the frequency is much lower than 100 MHz (Welkowitz

---

[36] The resonance of an electronic circuit. "Q" actually refers to quality factor. Q is a measure of the sharpness of a resonant peak. The term Q is often used interchangeably with "bandwidth." This is not entirely correct. It is more accurate to say that Q determines bandwidth (a subtle but distinct difference). Q is most often used in reference to synthesizer filters (sometimes referred to as resonance) and equalizers, but it also applies to capacitors (a measure of efficiency, the ratio of capacitive reactance to resistance at a high frequency) and speakers (a measure of directivity). In speakers, a Q of 1 means the system sends out energy equally in all directions; a speaker with a Q of 2 radiates in a 180 degree hemisphere; higher Q's correspond to smaller angles. (Sweetwater Sound Glossary)

317). Some other considerations pertaining to frequency include the fact that radio station interference may be troubling at night, when signals bounce in from remote areas. This may be dealt with by choosing an operating frequency outside of the radio station band. Frequencies above 1.5 MHz or below 500 kHz will bypass the more crowded radio bands. Another problem is the random noise from the building itself; often elevator motors and fluorescent lights are the culprits. (MacKay 251-252) A last relevant point is that some frequencies are legally restricted from use by the U.S. government's Federal Communications Commission (FCC). This, however, need not cause distress, as a 20% shift in frequency does not significantly affect telemetry system operation. (MacKay 255) So, while attenuation is the critical consideration in operating frequency choice, several other factors must be kept in mind.

Attenuation is a function of distance from the electromagnetic source. The attenuation factor is $e^{-\alpha z}$, where z is distance and α is the reciprocal of a term called the skin depth, or depth of penetration, h. In this distance, the signal is reduced by approximately 2/3 (MacKay 254). In other words, most of the signal resides in the skin depth. The variable alpha increases with the square roots of the material conductivity and frequency. Thus, in a conductive medium, the lower the frequency, the larger the skin depth. The design guideline suggests that a near-field telemetry system operating frequency should be chosen such that the distance through the conductive medium is much less than h, the skin depth (Welkowitz 316). The depth of penetration is given by

$$h = \sqrt{\frac{\rho}{\pi \mu f}}, \tag{62}$$

where ρ is the tissue resistivity, μ is the magnetic permeability of the tissue, and f is the operating frequency (Welkowitz 316). The skin depth is also given by the equation

$$\frac{1}{\alpha} = \sqrt{\frac{2}{\omega \mu \sigma}}, \tag{63}$$

where ω is the angular frequency and is equal to

$$\omega = 2\pi f \tag{64}$$

(MacKay 436) and σ is the tissue conductivity, also the inverse of the resistivity:

$$\sigma = \frac{1}{\rho} \tag{65}$$

(Welkowitz 315). The equations for the depth of penetration and the skin depth are equal:

$$h = \frac{1}{\alpha}, \tag{66}$$

easily proved by simple substitution and rearrangement. The operating frequency is chosen based on these equations.

In order to choose a first-pass operating frequency, the design guideline is approached: the distance through the tissue must be much less than the skin depth. To apply this guideline, a value for the distance through the conductive medium, the body tissue, is defined. This distance, z, is the distance from the transmitter coil to the skin-air interface. Although the transmitter position is defined as just within the capsular covering of the anterior portion of the liver or kidney, this position does not correlate to an exact distance from the surface of the body. Every individual body is different, so the distance ranges. The distance discrepancy is greatest between child patient and adult patient cases. There is no one value of z.

Fortunately, the design guideline specifies that z should be much less than the skin depth, so it is possible and acceptable to set z equal to a reasonable upper bound distance. In this methodology, if the distance through the tissue is less than z, then the signal will surely be received, and if the distance is equal to z, then this distance is exactly equal to the skin depth and the signal will just reach the receiver. In order to ensure that even a signal emerging from the upper bound value of z is received well, a safety factor of two is introduced to the distance approximation. Thus, the distance to be used as the distance between the transmitter and the skin-air interface is defined as:

$$z_1 = 2z\,. \tag{67}$$

With this inclusion, the distance through the tissue is assured to be much less than the depth of penetration, given by

$$h = z_1 >> z\,. \tag{68}$$

An upper bound distance value is found in the following fashion. A miniature survey of the adult population was conducted. Five individuals were measured about the midsection, and the anterior-to-posterior distance, referred to as the body thickness, was recorded for each. The results are summarized in the table below.

Table 9: Results of Body Thickness Measurement Survey

PERSON	BODY THICKNESS (IN.)
1	6.5
2	7.0
3	8.0
4	10.0
5	7.5

As is apparent, the upper bound value of the body thickness from the survey is ten inches. Assuming for the sake of simplicity that the anterior surface of the kidney or liver is halfway through this thickness, five inches is the upper bound value. Setting z equal to five inches yields a value of z_1 equal to ten inches. This then is the skin depth for which Equation 62 may be solved (Appendix B). Solving the equation for several values of h shows how the depth of penetration within the tissue varies with the operating frequency. As is clear in the graphs below, the depth of penetration increases with decreasing frequency (Appendix B).

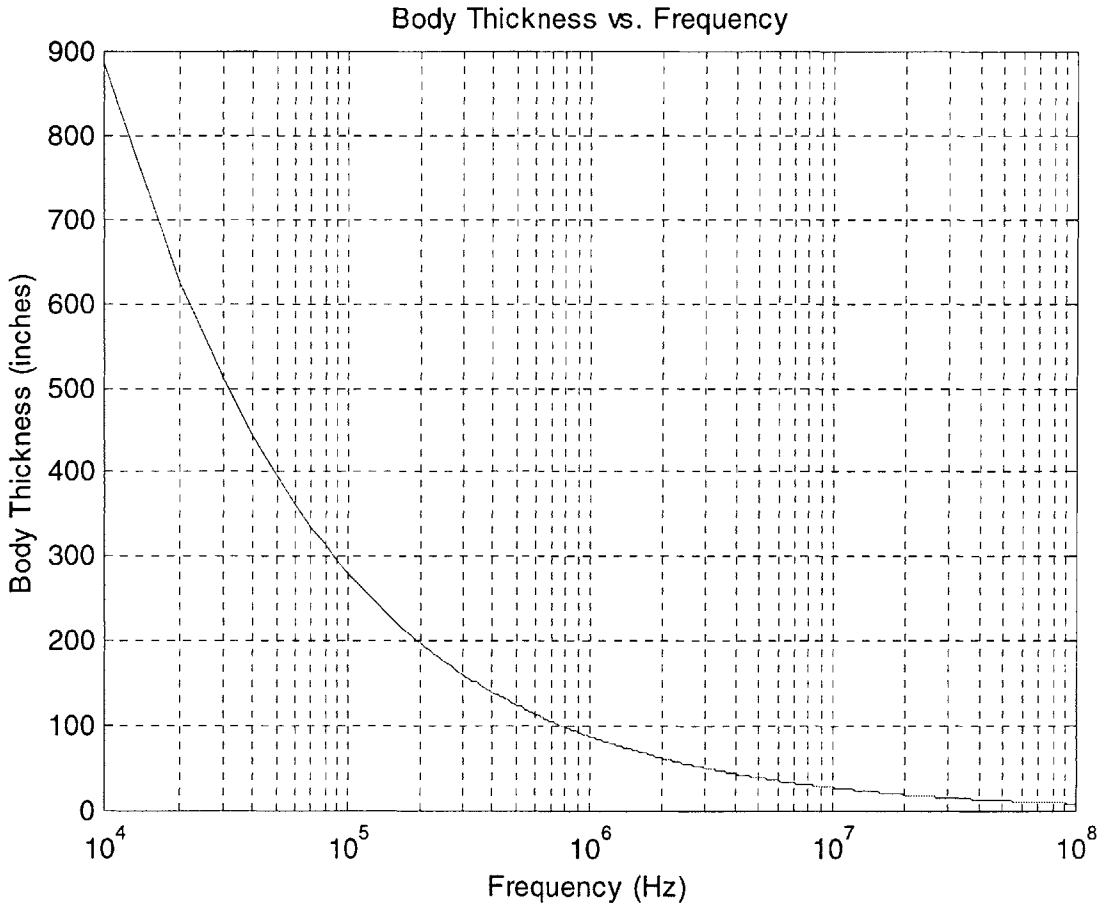

Figure 13: Body Thickness vs. Frequency

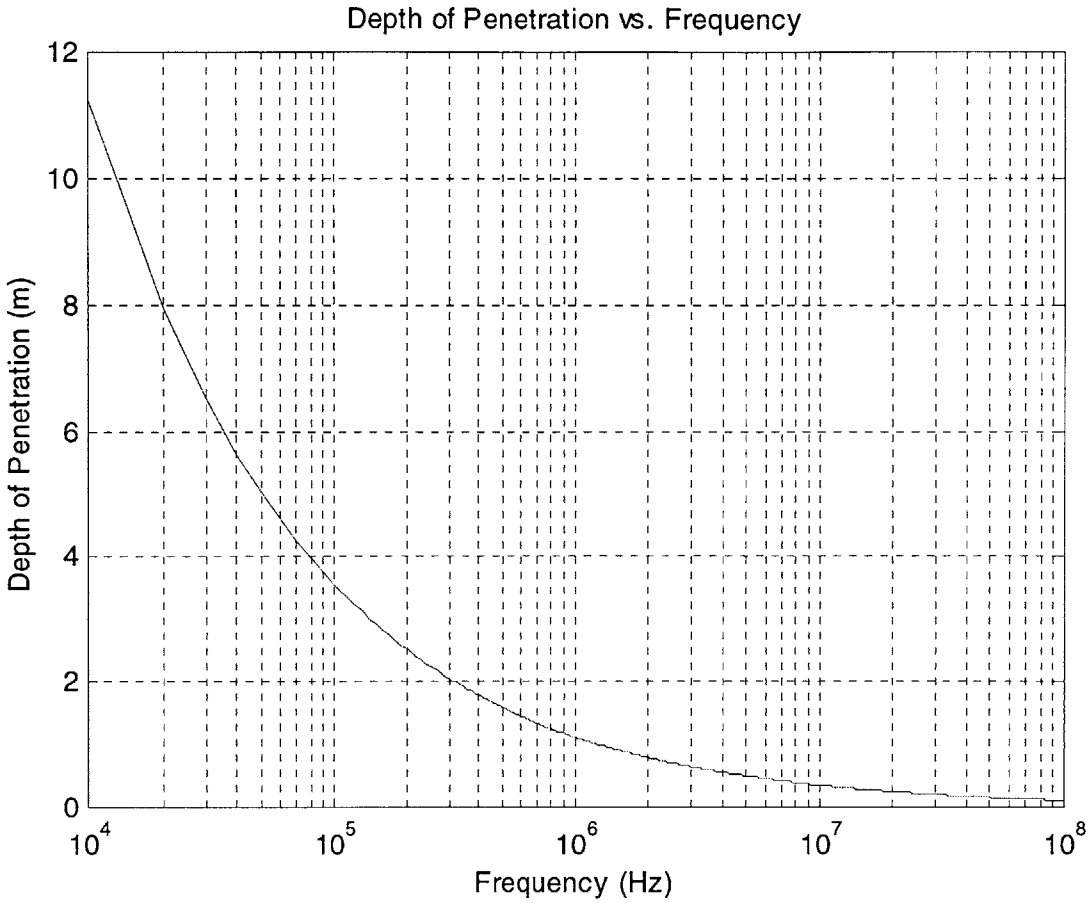

Figure 14: Depth of Penetration vs. Frequency

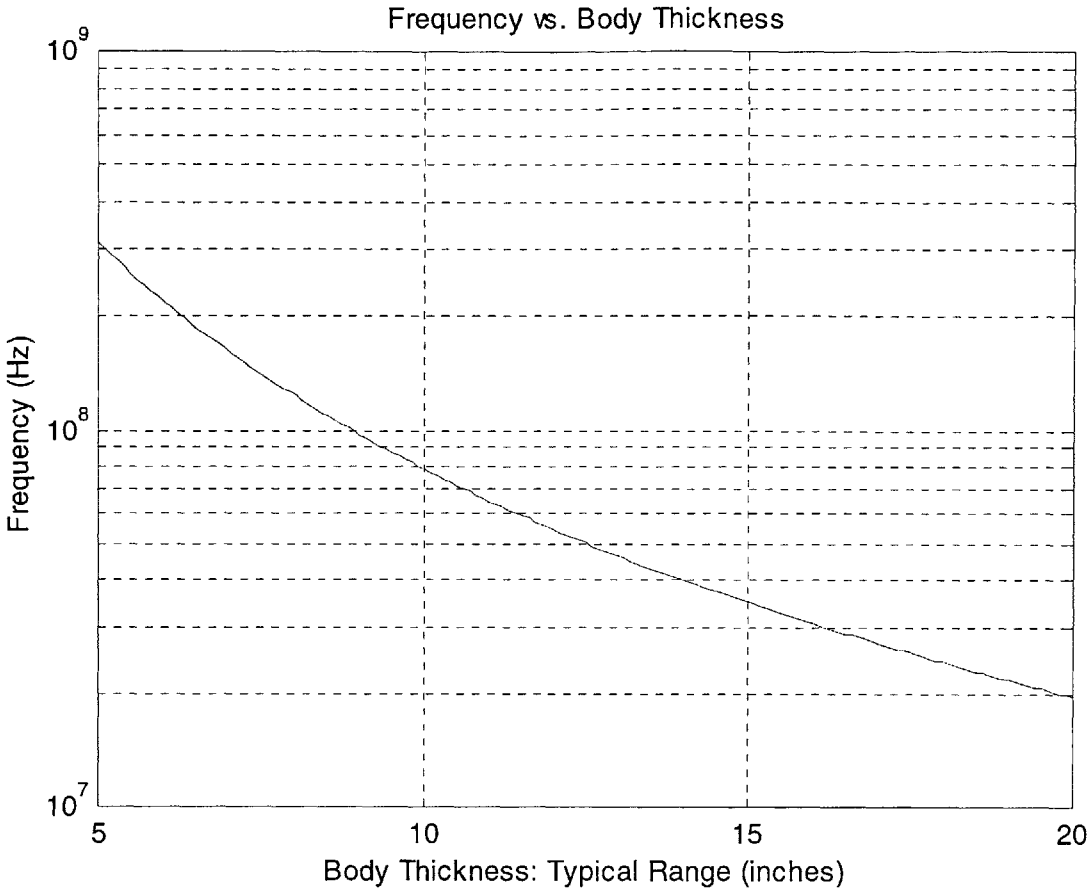

Figure 15: Frequency vs. Body Thickness (Typical Range)

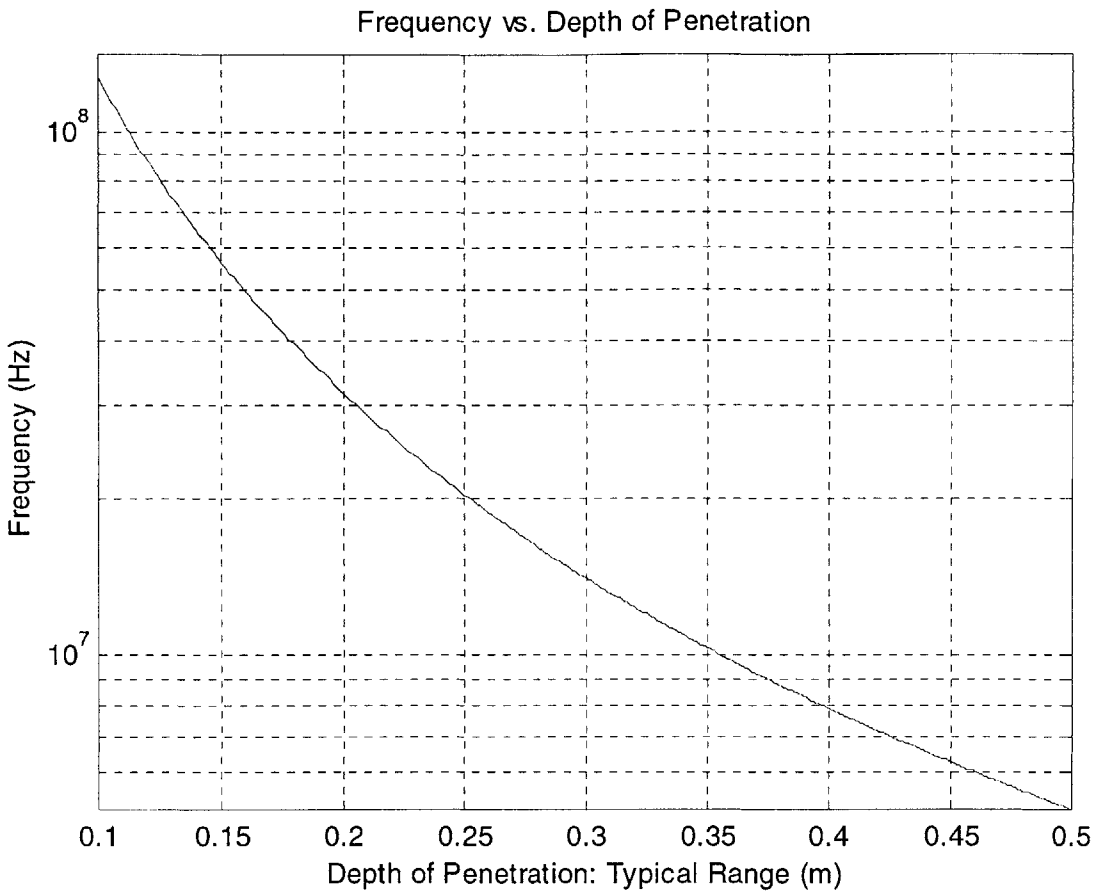

Figure 16: Frequency vs. Depth of Penetration (Typical Range)

For a skin depth upper bound value of ten inches, or 0.254 m, which corresponds to a body thickness of twenty inches, or 0.508 m, the necessary frequency is 1.96×10^7 Hz, or approximately 20 MHz. This is the highest frequency value that may accommodate the depth of penetration desired. While lower frequency values will penetrate even further through the tissue, 20 MHz is chosen as a compromise between the advantages of both low and high frequency operation. As discussed, high frequencies tend to better avoid atmospheric noise, while low frequencies exhibit less attenuation as is illustrated in the following figure, as well as other assets. Therefore, the first-pass operating frequency is defined as 20 MHz.

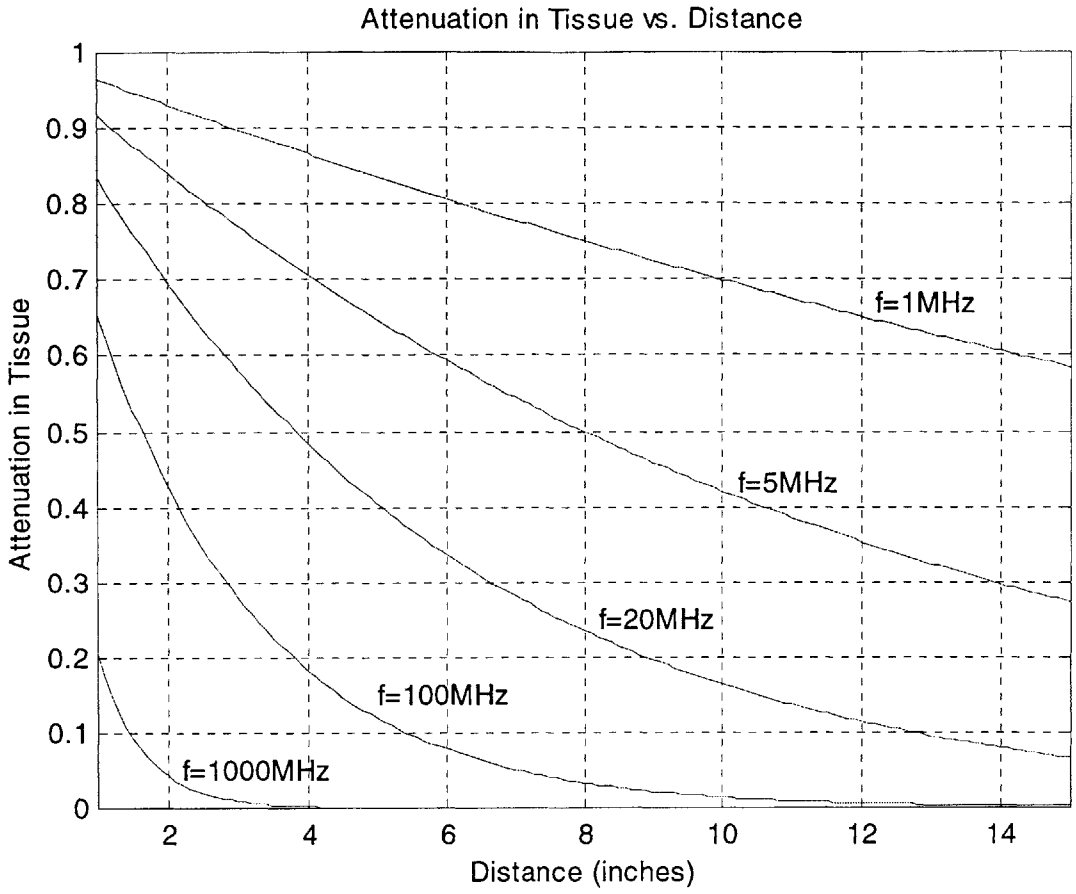

Figure 17: Attenuation in Tissue vs. Distance

The multiple considerations affecting this decision are visually represented in the diagram below.

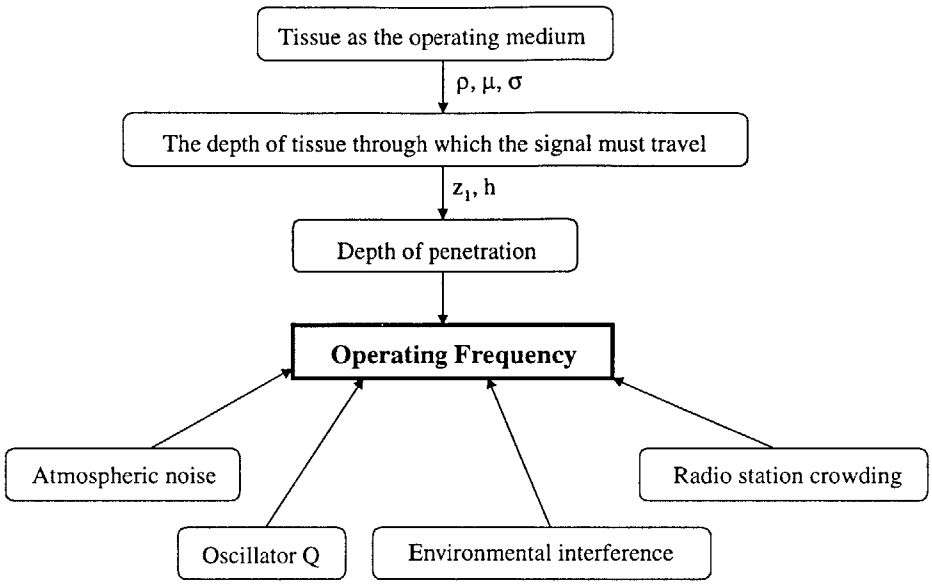

Figure 18: Factors Influencing Operating Frequency Design

Having set the operating frequency, the near-field assumption previously made is analyzed. In tissue, the wavelength is described by Equation 70. At a frequency of 20 MHz, the relative electric permittivity of muscle is 110.62, where relative permittivity K_e is given as:

$$K_e = \frac{\varepsilon}{\varepsilon_0} \tag{69}$$

(Hecht 56). The permittivity of free space is 8.854187817 x 10^{-12} C^2/Nm^2, thus the permittivity is 9.79450256 x 10^{-10} C^2/Nm^2. The magnetic permeability of tissue is estimated as essentially the permeability of free space, 4π x 10^{-7} N/A^2. Therefore, the wavelength in the tissue is given as

$$\lambda_t = \frac{1}{f\sqrt{\varepsilon\mu}} = \frac{1}{(2\times10^7\ \text{Hz})\sqrt{\varepsilon\mu}} = 1.425\ \text{m}. \tag{70}$$

The same analysis may be conducted for the path in air, except the electric permittivity of air is equal to the permittivity in vaccuum, or 8.854187817 x 10^{-12} C^2/Nm^2. So, the wavelength in the air is

$$\lambda_a = \frac{1}{f\sqrt{\varepsilon_0\mu_0}} = \frac{1}{(2\times10^7\ \text{Hz})\sqrt{\varepsilon_0\mu_0}} = 14.990\ \text{m}. \tag{71}$$

The field exists for z_1 at one speed and then exists for z_2 at another speed. The criteria for

the near-field is that the distance travelled is less than one-sixth of a wavelength. Therefore Equation 57:

$$z_1 + z_2 < \left(\frac{1}{6}\right)\lambda \tag{72}$$

decomposes into its specific cases as

$$z_1 < \left(\frac{1}{6}\right)\lambda_t \tag{73}$$

and

$$z_2 < \left(\frac{1}{6}\right)\lambda_a . \tag{74}$$

Both of these inequalities must be true to ensure near-field performance. If we assume, as before, that z_1 is equal to 0.254 m, and assume for argument that z_2 is half this distance, when it will be truly close to zero, then the above stipulations may be evaluated. In fact, both are very nearly true, as

$$z_1 = 0.254 \text{ m} \approx \left(\frac{1}{6}\right)\lambda_t = 0.238 \text{ m} \tag{75}$$

and

$$z_2 = 0.127 \text{ m} < \left(\frac{1}{6}\right)\lambda_a = 2.498 \text{ m} . \tag{76}$$

Although the tissue penetration depth is almost equal to one-sixth its wavelength, this is acceptable, as these are guidelines, not absolute rules. At a distance about equal to one-sixth of a wavelength, the near-field is still very present and does not become indiscernable until a distance a few times one-sixth of a wavelength. So, the telemetry system does operate within the near-field, as was originally assumed.

3.2.2.1.10 Coil Design

Primary and secondary coil design demands that the magnetic field generated by the primary coil will permeate the secondary and induce a voltage large enough to be detected. The first step is to approximate the minimum voltage level detectable at a representative receiver. A guideline exists that "a typical FM receiver only needs 2 or 3 μV" (Welkowitz 320). In the benchmarking case of a chronically-implanted glucose and oxygen transmitter operating at 27

MHz, a signal level of 50 μW was found at the receiver, corresponding to a voltage of 0.05 V with an antenna impedance of 50 Ω (McKean & Gough 527). In another benchmarking reference describing a subcutaneously-implanted glucose sensor system, an off-the-shelf receiver was used. When detecting frequencies of 25 MHz to 520 MHz, Realistic PRO-2006 Programmable Scanner from Tandy Corporation, with a 50 Ω antenna impedance, was sensitive to 3 μV (Shults 939). It seems that, while a voltage of 0.05 V was found at the receiver in a typical case of a subcutaneous implant, the minimum voltage required at a typical receiver could be estimated as 3μV.

The second step is to formulate an expression for the voltage in the secondary winding in terms of relevant design parameters. These parameters include the number of turns of the primary and secondary coils, N_P and N_S, the cross-sectional area of the primary and secondary coils, A_P and A_S, the distance from the transmitter to the receiver, $z_1 + z_2$, the current in the primary, I, and the permeability of the primary core, μ. Attenuation due to the dielectric properties of tissue must be taken into account. Attenuation occurs in all mediums with conductivity greater than zero. In this scenario, attenuation is calculated separately in the tissue over distance z_1 and in the air over distance z_2. From the transmitter to the skin-air interface, the attenuation factor is given as

$$k_1 = e^{-\alpha_1 z_1} \tag{77}$$

where

$$\alpha_1 = \sqrt{\frac{\omega \mu_1 \sigma_1}{2}} \tag{78}$$

and ω is the angular frequency of the electromagnetic radiation, μ_1 is the permeability of the material, and σ_1 is the conductivity of the material (MacKay 436). Similarly, for the path from the skin-air interface to the receiver antenna, the attenuation factor is

$$k_2 = e^{-\alpha_2 z_2} \tag{79}$$

and

$$\alpha_2 = \sqrt{\frac{\omega \mu_2 \sigma_2}{2}}. \tag{80}$$

Given that the frequency is 20 MHz, then from Equation 64, the angular frequency is equal to 1.3 x 10^8 rad/s. The permeability of tissue and air is assumed to be 4π x 10^{-7} N/A^2. The

conductivity of muscle at 20 MHz is 0.64267 S/m, and of air is 0 S/m (Andreuccetti). Calculation of α leads to:

$$\alpha_1 = \sqrt{\frac{\omega\mu_1\sigma_1}{2}} = 7.124\,\frac{1}{\mathrm{m}} \tag{81}$$

and

$$\alpha_2 = \sqrt{\frac{\omega\mu_2\sigma_2}{2}} = 0\,\frac{1}{\mathrm{m}}. \tag{82}$$

Consequently, the attenuation factors are

$$k_1 = e^{-\alpha_1 z_1} = 0.164 \tag{83}$$

and

$$k_2 = e^{-\alpha_2 z_2} = 1. \tag{84}$$

So, it becomes apparent that since the air has zero conductivity, there is no associated loss due to attenuation in that media. On the other hand, the tissue greatly reduces the signal, attenuating approximately 85%.

In order to find the voltage induced in the receiver, the vector potential of the physical magnetic dipole field is approximated as that of a pure magnetic dipole field, which allows the elucidation of the flux through the receiver coil, and consequently, the electromotive force induced in the secondary coil. This approximation correlates the primary coil to a point source in space from which a magnetic dipole emanates. As long as the primary winding is small in diameter compared to the secondary winding, which is located at a sufficient distance, the assumption is valid. Indeed, the primary winding diameter of 1 cm is small compared to the secondary winding diameter of 0.508 m. The vector potential of a pure magnetic dipole field is given by Griffiths (238) as:

$$\vec{A} = \left[\frac{\mu_0 A_p N_p i(t)}{4\pi r^2}\sin\theta\right]\hat{\phi}, \tag{85}$$

where r corresponds to the distance of observation from the center of the coil and i(t) is given assuming the current in the primary winding is sinusoidal over time, or may be decomposed to terms sinusoidal over time:

$$i(t) = I\cos(\omega t). \tag{86}$$

The current magnitude I may be assumed to be equal to 8 x 10^{-4} A during a telemetry burst and 7

μA during standby, as defined by benchmarking and discussed in the upcoming power requirement section. The primary and secondary coils are geometrically oriented as is shown in the following diagram.

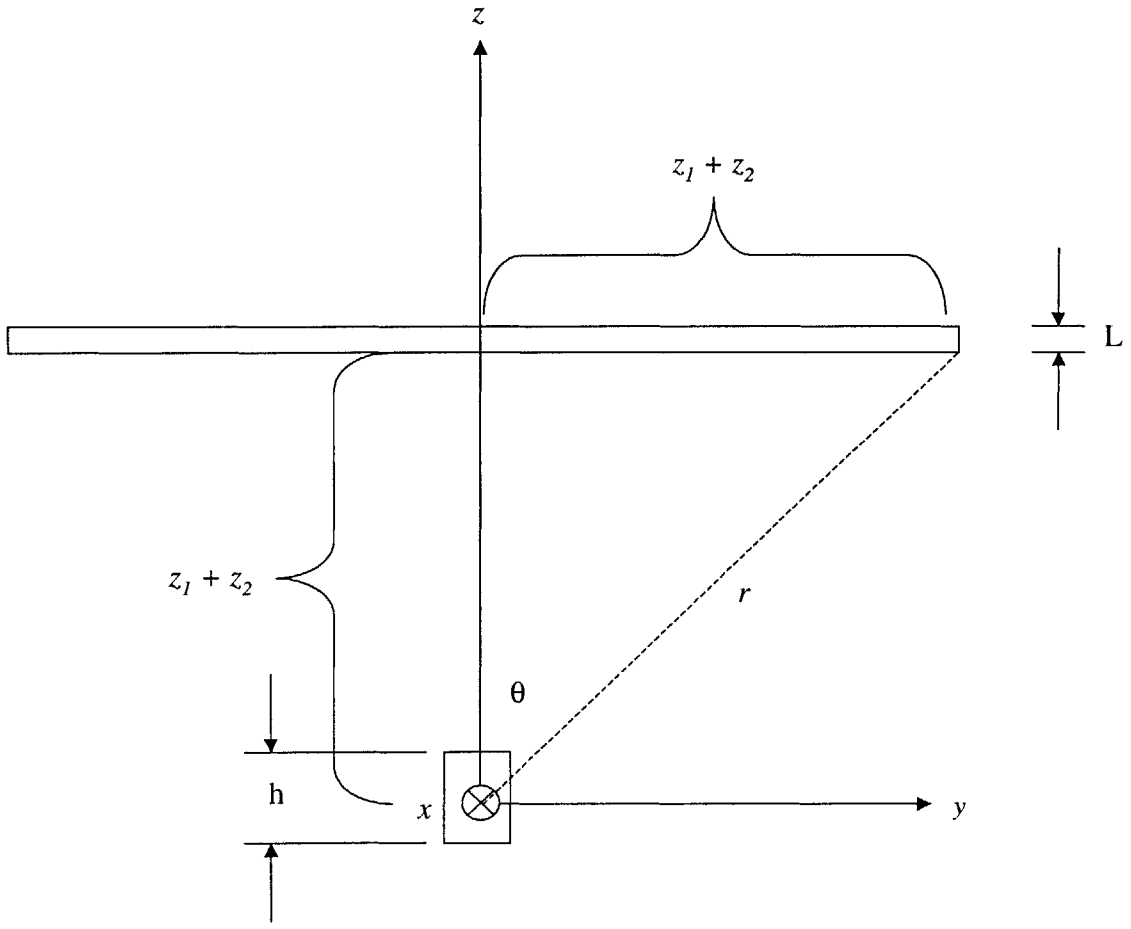

Figure 19: Primary and Secondary Coil Geometry (Side View)

It is obvious from the geometry that

$$\theta = \frac{\pi}{4} \tag{87}$$

and that the distance of observation at the edge of the coil is

$$r = \sqrt{2}(z_1 + z_2). \tag{88}$$

The vector potential is specifically:

$$\vec{A} = \left[\frac{\mu_0 A_P N_P i(t) k}{8\pi\sqrt{2}(z_1 + z_2)^2}\right]\hat{\phi}. \tag{89}$$

The magnetic flux through the secondary coil is:

$$\begin{aligned}\Phi_S &= \int \vec{B} \bullet d\vec{A} \\ &= \int \left(\vec{\nabla} \times \vec{A}\right) \bullet d\vec{A} \\ &= \oint \vec{A} \bullet d\vec{\ell}\,.\end{aligned} \tag{90}$$

In this case, it is clear that the path integral is easier to evaluate than the surface integral because $\vec{A}$ is parallel to $d\vec{\ell}$. Doing so yields the result:

$$\Phi_S = \frac{\mu_0 A_P N_P N_S i(t) k}{4\sqrt{2}(z_1 + z_2)} \tag{91}$$

(Appendix C). In order to find the voltage induced in the secondary coil, the mutual inductance must first be determined. It is:

$$M = \frac{\Phi_P}{i_S(t)} = \frac{\Phi_S}{i(t)}, \tag{92}$$

where $i_S(t)$ is the time-varying current induced in the secondary loop. The mutual inductance, combining Equations 91 and 92, may also written as:

$$M = \frac{\mu_0 A_P N_P N_S k}{4\sqrt{2}(z_1 + z_2)}. \tag{93}$$

Then, the voltage induced in the secondary coil is given by

$$\begin{aligned}e_S(t) &= -M\frac{di}{dt} \\ &= \frac{\mu_0 \omega A_P N_P N_S I k}{4\sqrt{2}(z_1 + z_2)} \sin(\omega t)\end{aligned} \tag{94}$$

and the root-mean-squared value is derived to be

$$\langle e_S \rangle_{RMS} = \frac{\mu_0 \omega A_P N_P N_S k}{4\sqrt{2}(z_1 + z_2)} \langle i \rangle_{RMS}, \tag{95}$$

where the root-mean-squared value of the current in the primary coil is

$$\langle i \rangle_{RMS} = \frac{I}{\sqrt{2}}. \tag{96}$$

The final expression for the voltage induced in the secondary winding in terms of pertinent design parameters is:

$$\langle e_S \rangle_{RMS} = \frac{\mu_0 \omega A_P N_P N_S I k}{8(z_1 + z_2)}. \tag{97}$$

Now all that remains to be done is to define the design parameters that have not been previously

set. The distance between the transmitter and receiver has been estimated in the previous section as 0.254 m. The angular frequency is quickly known from the operating frequency of 20 MHz, as

$$\omega = 2\pi f \ , \tag{98}$$

yielding 1.3 x 10^8 rad/s. Knowing that the voltage induced in the secondary coil should be at least 3 μV, the number of turns and cross-sectional area of the primary may be determined. In setting the secondary winding area, it is useful to recall that the diameter of the secondary coil should be twice the distance between the transmitter and receiver, as mentioned in Section 3.2.2.1.4. Given that

$$A_S = \frac{\pi d_S^2}{4} = \frac{\pi[2(z_1 + z_2)]^2}{4} = \pi(z_1 + z_2)^2 \ , \tag{99}$$

then the cross-sectional area of the receiver coil is approximately 0.2 m^2. It is also helpful to consider that the primary coil size should be minimized, as it resides within the body, a limited space container. Given this guide, Equation 97 may be solved for several values of N_P, N_S, and A_P (Appendix D). The area of the primary coil depends on the diameter of the coil. If the diameter is restricted to 1 cm, then the area is equal to 7.85 x 10^{-5} m^2. If the number of turns of the primary is restricted to 2 turns, then the number of turns of the secondary is 1.8, about 2. This feasible solution will yield the minimum signal necessary for pickup at the receiver. In order to increase the signal, the number of turns or the area of the primary may be increased. To ensure signal reception, a safety factor of 10 is included so that the number of turns at the secondary is 20.

Given that the transmitter and receiver antennas are loops, there are a number of ways in which their signal transmission and reception may be made more effective. In many cases, the transmission range can be substantially increased by connecting a trailing length of wire to one side of the loop (MacKay 249). Of course, advantage is also conferred upon those antennas with ferrite cores. In fact, flux concentrations may increase tenfold as a result. (MacKay 231)

3.2.2.1.11 Power Requirements

Power is necessary to drive both internal and external portions of the device. Because external power requirements may easily be met through the use of conventional sources, such as a wall outlet line, this discussion focuses on meeting the implantable system power requirements.

To this end, a portable power source, or battery, is an ideal solution. A battery will provide the required power in a compact, on-site, enclosed container. Several types of batteries are readily available in all shapes, sizes, and capacities. Custom designs are available, but perhaps not necessary for this application.

The internal system circuitry is comprised of subsystems with differing power requirements. These may be described in general, although specific design is not an aim of this thesis and will not be presented. The sensing element outputs plate-wave frequency and amplitude information to a circuit which translates this data into electrical energy. This energy then would typically proceed through an amplifier circuit and a data processing circuit. In the particular design, an amplifier circuit is not necessary due to the fact that the operating frequency chosen for the telemetry system is roughly equal to the range of frequencies produced by the flexural plate-wave sensors. The signals are then sent to an oscillator circuit, which sends a current I into the transmitter antenna loop. Each one of these subsystems may require a different power, thus, it is essential that a power conversion circuit exist. Such a circuit changes the power from the battery into the amounts of power needed at each separate subsystem. It may typically be assumed to work at an efficiency of 80%. Such a system may be visualized as in the following diagram.

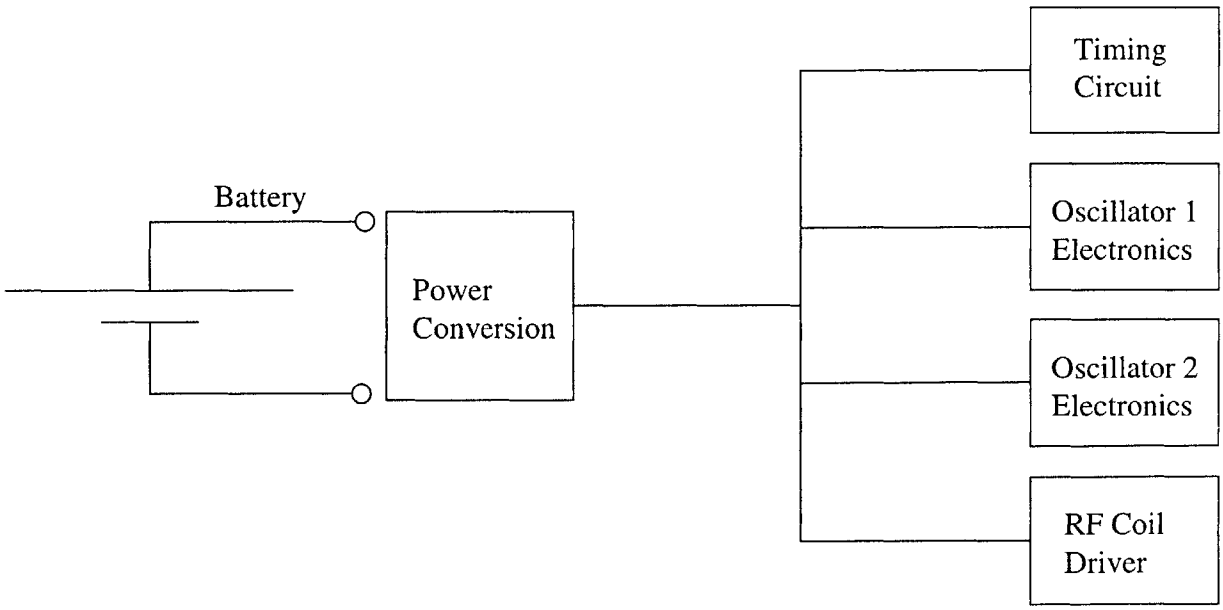

Figure 20: Power Conversion Concept

While a conversion block can convert the power to be used, the battery must be capable of outputting enough power to supply all of the subsystems. Therefore, in order to choose a battery, the subsystem power levels must be at least roughly defined.

Implantable sensor circuitry is usually composed of low-power, CMOS[37] elements. Although the power requirements for individual components are only obtained by specifically defining those components, which is outside the scope of this thesis, it is possible to obtain a general value from benchmarking analysis. A glucose and oxygen sensor designed in 1988 utilized a lithium-bromide cell, Wilson-Greatbatch BCX-72, with potential 3.8 V and a capacity of 1 A-h. The average current drain was 250 μA in standby mode and 500 μA in transmit mode. (McKean & Gough 527-529) A subcutaneously-implantable glucose sensor designed and implemented in 1994 was able to transmit glucose levels for up to 2.5 years at the least frequent transmission interval using two lithium coin cells, Panasonic BR2330, with capacity 0.25 A-h and potential 5.6 V. This sensor experienced an overall current load of 7 μA in standby mode and 3 mA in transmit mode. (Shults 938) The current load information might be considered indicative of the overall current loading in this particular application. While this information may be considered in choosing a battery, it is still helpful to define, where possible, the power requirements of individual subsytems, for example, the telemetry system.

Within the telemetry system, the power requirement of the primary coil must be ascertained, as it represents a fundamental power consumption. If the coil were to exist in free space and were to be considered small enough so that radiation might be neglected, there would be no power delivered to the surrounding space. This is analogous to the previously-discussed case of the ideal voltage transformer. Because the coil is imperfect and exists within a conducive material, there are associated losses that must be taken into account. One loss is due to the resistivity of the coil material. Another loss is derived from the use of a magnetic core material within the coil. A third loss is attributed to current induced in the conducive surroundings, the

[37] CMOS is an acronym for complementary metal-oxide semiconductor. "CMOS is the semiconductor technology used in the transistors that are manufactured into most of today's computer microchips. Semiconductors are made of silicon and germanium, materials which conduct electricity, but not enthusiastically. Areas of these materials that are 'doped' by adding impurities become full-scale conductors of either extra electrons with a negative charge (N-type transistors) or of positive charge carriers (P-type transistors). In CMOS technology, both kinds of transistors are used in a complementary way to form a current gate that forms an effective means of electrical control. CMOS transistors use almost no power when not needed. As the current direction changes more rapidly, however, the transistors become hot. This characteristic tends to limit the speed at which microprocessors can operate." (Whatis.com)

tissue. These three losses may be modeled as a single lumped resistance R in series with the primary winding. In order to find the lumped resistance R, consider the three losses in series, so that

$$R = R_{Tissue} + R_{Coil} + R_{Core}. \tag{100}$$

The resistance due to the tissue conductivity may be estimated using the following methodology. Given an ideal transmitter coil and an ideal receiver coil operating in free space,[38] the power in the magnetic field at the receiver has a certain value, P_{FS}. Consider the same situation, where the only variation is that the space between the transmitter and receiver is now filled by a conducive material instead of by free space. Now, the power in the magnetic field at the receiver is a value less than P_{FS}, and may be called P_T. The difference between these two power values is the power lost due to the conductivity of the material, P_L, where

$$P_{FS} = P_T + P_L. \tag{101}$$

This power loss may be modeled in terms of a resistivity, R_{Tissue}. The root-mean-squared power loss is

$$\langle P_L \rangle_{RMS} = \frac{I^2 R_{Tissue}}{2}, \tag{102}$$

where I is a term present in the time-varying current, $i(t) = I \cos \omega t$. Once the root-mean-squared power loss is known, R_{Tissue} is easily found.

First, the B-field is modeled mathematically. Second, an expression is given for the energy density, which is proportional to the B-field in the ideal case, squared. Thirdly, the energy density equation is integrated spatially to yield the energy in the specific region of space bounded by the dimensions of the secondary coil. Next, the power in this region of space, P_{FS}, is found by taking the time derivative of this energy. The power in the tissue case is related to the power in the free space case by some reducing factor, a function of the attenuation, $e^{-\alpha z}$. In order to ascertain this function, it is helpful to consider that attenuation affects both the magnitude and the phase of the magnetic field along the primary coil axis as:

$$B_z(z,t) = B_0 e^{-\alpha z} \cos(\omega t - \alpha z), \tag{103}$$

where B_z represents the magnetic field along the primary coil axis a distance z from the center of

[38] The ideal case is that for which there are no losses associated with (1) resistivity of the coil material, (2) permeability of the core material, and (3) conducive surroundings.

the primary coil surrounded by tissue, B_0 signifies the amplitude of the magnetic field at a distance z in free space, and $-\alpha z$ is the phase shift of B_z relative to B_0. Power is proportional to the square of the B-field, so that the reducing factor is elucidated as $e^{-2\alpha z}$. To simplify notation, this is referred to as k^2. So, the powers are related by:

$$k^2 P_{FS} = P_T . \tag{104}$$

Combining this equation with Equation 86 above, the power loss may be described as:

$$P_L = P_{FS}\left(1 - k^2\right). \tag{105}$$

Taking the root-mean-squared value of this power loss and equating to Equation 87 allows determination of R_{Tissue}.

The vector potential $\bar{A}$ for a magnetic dipole is given by Griffiths as:

$$\bar{A} = \left[\frac{\mu_0 A_P N_P i(t)}{4\pi r^2}\sin\theta\right]\hat{\phi}, \tag{106}$$

where r is the distance of observation (238). Since the B-field and the vector potential are related by

$$\vec{B} = \vec{\nabla} \times \bar{A}, \tag{107}$$

the magnetic flux density field in the $r>>R_P$ region of an ideal magnetic dipole is appropriately described by the vector equation:

$$\vec{B} = \left[\frac{\mu_0 N_P R_P^2 i(t)}{2\pi r^3}\cos\theta\right]\hat{r} + \left[\frac{\mu_0 N_P R_P^2 i(t)}{4\pi r^3}\sin\theta\right]\hat{\theta}, \tag{108}$$

where the coordinate system and loop position are such as is diagrammed in Figure 15. Since the energy density is proportional to the field squared, it is necessary to calculate the square, which is

$$B^2 = \left(\frac{\mu_0^2 N_P^2 R_P^4 [i(t)]^2}{16 r^6}\right)\left(3\cos^2\theta + 1\right) \tag{109}$$

(Appendix C). The energy density is then given by

$$\begin{aligned} w(t) &= \frac{B^2}{2\mu_0} \\ &= \left(\frac{\mu_0 N_P^2 R_P^4 [i(t)]^2}{32 r^6}\right)\left(3\cos^2\theta + 1\right). \end{aligned} \tag{110}$$

In order to find the energy contained in the space of the secondary winding, consider a solenoid of short height L and large radius $z_1 + z_2$, a distance $z_1 + z_2$ away from the primary coil, where L is equal to the diameter of the secondary winding wire times the number of turns:

$$L = d_{wS} N_S . \tag{111}$$

Integration is most simple in cylindrical coordinates, so spherical coordinate system (r, θ, ϕ) is changed to cylindrical coordinate system (ρ, ϕ, z) by the transformations

$$r^2 = \rho^2 + z^2 \tag{112}$$

and

$$\cos\theta = \frac{z}{\sqrt{\rho^2 + z^2}} . \tag{113}$$

Thus, the energy density is converted to

$$w(t) = \left(\frac{\mu_0 N_P^2 R_P^4 [i(t)]^2}{32(\rho^2 + z^2)^3} \right) \left(\frac{3z^2}{\rho^2 + z^2} + 1 \right). \tag{114}$$

The energy in the space of the secondary coil is

$$\begin{aligned} E(t) &= \int_0^{z_1+z_2} \int_{z_1+z_2}^{z_1+z_2+L} \int_0^{2\pi} \left(\frac{\mu_0 N_P^2 R_P^4 [i(t)]^2}{32(\rho^2 + z^2)^3} \right) \left(\frac{3z^2}{\rho^2 + z^2} + 1 \right) d\phi dz (\rho d\rho) \\ &= \left(\frac{\mu_0 N_P^2 R_P^4 [i(t)]^2}{32} \right) (2\pi) \int_0^{z_1+z_2} \int_{z_1+z_2}^{z_1+z_2+L} \left[\frac{\rho}{(\rho^2 + z^2)^3} + \frac{3\rho z^2}{(\rho^2 + z^2)^4} \right] dz d\rho . \end{aligned} \tag{115}$$

Since $z_1 + z_2 >> L$, and $z_1 + z_2 \le z \le z_1 + z_2 + L$, z may be approximated in the integrand as equal to $z_1 + z_2$, a constant value, while the term outside of the integral may be multiplied by the differential in z, in other words, L. Having made this adjustment, the energy equation is now:

$$E(t) = \left(\frac{\mu_0 N_P^2 R_P^4 [i(t)]^2 L\pi}{16} \right) \int_0^{z_1+z_2} \left[\frac{\rho}{\left[\rho^2 + (z_1 + z_2)^2\right]^3} + \frac{3\rho(z_1 + z_2)^2}{\left[\rho^2 + (z_1 + z_2)^2\right]^4} \right] d\rho . \tag{116}$$

Trigonometric substitution yields the final equation for the energy:

$$E(t) = \frac{5\pi\mu_0 N_P^2 R_P^4 [i(t)]^2 L}{128(z_1 + z_2)^4} . \tag{117}$$

The power in this space is then given as

$$P(t) = \frac{dE}{dt} = -\frac{5\pi\mu_0 N_P^2 R_P^4 I^2 L\omega}{128(z_1 + z_2)^4} \sin 2\omega t . \tag{118}$$

This is the power in the space when it is filled by vacuum, P_{FS}. According to Equation 105 above, the power lost between the free space and tissue cases is

$$P_L(t) = -(1-k^2)\frac{5\pi\mu_0 N_P^2 R_P^4 I^2 L\omega}{128(z_1+z_2)^4}\sin 2\omega t. \tag{119}$$

The root mean squared value of this power is

$$\langle P_L \rangle_{RMS} = (1-k^2)\frac{5\pi\mu_0 N_P^2 R_P^4 I^2 L\omega}{128\sqrt{2}(z_1+z_2)^4}. \tag{120}$$

Modeling this power loss due to attenuation as a resistor, the root mean squared value is matched to the average power output of such a resistor:

$$\langle P_L \rangle_{RMS} = \frac{I^2 R_{Tissue}}{2}, \tag{121}$$

and the resistance is then

$$R_{Tissue} = (1-k^2)\left[\frac{5\omega\mu_0 N_P^2 A_P^2 L}{64\pi\sqrt{2}(z_1+z_2)^4}\right]. \tag{122}$$

The resistance associated with the coil wire material may be calculated by the equation

$$R_{Coil} = \frac{\rho\ell}{A}, \tag{123}$$

where ℓ is the length of the uncoiled wire, equal to

$$\ell = 2\pi N_P R_P, \tag{124}$$

ρ is the resistivity, and A is the cross-sectional area of the wire. This area depends on the diameter of the wire. A reasonable wire diameter choice is 1 mm. Copper is chosen as the wire material for its low resistivity. A table of material resistivity is given below.

Table 10: Resistivity Values of Some Materials

MATERIAL	RESISTIVITY AT 20 °C (Ω-M)
Silver	1.59×10^{-8}
Copper	1.7×10^{-8}
Gold	2.44×10^{-8}
Aluminum	2.82×10^{-8}
Tungsten	5.6×10^{-8}
Iron	10×10^{-8}
Platinum	11×10^{-8}
Lead	22×10^{-8}
Nichrome	150×10^{-8}

MATERIAL	RESISTIVITY AT 20 °C (Ω-M)
Carbon	3.5×10^{-5}
Germanium	0.46
Silicon	640
Glass	$10^{10} - 10^{14}$
Hard rubber	10^{13}
Sulfur	10^{15}
Quartz (fused)	75×10^{16}

The resistance stemming from the permeability of the core material is derived in a fashion similar to that of the tissue resistance. The magnetic field intensity within the primary winding is given for a long solenoid as

$$H(t) = \frac{N_P i(t)}{h}, \tag{125}$$

where N_P is the number of turns and h is the height of the wound wire, equal to the diameter of the primary winding wire times the number of turns:

$$h = d_{wP} N_P . \tag{126}$$

The energy density in this space is given as

$$w(t) = \frac{\mu H^2}{2}, \tag{127}$$

where μ is the permeability of the core material. The energy is derived from multiplying the energy density by the volume of the space, then substituting in Equation 125 for H so that

$$\begin{aligned} E(t) &= \left(\frac{\mu H^2}{2}\right)\left(\pi R_P^2 h\right) \\ &= \frac{\mu N_P^2 \pi R_P^2 [i(t)]^2}{2h}, \end{aligned} \tag{128}$$

where R_P is the radius of the primary winding. From this equation, it may be seen that the energy in the space filled by a material is equal to an expression in terms of the energy in the space when it is filled by vacuum:

$$\begin{aligned} E(t) &= K_m E_{FS} \\ &= K_m \left(\frac{\mu_0 N_P^2 \pi R_P^2 [i(t)]^2}{2h}\right), \end{aligned} \tag{129}$$

where E_F is the energy in the volume in free space and K_m is the relative permeability of the material, given as

$$K_m = \frac{\mu}{\mu_0}. \tag{130}$$

The primary core permeability is a material property determined directly from the choice of core material. Core material is chosen as ferrite based on benchmarking. The relative permeability of ferrite is 1.1 (Ida 114). The power is the time derivative of the energy, hence the power in the case of a core material and the power in the absence of a material are related as

$$P = K_m P_{FS}. \tag{131}$$

The power discrepancy between the two cases is the amount of power lost due to the permeability property of the core. This discrepancy correlates to the lesser amount of power available to be picked up at the receiver, namely

$$P_L = P - P_{FS}. \tag{132}$$

Combining the previous two equations yields an expression for the power lost in terms of the relative permeability and the power in free space:

$$P_L = (K_m - 1)P_{FS}, \tag{133}$$

where P_{FS} is expressly defined as

$$\begin{aligned} P_{FS}(t) &= \frac{dE_{FS}}{dt} \\ &= -\frac{\mu_0 N_P^2 \pi R_P^2 I^2 \omega}{2h} \cos\omega t \sin\omega t \\ &= -\frac{\mu_0 N_P^2 \pi R_P^2 I^2 \omega}{2h} \sin 2\omega t. \end{aligned} \tag{134}$$

Then, P is appropriately given as

$$\begin{aligned} P(t) &= K_m P_{FS} \\ &= -\frac{K_m \mu_0 N_P^2 \pi R_P^2 I^2 \omega}{2h} \sin 2\omega t. \end{aligned} \tag{135}$$

So, P_L is then

$$P_L(t) = -\frac{(K_m - 1)\mu_0 N_P^2 \pi R_P^2 I^2 \omega}{2h} \sin 2\omega t. \tag{136}$$

The power lost may also be expressed in terms of a resistance and its root mean squared power:

$$\langle P_L \rangle_{RMS} = \frac{I^2 R_{Core}}{2} = \frac{(K_m - 1)\mu_0 N_P^2 \pi R_P^2 I^2 \omega}{h2\sqrt{2}}. \tag{137}$$

The resistance due to the presence of the core material is then

$$R_{Core} = \frac{(K_m - 1)\mu_0 N_P^2 \pi R_P^2 \omega}{h2\sqrt{2}}. \tag{138}$$

Thus, combining the resistances associated with the tissue, the coil, and the core yields the lumped resistance:

$$R = \left(1 - e^{-2\alpha_1 z_1}\right)\left[\frac{5\omega\mu_0 N_P^2 A_P^2 L}{64\pi\sqrt{2}(z_1 + z_2)^4}\right] + \frac{2\pi\rho N_P R_P}{A} + \frac{(K_m - 1)\mu_0 N_P^2 \pi R_P^2 \omega}{h2\sqrt{2}}. \tag{139}$$

The three resistances that comprise the lumped resistance may be solved separately and added (Appendix E). The resultant resistance is equal to 0.9086 Ω, or about 1 Ω.

The battery voltage necessary to induce a minimum voltage in the receiver remains to be found. A voltage-limited condition, in other words, the use of a battery with an open cell potential of e_B, is assumed. It is also assumed that the coil reactance may be cancelled and that the source resistance is negligible, as these may both be easily accomplished with circuit design. A simple diagram shown below illustrates the basic circuit approach.

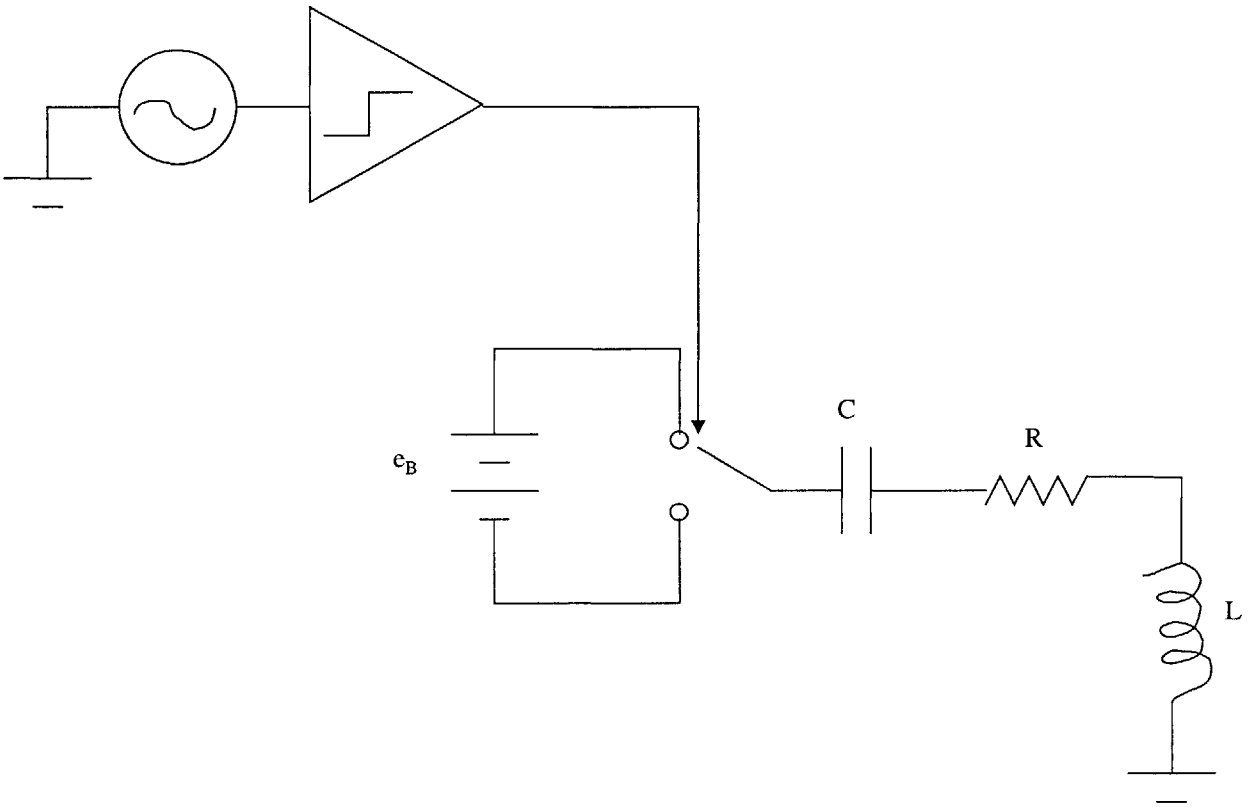

Figure 21: Circuit Approach Concept

Then, if the coil current is switched between the battery voltage and ground with zero impedance, its root-mean-squared value may be described as

$$\langle i \rangle_{RMS} = \frac{\langle e_B \rangle_{RMS}}{R}, \tag{140}$$

where $\langle e_B \rangle_{RMS}$ is the root-mean-squared value of the battery voltage and R is the lumped resistance previously determined. Combining these equations leads to an easily-solved expression for the battery voltage:

$$\langle e_B \rangle_{RMS} = \frac{4\sqrt{2}(z_1 + z_2)kR}{\mu_0 \omega A_P N_P N_S} \langle e_S \rangle_{RMS}. \tag{141}$$

Inserting appropriate variable values and solving gives the result that the minimum battery voltage required is 1.25×10^{-6} V. This requirement may be easily met by any number of commercially-available batteries. In fact, a battery may be chosen with a larger than specified open cell voltage, as a power conversion circuit can easily separate and distribute the proper

voltage values to power-requiring components.

In the glucose telemetry-instrumentation system designed by Shults and others in 1994, the implanted sensor used a pair of lithium coin cells, Panasonic BR2330, each with capacity of 0.25 A-h. The power source remains over 5.6 V throughout most of the battery lifetime. The current demand of the device is 7 μA in standby mode and 3 mA in transmit mode. This yields a battery lifetime of 3.5 years in standby mode, 2.5 years at the longest transmitting interval able to be set, and 45 days at the shortest transmit interval. The authors assumed that the shortest transmit interval would be used approximately 24 hours per month, while the longest transmit interval would be used the rest of the time. With these assumptions, a battery lifetime of about 1.5 years is expected. (Shults 938) These calculations are made in the following fashion.

Given the length of time of a telemetry transmission burst b, the transmission interval i, the standby state drain s, and the transmission state drain t, it is possible to calculate the total drain on the battery D for a certain transmission interval:

$$D = \left(\frac{i}{i+b}\right)s + \left(\frac{b}{i+b}\right)t \text{ (A).} \tag{142}$$

Now, given the battery capacity C, one may arrive at the battery lifetime L for a given transmission interval:

$$L_h = \frac{C}{D} \text{ (hours).} \tag{143}$$

Of course, the battery lifetime may also be calculated in terms of days or years, as

$$L_d = \frac{L_h}{24} = \frac{C}{24D} \text{ (days)} \tag{144}$$

or

$$L_y = \frac{L_d}{365} = \frac{L_h}{8760} = \frac{C}{8760D} \text{ (years).} \tag{145}$$

Once L_y is known for each operating interval, the total battery lifetime may be derived. If one mode is used A days out of a year, and a second mode is used B days out of a year, where A + B equals 365 days, and L_{yA} is the battery lifetime in the first mode and L_{yB} is the lifetime in the second mode, then the overall battery lifetime L_T is

$$L_T = \left(\frac{A}{A+B}\right)L_{yA} + \left(\frac{B}{A+B}\right)L_{yB} \text{ (years).} \tag{146}$$

Since the necessary battery lifetime has been specified by functional requirement number

7, the given value of L_T is 4 weeks, or about 7.7×10^{-2} years. Assume that a transmission interval of 300 s, or one reading per 5 minutes, is used for continuous monitoring throughout the product lifetime and that a telemetry burst takes 1/3 of a second and 8×10^{-4} A, as was assumed in the previous section. The standby period is characterized by a low-level input of 7 μA, as is assumed in the benchmarking case of the device by Shults. Given these assumptions, the necessary capacity is calculated as roughly 9×10^{-6} A-h (Appendix F).

Another way to approach the problem is to selectively arm the sensor electronics. Instead of remaining powered up continuously, the electronics would operate only to send a reading and then power down. Activation could be stimulated by a signal sent from the receiver coil to the transmitter coil. In this scenario, readings could be taken whenever necessary at the discretion of the physician. Power is not wasted, and hence, a smaller power source may be implemented. Next, the battery size specification should be met.

Oak Ridge National Laboratory has developed thin-film batteries which are extremely small; the batteries are made 10 to 15 μm thick. They have high energy and power densities and may be fabricated in essentially any shape and any required size. Their single cell operation runs at 4 V and is capable of discharging continuous currents up to several mA/cm^2. These lithium batteries operate within a wide temperature range of -25 °C up to 125 °C. (Bates)

Battery placement must also be addressed. It should not be placed inside the antenna loop in order to avoid the "shorted turn" effect, which would reduce the radiated signal. If it must be placed inside the loop, MacKay suggests "the loop should be several times the diameter of the battery case and the battery should be centered" (248). However, it is best if the battery is placed outside the loop, even if placed close to the loop. It has been found that even very close placement "does not much degrade coil performance" (MacKay 248).

Having specified the operating frequency, coil designs, and the power source, the circuitry description remains. Unfortunately, detailed circuit design is outside the designer's realm of knowledge and will not be attempted in this thesis. Instead, a representative design is recommended, which may be modified to suit this application. The chosen design is one for a system capable of monitoring several *in vivo* glucose sensors in a single clinical area. It is small, lightweight, and runs on low power. It contains data check parameters and failsafes to ensure viable and accurate information transfer. Designed in 1994, it appears in a *IEEE Transactions of Biomedical Engineering* journal article written by Mark Shults and others.

3.2.2.2 DATA DISPLAY

The data display should meet the standards set forth by the functional requirements and, ultimately, meet metric levels defined in consideration of those functional requirements. Requirements number 28 through 31 apply. The display unit should be easy to read, quantified by a non-skilled user being able to obtain target marker information in less than 1 minute. The display should be easy to manipulate. This requirement is met by having at most 5 different displays that may be toggled. Another standard is that visual and audio warnings should be included. If target marker levels match rejection, infection, or occlusion signature concentrations, both visual and audio alarm devices should alert a medical professional. These standards may be quantified by a certain lux value of light and the use of vibrant colors, as well as sounds at a certain decibel level at a certain frequency. These levels should be set as to be most effective at obtaining a person's attention. This thesis does not attempt to determine these values, which are most likely best ascertained through experimentation.

3.2.3 Remain Biocompatible

3.2.3.1 HOUSING

The overall size of the implant is determined by the housing. While larger devices may cause a greater degree of tissue injury upon implantation, perhaps leading to increased inflammation and a thicker fibrous capsule, very small implants may be prone to phagocytic response, stimulating macrophages and foreign body giant cells (Fraser 142). Because the size of the interior components will disallow the housing size from being small enough to be considered particulate-like, design effort should be directed at making the housing as small as possible.

The shape of the housing is also very important. It has been shown that rounded edges and smooth transitions between surfaces, rather than sharp corners, reduce the negative tissue response:

> ...the local tissue response was generally greater around the corners, e.g. shape contours of a device (this is referred to as "clubbing"), suggesting that a component of the tissue reaction around implants is probably...due to the mechanical trauma produced by the presence of the implant (Fraser 142).

In fact, triangular shaped-implants have been shown to promote a greater tissue reaction, measured histologically, than pentagonal or circular shapes (Fraser 142).

The housing material chosen is polyethylene, which has fared well in other sensors. The polyethylene shell is coated in two parts. The area surrounding the fluid chamber and sensing element is coated with PC-heads, while the remaining surface area is covered with a porous substance incorporating fibronectin. These areas will discourage protein adsorption and encourage tissue ingrowth, respectively.

In order to seal closed the two-part housing, hot melt adhesive may be used, as this type of sealant has been previously used successfully in a chronically-implanted device (Shults 940).

3.2.3.2 Encapsulant and Gasketing

The internal sensor components should be encapsulated in order to (1) reduce the possibility of breakage, (2) prevent leakage of body fluids into the device in the unlikely event that fluid should penetrate the outer housing, and (3) prevent the leaching of battery fluids into the tissue in the unlikely event that the battery should leak and that the outer housing is permeable. The encapsulant should be chosen keeping in mind the working temperature range of the battery, the circuitry components, and the housing material. It should also be chosen to best adhere to the internal components and the housing material. The third consideration is that the potting material should be chosen to best minimize fluid penetration. These three specifications guide the encapsulant choice.

A benchmarking example is available. In the benchmarking example of the implantable telemetry device designed by Shults et al., the chosen encapsulant composition was 54% PW 130/35 H wax, 40% MVO 2528 resin, and 6% 93.04 resin (Shults 940).

It is helpful to consider that potting can shift the operating frequency down by as much as 20%. If the antenna wire is coated in Q-dope or Teflon, this effect may become negligible (MacKay 107).

Gasketing the device is an important method of ensuring a hermetic seal against fluid penetration. A European standard, European Council Directive 93/42/EEC stresses that "the device must be designated and manufactured in such a way as to reduce to a minimum the risks posed by substances leaking from the device" (Fraser 154).

3.3 Layout

The interior sensor system may be conceptualized in such a way so that all the necessary components fit into the smallest space with minimum physical or effective interference. While other configurations are possible, the author presents one. Several factors are considered.

The housing is split into two pieces for ease of manufacturability and assembly. Made as two parts, both components may be formed through injection molding, a cost-effective and highly reproducible manufacturing method. Mold design and production is to occur in-house; small numbers of a part, made for a prototype, are to be injection-molded by an outside vendor, a machine shop with injection molding machine access. Depending on production ramp-up numbers and schedule, it may also be most cost-effective to utilize an outside vendor for sensor production runs, as an injection molding machine represents an appreciable start-up cost. The housing is assembled as follows. Assembly of inner components is first accomplished, followed by capping with the top and bottom housing. The entire assembly is then fused with sealant. The top and bottom housing form a shape with a definite top and bottom, to facilitate proper orientation during sensor implantation. The edges are rounded to ease tissue aggravation.

The semi-permeable membrane is stretched over an opening in the top housing and is, thus, in direct contact with the environment to be sensed. This positioning allows diffusion through the membrane to occur most readily. Rapidity of target diffusion is relative to the overall sensor response time, as well as the sensing element membrane lifetime, as was previously discussed in Section 3.2.1.2.

The sensing element surface is placed as near to the interior surface of the semi-permeable membrane as is possible, without actual physical contact. It is crucial that physical contact between the two surfaces is avoided, as such contact and resultant friction could possibly dislodge relevant portions of the molecular coating, rendering the sensing element inaccurate and ineffective. A finite distance is, then, left present between the two surfaces. This space is referred to as the fluid chamber, and may be visualized as in Figure 9.

The sensing element couples directly to the circuit board. Minimum wiring distance reduces the possibility of connection failure, which could be due to sensor component vibration from normal operation or patient movement. Minimal overall space constraint is also a consideration. For the same reasons, the internal power source, the battery, directly abuts the opposite side of the circuit board. The transmitter antenna loop is oriented parallel to the

receiver coil, as is depicted in Figure 2. The battery remains outside of the transmitter loop, as was recommended in Section 3.2.2.1.11. Wiring and circuitry components on both sides of the board are encased in encapsulant.

In the model given, the shapes and placements of the components are not to be construed as exact and final. This is a concept model, which is lacking gasketing and component anchoring mechanisms, which would be necessary to include within a prototype device. Encapsulant and sealant are also absent, although the space which the encapsulant would fill is included. The ProEngineer model developed does, however, fulfill the present purpose: allow the reader to easily envision the design concept. Several views are given so that the reader may better imagine component placement.

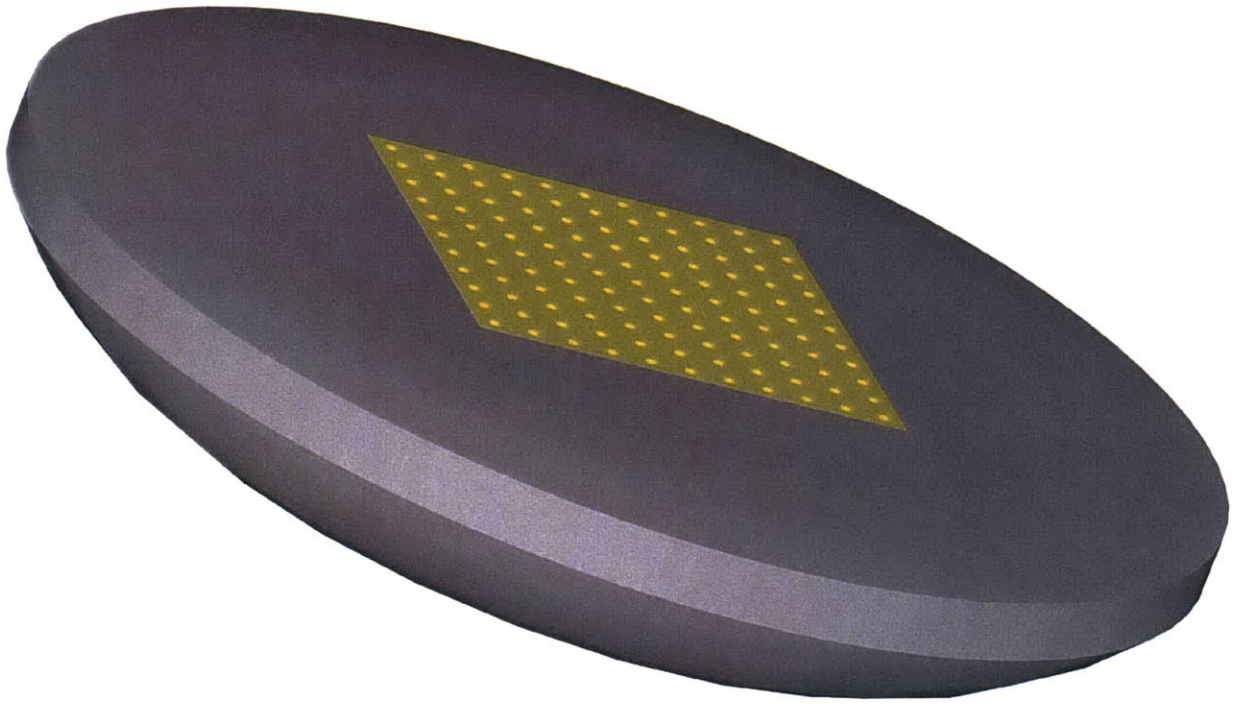

Figure 22: Design Model (External View, Color)

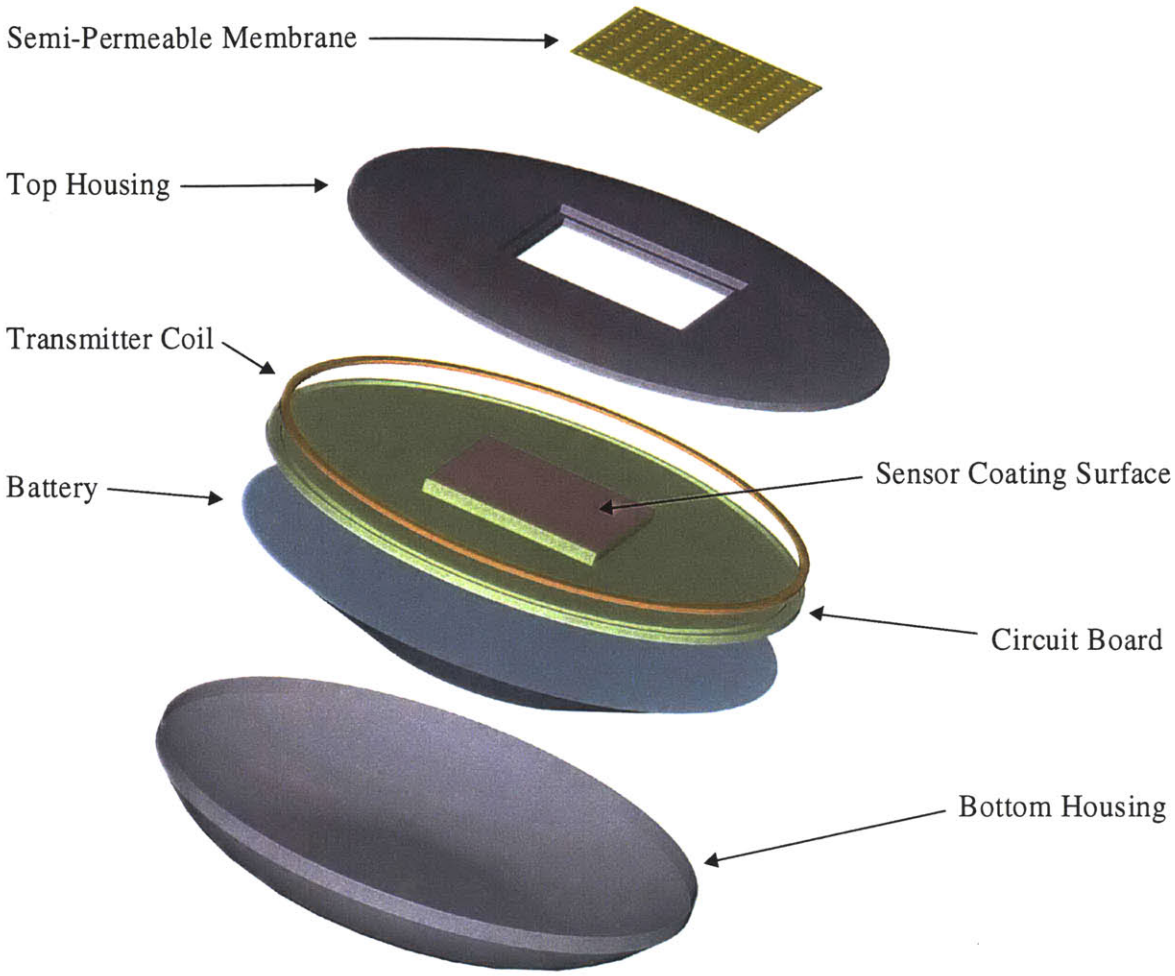

Figure 23: Design Model (Exploded View, Color)

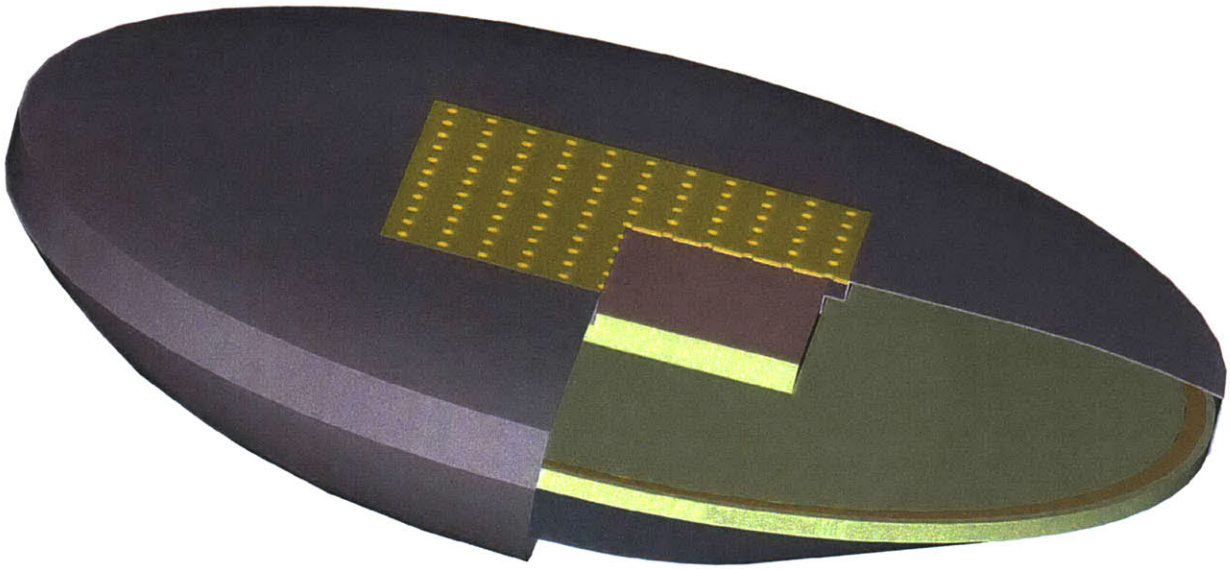

Figure 24: Design Model (Cut-away, Downward Tip View, Color)

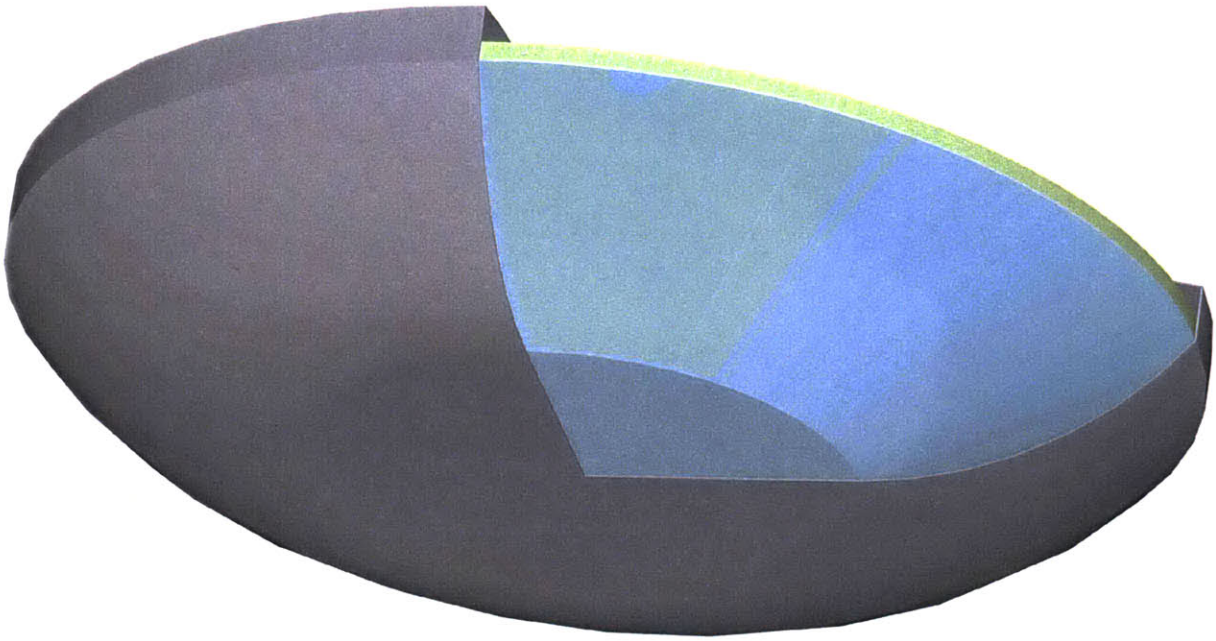

Figure 25: Design Model (Cut-away, Upward Tip View, Color)

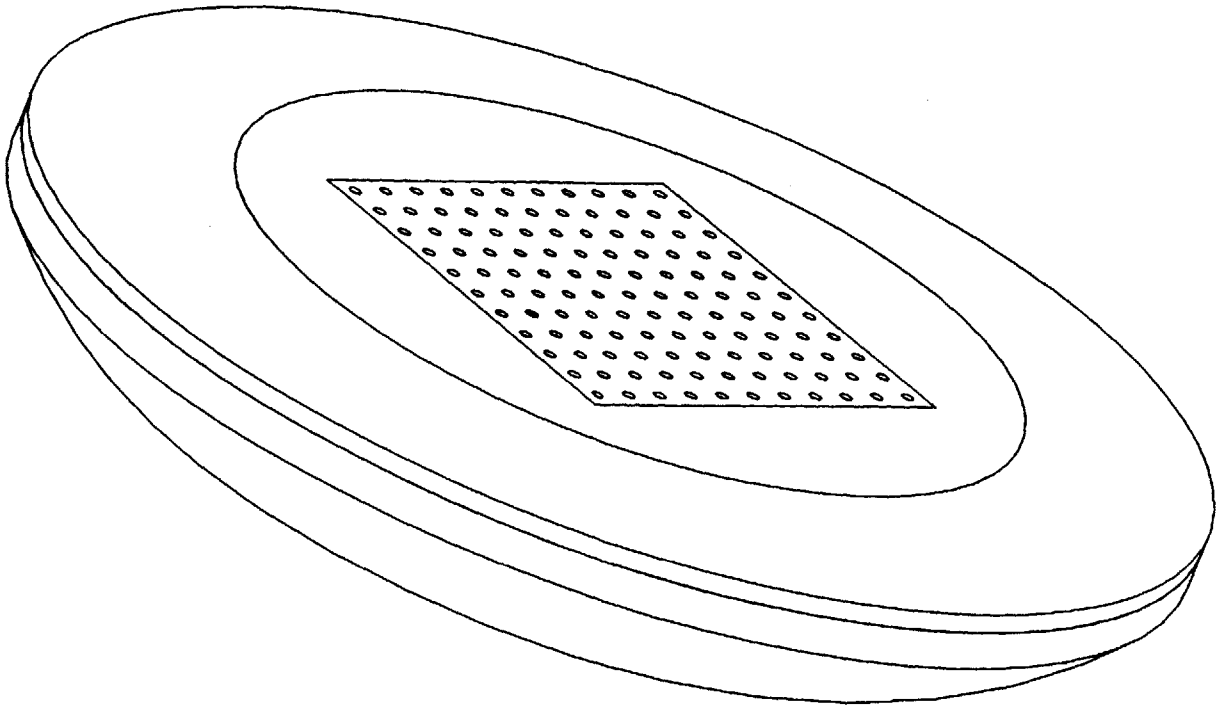

Figure 26: Design Model (External View, Black and White)

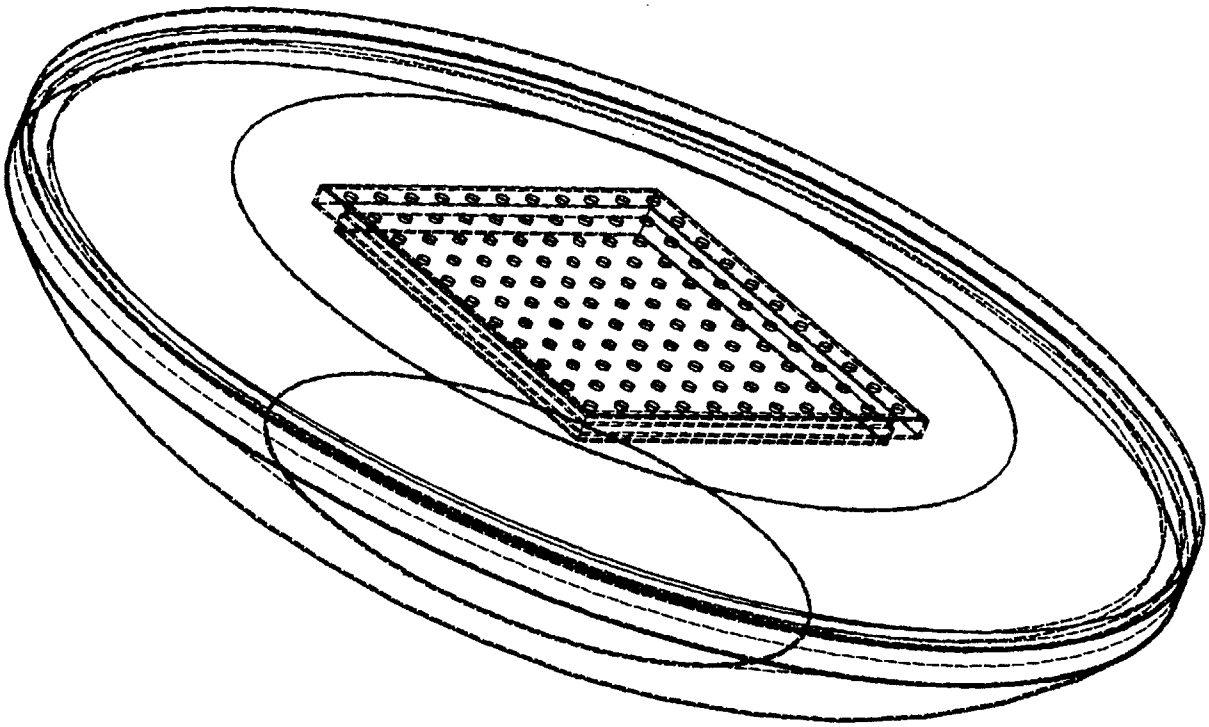

Figure 27: Design Model (External View, Black and White, Hidden Line)

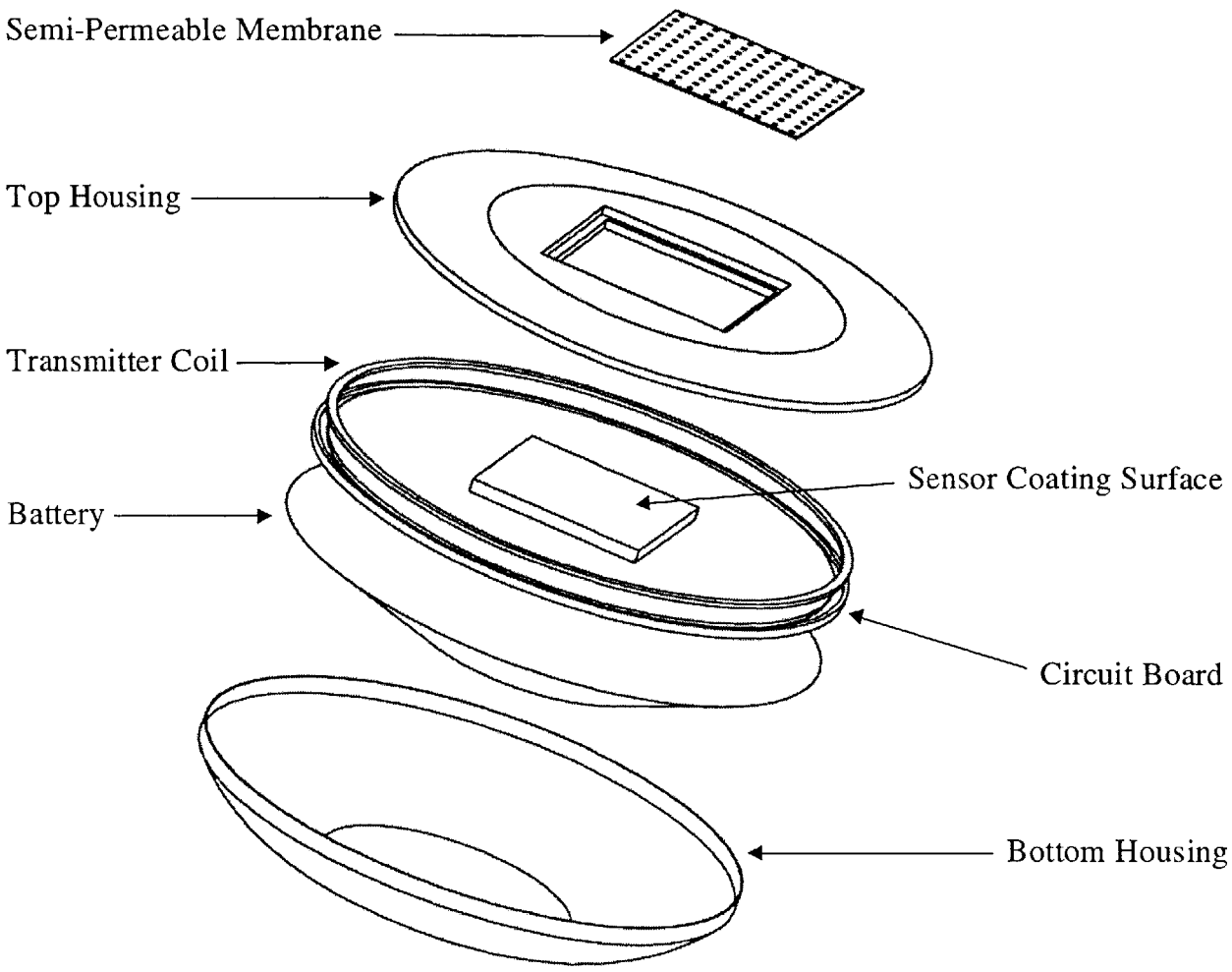

Figure 28: Design Model (Exploded View, Black and White)

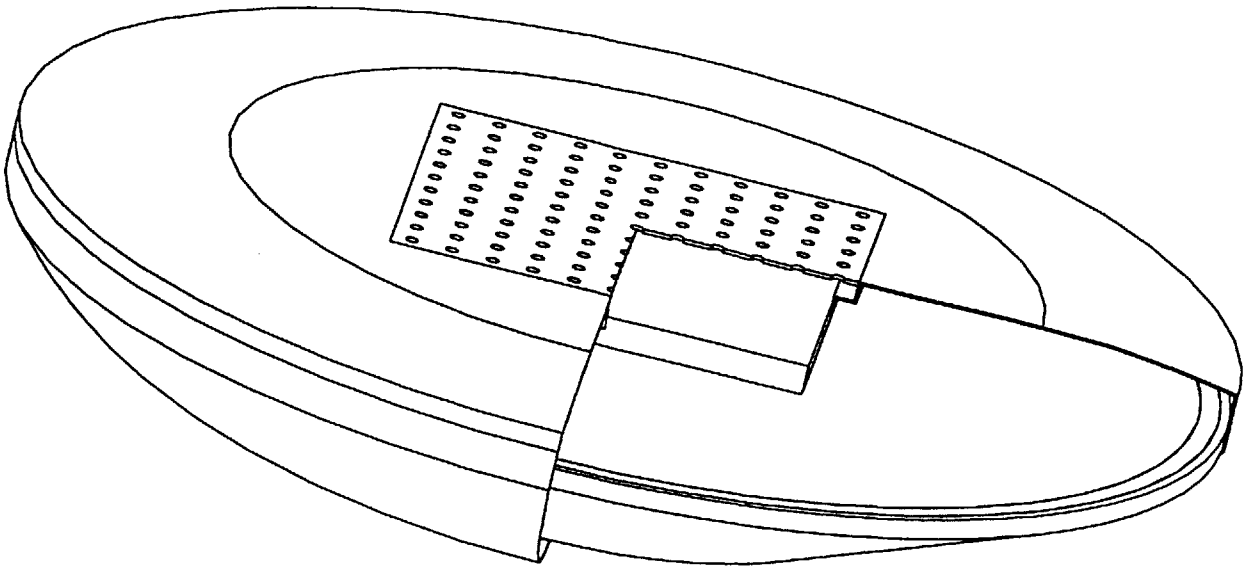

Figure 29: Design Model (Cut-away, Downward Tip View, Black and White)

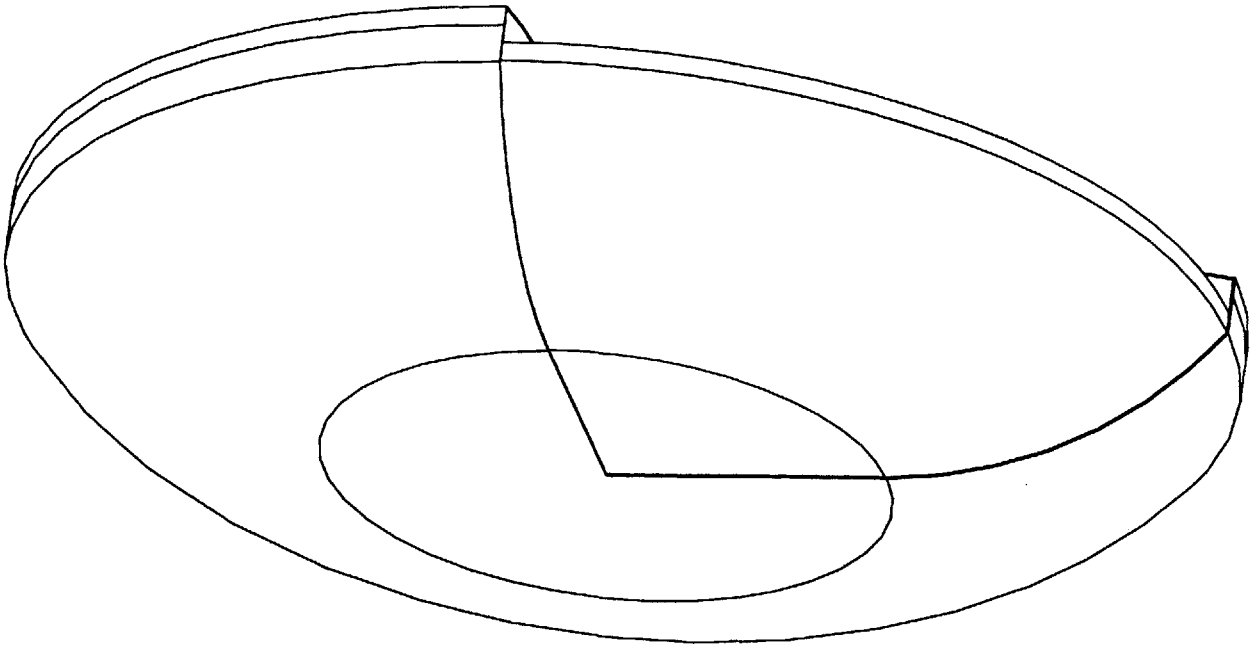

Figure 30: Design Model (Cut-away, Upward Tip View, Black and White)

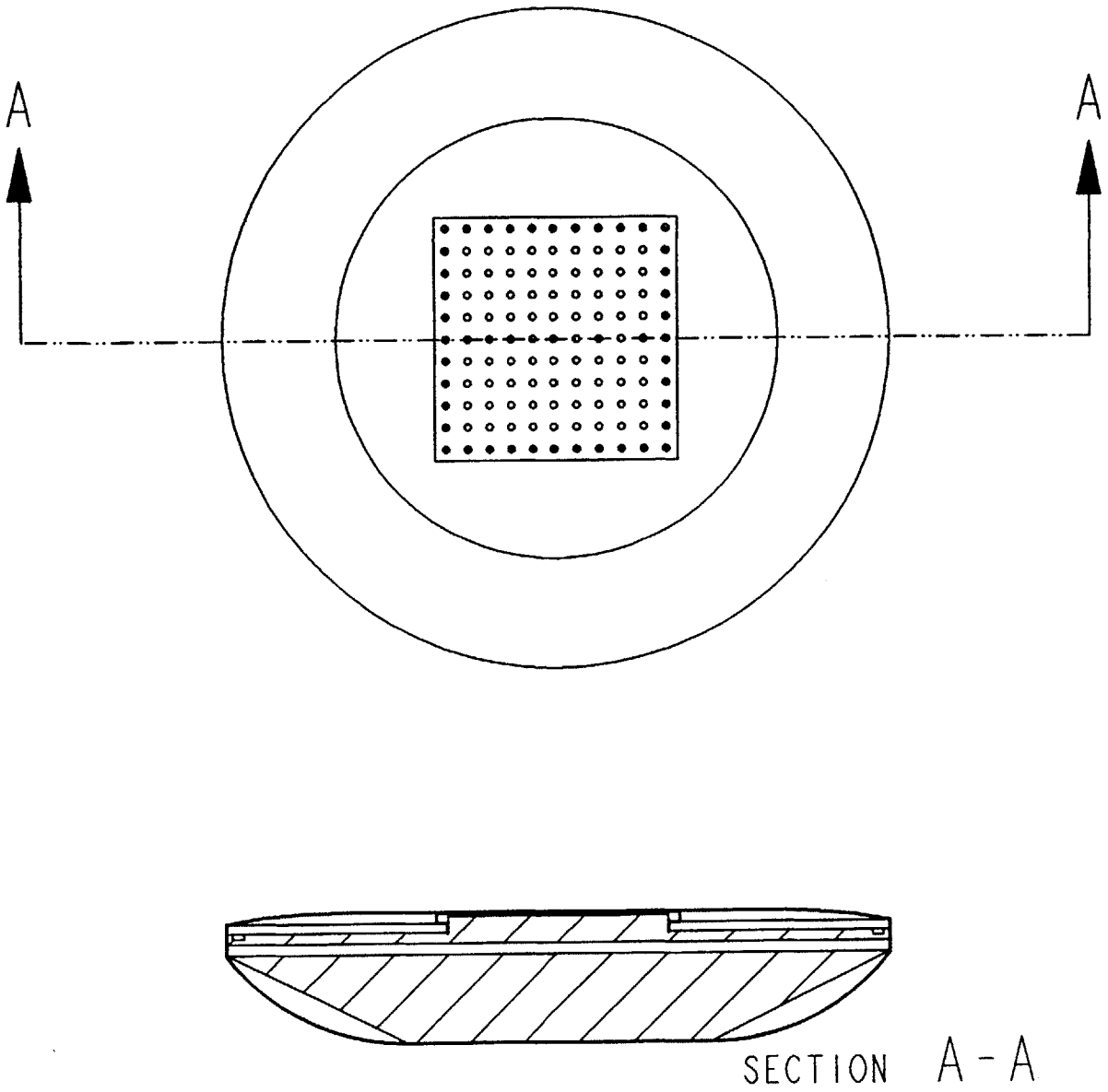

Figure 31: Design Model (Cross-Section View, Black and White)

3.4 Other Specifications

3.4.1 Implantation Procedure

Sensor implantation may occur either prior to organ implantation or during transplantation surgery. By choosing one of these times to implant, the sensor is effectively non-invasive, as it is opportunistic and does not require any bodily perforation. Since organ transplant recipients are the target users, and since the sensor is to be used up to one month post-transplant, one of these two times only makes sense.

Because a surgeon may choose to implant the device during transplantation surgery, the method of implantation must be easy. Ease of implantation may be described as the surgeon making 5 or less separate movements to install the sensor. This is within reason, as the site of implantation, the anterior side of the organ capsule, is readily exposed following a kidney or liver transplant. Because the implantation site is shallow and the sensor housing is porous and coated with adhesion-encouraging agents, no mechanical anchorage is necessary. The surgeon must make a small slit in the organ capsule, slip the sensor inside, and then may or may not choose to suture the capsule. Since the incision has no need to be greater than the sensor size, suture may not be necessary. When slipping the sensor inside the organ, the surgeon should take care to insert the device with the top facing the anterior position; this will set the direction of magnetic radiation and, hence, the orientation of the receiver.

The sensor implantation method should also be swift. This may mean that the procedure may be finished in 3 minutes or less. Given the events in the implantation sequence, this should not be troublesome.

4 Conclusion

This thesis presented a problem within the medical community for which there is no currently developed solution, the delayed and nonideal means of positive identification of acute rejection, infection, and vascular occlusion in the transplanted kidney and liver. Issues of interest with respect to the problem were explored. These consisted of: kidney and liver anatomy, history of transplantation surgery, post-operative complications of transplantation surgery, immunology events, literature review of chemical correlates associated with the three problems, biomaterial-tissue interaction events, literature review of biomaterials, biosensor benchmarking, analysis of the flexural plate-wave gravimetric sensor, and biotelemetry. A

design methodology was described and its results were given. Finally, a preliminary design was presented as a feasible solution to the problem posed.

In brief, the design describes a non-invasive, chronically-implantable biosensor able to detect concentration levels of cytokines or other chemical species indicative of acute rejection, infection, or vascular occlusion. The sensor is designed in consideration of long-term biocompatibility, as retrieval is not anticipated. The transducer element is the flexural plate-wave sensor which may be coated with antibody for any chemical species. The detected levels are transmitted via radiotelemetry to an external receiver, where the data is displayed and stored.

Further work is necessary in order to yield a usable product. Future steps are suggested. A prototype should be constructed based on the theoretical design given in order to obtain experimental design parameters, which may vary from theory given unforeseen factors. Biocompatibility testing should be run in order to best predict long-term *in vivo* performance and stability. A cost analysis should be undertaken to prove that the concept is monetarily attractive to potential developers. Finally, a manufacturing plan should be constructed to allow timely and efficient product production and implementation.

The concepts developed in this thesis and the further work accomplished will comprise the development of the implantable organ biosensor, a product that is necessary to solve a problem facing organ transplant recipients today.

References

Books:

Andrade, Joseph D., ed. Surface and Interfacial Aspects of Biomedical Polymers, Volume 2: Protein Adsorption. New York: Plenum Press, 1985.

Berkow, Robert, M.D., ed. The Merk Manual of Medical Information, Home Edition. Whitehouse Station: Merck Research Laboratories, 1997.

Berne, Robert M., et al. Physiology, Fourth Edition. St. Louis: Mosby, 1988.

Bronzino, Jospeh D., ed. The Biomedical Engineering Handbook. Boca Raton: CRC Press LLC, 1995.

Campbell, Neil A. Biology, Second Edition. Redwood City: The Benjamin/Cummings Publishing Company, Inc., 1990.

Carden, Frank. Telemetry Systems Design. Boston: Artech House, 1995.

Cheng, David K. Field and Wave Electromagnetics. Reading: Addison-Wesley Publishing Company, 1983.

Crank, J. The Mathematics of Diffusion, Second Edition. Oxford: Clarendon Press, 1975.

Eggins, Brian R. Biosensors: An Introduction. Chichester: Wiley Teubner, 1996.

Forsythe, John L.R., ed. Transplantation Surgery. London: W. B. Saunders Company Ltd., 1997.

Fraser, David M., ed. Biosensors in the Body: Continuous in vivo Monitoring. Chichester: John Wiley & Sons Ltd., 1997.

Guralnik, David B., ed. Webster's New World Dictionary of the American Language, Second College Edition. New York: Simon and Schuster, 1986.

Halliday, David, et al. Fundamentals of Physics, Fourth Edition. New York: John Wiley & Sons, Inc., 1974.

Hecht, Eugene. Optics, Second Edition. Reading: Addison-Wesley Publishing Company, 1987.

Ida, Nathan, and Baston, Joao P. A. Electro-Magnetics and Calculation of Fields, Second Edition. New York: Springer, 1997.

Lachmann, P. J., ed. Clinical Aspects of Immunology, Fifth Edition. Boston: Blackwell Scientific Publications, 1993.

MacKay, R. Stuart. Bio-Medical Telemetry: Sensing and Transmitting Biological Information from Animals and Man, Second Edition. New York: IEEE Press, 1993.

Netter, Frank H. The CIBA Collection of Medical Illustrations: a Compilation of Pathological and Anatomical Paintings. Summit: Ciba Pharmaceutical Products, 1959-1993.

Rubin, E., and Farber, J. L., eds. Pathology. Philadelphia: J. B. Lippincott, 1988.

Serway, Raymond A. Physics for Scientists and Engineers, with Modern Physics, Third Edition. Philadelphia: Saunders College Publishing, 1990.

Ulrich, Karl T., and Eppinger, Steven D. Product Design and Development. New York: McGraw-Hill, Inc., 1995.

Vander, Arthur J., et al. Human Physiology: The Mechanisms of Body Function, Sixth Edition. New York: McGraw-Hill, Inc., 1994.

Welkowitz, Walter, et al. Biomedical Instruments: Theory and Design. San Diego: Harcourt Brace Jovanovich, 1992.

Williams, Peter L., ed. Gray's Anatomy, Thirty-Eighth Edition. Edinburgh: Churchill Livingstone, 1995.

Zahn, Markus. Electromagnetic Field Theory: A Problem Solving Approach. New York: John Wiley & Sons, 1979.

Internet Sources:

1998 SR & OPTN Annual Report, Data Highlights, Graft and Patient Survival Rates. UNOS (United Network for Organ Sharing). 11 Jan. 2000 <http://www.unos.org/frame_Default.asp?Category=anrpt>.

Andreuccetti, Daniele, et al. Dielectric Properties of Body Tissues. Brooks Air Force Base, 1997-1998 <http://safeemf.iroe.fi.cnr.it/tissprop/htmlclie/htmlclie.htm>.

Assays Currently Available. Genox Corporation. 11 Jan. 2000 <http://www.genox.com/>.

Bates, John B. Thin-Film Rechargeable Lithium and Lithium-Ion Batteries. Oak Ridge National Laboratory, Computer Science and Mathematics Division. 1 May 1998 <http://www.ccs.ornl.gov/3M/bates.html>.

Brabson, John, and Enfield, Adrienne. Biochemistry Web Pages. Mills College, 14 Nov.1997 <http://www.mills.edu/RESEARCH/FUTURES/JOHNB/structurefunction/711.html>.

CIMIT Staff. CIMIT (Center for Innovative Minimally-Invasive Therapy). 22 Feb. 2000 (http://www.cimit.org/main/about/staff/index.html>.

Critical Data. UNOS (United Network for Organ Sharing). 14 Sept. 1999 <http://www.unos.org/Frame_default.asp?Category=Newsdata>.

Davison, Shane. Refraction Index. 1995 <http://www.is.kiruna.se/~cjo/d2i/REFRACTION.INDEX3.html>.

"Free Radicals and Oxidative Stress." The Cytokine Bulletin Spring 1996. R & D Systems. <http://cytokine.rndsystems.com/cb/cbsp96/cbsp96a3.html>.

Glossary of HIV/AIDS-Related Terms. 11 Jan. 2000 <http://www.hivatis.org/glossary/cglosary.html>.

"Ischemia/ Reperfusion Injury." The Cytokine Bulletin Spring 1996. R & D Systems. <http://cytokine.rndsystems.com/cb/cbsp96/cbsp96a3.html>.

Newcomer, Jeffrey P. Glossary of Oncology Terms. The Kingsbury Center for Cancer Care. 11 Jan. 2000 <http://www.cheshire-med.com/programs/kingsbur/terms.html#Ultrasound>.

Olhoeft, Gary R. Ground Penetrating Radar (GRORADAR). 22 Feb. 2000 <http://www.g-p-r.com/groradar.htm>.

On-Line Medical Dictionary. Gray Laboratory Cancer Research Trust. 18 Nov. 1997 <http://www.graylab.ac.uk/cgi-bin/omd?granulation+tissue>.

Subcutaneous Glucose Monitoring System: Fact Sheet. MiniMed Inc. 22 Feb. 2000 <http://www.minimed.com/files/snsr_fac.htm>.

Sweetwater Sound Glossary. Sweetwater Sound. 22 Feb. 2000 <http://www.sweetwater.com/insync/wftd/>.

Whatis.com. 29 Feb. 2000 <http://whatis.com/nfindex.htm>.

Journals:

Atanasov, P., et al. "Implantation of a Refillable Glucose Monitoring-telemetry Device." Biosensors & Bioelectronics Vol. 12, No. 7, (1997): 669-680.

Baker, Dale A., and Gough, David A. "A Continuous, Implantable Lactate Sensor." Analytical Chemistry Vol. 67, (1995): 1536-1540.

Bergan, A. "Ancient Myth, Modern Reality: A Brief History of Transplantation." Journal Biocommunity Vol. 24, No. 4 (1997): 2-9.

Bordji, K., et al. "Cytocompatibility of Ti-6Al-4V and Ti-5Al-2.5Fe Alloys According to Three Surface Treatments, Using Human Fibroblasts and Osteoblasts." Biomaterials Vol. 17, No. 9, (1996): 929-940.

Bruno, Alfredo E., et al. "All-Solid-State Miniaturized Fluorescence Sensor Array for the Determination of Critical Gases and Electrolytes in Blood." Analytical Chemistry Vol. 69, (1997): 507-513.

Budde, Klemens, et al. "Interleukin-8 Expression in Patients After Renal Transplantation." American Journal of Kidney Diseases Vol. 29, No. 6, June (1997): 871-880.

Chang, Kuo Wei, et al. "Validation and Bioengineering Aspects of an Implantable Glucose Sensor." Transactions - American Society for Artificial Internal Organs Vol. 19, (1973): 352-360.

Charpentier, B., et al. "Release of Interleukins During Tolerance and Rejection of Human Renal Allografts." Transplantation Proceedings Vol. 19, No. 1, Feb. (1987): 1572-1573.

Collier, T. O., et al. "Protein Adsorption of Chemically Modified Surfaces." Biomedical Sciences Instrumentation Vol. 33, (1997): 178-183.

Cosenza, Carlos A., et al. "Intragraft Cytokine Gene Expression in Human Liver Allografts." Liver Transplantation and Surgery Vol. 1, No. 1, Jan. (1995): 16-22.

Cosofret, Vasile V., et al. "Electroanalytical and Surface Characterization of Encapsulated Implantable Membrane Planar Microsensors." Analytica Chimica Acta Vol. 314, (1995): 1-11.

Csoregi, Elisabeth, et al. "Design, Characterization, and One-Point In Vivo Calibration of a Subcutaneously Implanted Glucose Electrode." Analytical Chemistry Vol. 66, (1994): 3131-3138.

Ferdman, Ariel G., and Yannas, Ioannis V. "Scattering of Light from Histologic Sections: A New Method for the Analysis of Connective Tissue." The Journal of Investigative Dermatology Vol. 100, No. 5, May (1993): 710-716.

Fischer, U. "Continuous in vivo Monitoring in Diabetes: the Subcutaneous Glucose Concentration." Acta Anaesthesiologica Scandinavica Vol. 39, (1995): 21-29.

Gough, David A., and Armour, Jon C. "Development of the Implantable Glucose Sensor: What are the Prospects and Why is it Taking So Long?" Diabetes Vol. 44, No. 9, Sept. (1995): 1005-1009.

Gretzer, C., et al. "Monocyte Activation on Titanium-sputtered Polystyrene Surfaces In Vitro: the Effect of Culture Conditions on Interleukin-1 Release." Biomaterials Vol. 17, (1996): 851-858.

Herold, Nicole, et al. "Measurements of Behavior in the Naked Mole-Rat after Intraperitoneal Implantation of a Radio-Telemetry System." Journal of Neuroscience Methods Vol. 81, (1998): 151-158.

Humar, Abhinav, et al. "The Acutely Ischemic Extremity After Kidney Transplant: An Approach to Management." Surgery Vol. 123, No. 3, March (1998): 344-350.

Kutukculer, N., et al. "The Value of Posttransplant Monitoring of Interleukin (IL)-2, IL-3, IL-4, IL-6, IL-8, and Soluble CD23 in the Plasma of Renal Allograft Recipients." Transplantation Vol. 59, No. 3, Feb. 15 (1995): 333-340.

Lang, Thomas, et al. "Production of IL-4 and IL-10 Does Not Lead to Immune Quiescence in Vascularized Human Organ Grafts." Transplantation Vol. 62, No. 6, Sept. 27 (1996): 776-780.

Lee, Po-Huang, et al. "Serum Interleukin-2 and Soluble Interleukin-2 Receptor in Renal Transplant Recipients." Journal of the Formosan Medical Association Vol. 91, No. 9, Sept. (1992): 844-848.

Li, Xian Chang, et al. "Differential Expression of T-Cell Growth Factors in Rejecting Murine Islet and Human Renal Allografts." Transplantation Vol. 66, No. 2, July 27 (1998): 265-268.

Lipman, Mark L., et al. "Immune-activation Gene Expression in Clinically Stable Renal Allograft Biopsies: Molecular Evidence for Subclinical Rejection." Transplantation Vol. 66, No. 12, Dec. 27 (1998): 1673-1681.

Maury, C.P.J., and Teppo, A.M. "Serum Immunoreactive Interleukin 1 in Renal Transplant Recipients." Transplantation Vol. 45, No. 1, Jan. (1988): 143-147.

McKean, Brian D., and Gough, David A. "A Telemetry-Instrumentation System for Chronically Implanted Glucose and Oxygen Sensors." IEEE Transactions on Biomedical Engineering Vol. 35, No. 7, July (1988): 526-532.

Meffert, Roland M. "Do Implant Surfaces Make a Difference?" Current Opinion in Periodontology Vol. 4, (1997): 104-108.

Mercado, R. C., and Moussy, F. "In Vitro and In Vivo Mineralization of Nafion Membrane Used for Implantable Glucose Sensors." Biosensors & Bioelectronics Vol. 13, No. 2, (1998): 133-145.

Mora Durban, M., et al. "Non-functioning Renal Graft: Indications for Transplant Excision." Archivos Espanoles De Urologia Vol. 42, No. 9, Nov.-Dec. (1989): 873-878.

Munoz, R., et al. "Renal Graft Survival in Children with Early Acute Rejection." Pediatric Transplantation Vol. 2, No. 4, Nov. (1998): 294-298.

Ogiso, M., et al. "The Process of Physical Weakening and Dissolution of the HA-coated Implant in Bone and Soft Tissue." Journal of Dental Research Vol. 77, No. 6, (1998): 1426-1434.

Ohashi, Eiji, and Karube, Isao. "Development of a Thin Membrane Glucose Sensor Using β-type Crystalline Chitin for Implantable Biosensor." Journal of Biotechnology Vol. 40, (1995): 13-19.

Oliveira, Gerardo, et al. "Cytokine Analysis of Human Renal Allograft Aspiration Biopsy Cultures Supernatants Predicts Acute Rejection." Nephrology, Dialysis, Transplantation Vol. 13, No. 2, Feb. (1998): 417-422.

Patzer, John F. II, et al. "A Microchip Glucose Sensor." American Society for Artificial Internal Organs Journal Vol. 41, No. 3, July (1995): M409-M413.

Pikoulis, Emmanouil, et al. "Rapid Arterial Anastomosis with Titanium Clips." American Journal of Surgery Vol. 175, No. 6, June (1998): 494-496.

Quinn, C. P., et al. "Kinetics of Glucose Delivery to Subcutaneous Tissue in Rats Measured with 0.3-mm Amperometric Microsensors." American Journal of Physiology Vol. 269, Vol. 1, July (1995): E155-E161.

Rabinovitz, Raphael S., et al. "Implantable Sensor for Intraoperative and Postoperative Monitoring of Blood Flow: A Preliminary Report." Journal of Vascular Surgery Vol. 12, No. 2, Aug. (1990): 148-157.

Reach, Gerard, and Wilson, George S. "Can Continuous Glucose Monitoring Be Used for the Treatment of Diabetes?" Analytical Chemistry Vol. 64, No. 6, March 15 (1992): 381A-386A.

Rosengren, Agneta, et al. "Immunohistochemical Studies on the Distribution of Albumin, Fibrinogen, Fibronectin, IgG and Collagen Around PTFE and Titanium Implants." Biomaterials Vol. 17, No. 18, (1996): 1779-1786.

Schmouder, Robert L., et al. "Epithelial-derived Neutrophil-activating Factor-78 Production in Human Renal Tubule Epithelial Cells and in Renal Allograft Rejection." Transplantation Vol. 59, No. 1, Jan. 15 (1995): 118-124.

Sharma, V. K., et al. "Molecular Correlates of Human Renal Allograft Rejection." Transplantation Proceedings Vol. 30, No. 5, Aug. (1998): 2364-2366.

Shichiri, Motoaki, et al. "Telemetry Glucose Monitoring Device with Needle-Type Glucose Sensor: A Useful Tool for Blood Glucose Monitoring in Diabetic Individuals." Diabetes Care Vol. 9, No. 3, May-June (1986): 298-301.

Shortkroff, S., et al. "Healing of Chondral and Osteochondral Defects in a Canine Model: the Role of Cultured Chondrocytes in Regeneration of Articular Cartilage." Biomaterials Vol. 17, No. 2, Jan. (1996): 147-154.

Shults, Mark C., et al. "A Telemetry-Instrumentation System for Monitoring Multiple Subcutaneously Implanted Glucose Sensors." IEEE Transactions on Biomedical Engineering Vol. 41, No. 10, Oct. (1994): 937-942.

Shultz, Jerome S., et al. "Affinity Sensor: A New Technique for Developing Implantable Sensors for Glucose and Other Metabolites." Diabetes Care Vol. 5, No. 3, May-June (1982): 245-253.

Smith, Brian, et al. "An Externally Powered, Multichannel, Implantable Stimulator-telemeter for Control of Paralyzed Muscle." Transactions of Biomedical Engineering Vol. 45, No. 4, April (1998): 463-475.

Thompson, Michael, & Vandenberg, Elaine T. "In Vivo Probes: Problems and Perspectives." Clinical Biochemistry Vol. 19, No. 5, Oct. (1986): 255-261.

Turner, Robin F. B., et al. "Preliminary In Vivo Biocompatibility Studies on Perfluorosulphonic Acid Polymer Membranes for Biosensor Applications." Biomaterials Vol. 12, May (1991): 361-368.

Van Kooten, Cees, et al. "Interleukin-17 Activates Human Renal Epithelial Cells In Vitro and is Expressed During Renal Allograft Rejection." Journal of the American Society of Nephrology Vol. 9, No. 8, Aug. (1998): 1526-1534.

Van Kooten, Theo G., et al. "Influence of Silicone (PDMS) Surface Texture on Human Skin Fibroblast Proliferation as Determined by Cell Cycle Analysis." Journal of Biomedical Materials Research Vol. 53, No. 1, Spring (1998): 1-14.

Vandenbroecke, Catherine, et al. "Differential In Situ Expression of Cytokines in Renal Allograft Rejection." Transplantation Vol. 51, No. 3, Mar. (1991): 602-609.

Wenzel, Stuart W., and White, Richard M. "Flexural Plate-wave Gravimetric Sensor." Sensors and Actuators Vol. A21-A23, (1990): 700-703.

Weston, S. D., et al. "Lack of Correlation of Soluble E-selectin Level with Renal Transplant Rejection." Transplant Immunology Vol. 3, No. 1, March (1995): 50-54.

Wong, W.W., and Bain, V.G. "Update in Liver Transplantation." Canadian Family Physician Vol. 45, May (1999): 1241-1249.

Xu, Guo-Ping, et al. "Intragraft Expression of IL-10 messenger RNA: A Novel Correlate of Renal Allograft Rejection." Kidney International Vol. 48, No. 5, Nov. (1995): 1504-1507.

Yang, Qingling, et al. "A Needle-Type Sensor for Monitoring Glucose in Whole Blood." Biomedical Instrumentation and Technology Vol. 31, No. 1, Jan. (1997): 54-62.

Zervas, Nicholas T., et al. "A Pressure-balanced Radio-telemetry System for the Measurement of Intracranial Pressure: A Preliminary Design Report." Journal of Neurosurgery Vol. 47, (1977): 899-911.

Personal Communication:

Carpenter, C. B. Laboratory of Immunogenetics and Transplantation, Brigham and Womens' Hospital. Personal Interview. 9 June 1999.

Dawson, Steve. Head of Abdominal Interventional Radiology and Program Director of Interventional Radiology Fellowship Program at Massachusetts General Hospital. Assistant Professor of Radiology at Harvard Medical School. Visiting Scientist at the Massachusetts Institute of Technology. Personal Interview. 22 June 1999.

Appendix A: Notes, Interview with Joseph P. Vacanti, M. D.

11/9/98

Meeting Summary

Attending: Joseph P. Vacanti, M.D.
Brian T. Cunningham
Megan M. Owens

Date: Monday, November 2, 1998

Location: MGH

Purpose: To report status of sensor development,
To ask the customer (doctor) what features are needed or wanted,
To gain further insight about the general concept of the project.

Notes:

The critical period, the period we should design the lifetime of the sensor to meet, is the first few weeks following transplant. Sometimes, a patient will show external signs of trouble, i.e. a fever, that may be interpreted one of three phenomena, whose symptoms overlap: rejection, vascular occlusion, and infection. The desired approach would be to test locally to determine exactly what is going on, however, current methods only allow global testing, through the blood etc., or biopsies. It is therefore possible for a doctor to misdiagnose and administer treatment which could hurt the patient. For example, if a child is suffering from infection, but the doctor thinks it is rejection, the doctor will administer immunosuppressive therapy of some sort, which will lower the body's defense mechanisms, allowing the infection to thrive.

Rejection can be sensed through cytokines and complement fixation, while vascular occlusion can be sensed through acid production or ATP depletion, etc.

It is the opinion of this doctor that a removable sensor, or a sensor with leads coming out of the body, is preferable to a sensor that is left inside the body in its entirety.

As far as designing the attachment mechanism, this doctor feels that the mechanism does not have to be different for different organs since the tissues are all surprisingly similar. We do want to ensure that the sensor does not "damn itself" and cause more damage than it is worth. The attachment mechanism should not hurt the organ, however, probes as long as an inch have been stuck into an organ without considerable damage.

As far as whether the device must be continuous or snapshot, this doctor feels that the snapshot sensor is currently a better approach, and it will adequately fulfill the purpose of the device.

Other recommended reading: Journal of Transplantation, Transplantation Proceedings,

Transplantation Reviews.

The sensor placement should be local to the organ.

Only one sensor per organ is needed since the three phenomena occur all over if they occur at all.

When asked whether or not he had any knowledge of similar devices, the doctor replied that he knows of no similar devices on the market.

When asked about maximum safe size, he said that it was not at all critical, that a silver-dollar-sized patch would even be okay, to just leave it on the surface of the organ and extract the leads when use is done.

Summary of J. Vacanti's opinions:

1. Lifetime of the device must be at least as long as the critical period, a few weeks post-transplant.
2. Purpose of the device is to detect indications of at least two of the three phenomena: rejection, vascular occlusion, and infection.
3. Device should be implanted locally.
4. Sensor could have removable leads.
5. The same attachment mechanism may be used for all organs; only one sensor package design is necessary.
6. Shapshot sensor is appropriate.
7. One sensor per organ.
8. No similar device on the market.
9. Size is not critical.

More information needed about:

What exactly are we trying to sense? J. Vacanti was not firm about this. He suggested we speak to other sources. We must find out what we are looking for.

Appendix B: Matlab Script, Determine Operating Frequency

M-File Script

```
% Choosing operating frequency:
% Depth of penetration

% In the case of an implant near the center of an animal's body,
the distance to
% the surface of the animal should be much less than the depth
of penetration in
% order to guarantee that sufficient magnetic field strength
exists in the air for
% external pickup.

% Regarding this, note that NO SAFETY FACTORS built in to these
calculations.
% These are strictly to show the relationship between frequency
and depth of
% penetration in the human body.

clear all;
close all;

% SINGLE VALUE CALCULATIONS

disp('DEFINE FREQUENCY TO YIELD THICKNESS')
disp('Resistivity (Ohm-m)')
rho = 5
disp('Magnetic permeability (H/m)')
mu = (4*pi)*1e-7
disp('Frequency (Hz)')
f = 4e5
disp('Depth of penetration')
h_in_m = (rho/(pi*mu*f))^0.5
h_in_inch = h_in_m*(39.37008)
disp('Body thickness')
x_in_m = 2*h_in_m
x_in_inch = x_in_m*(39.37008)

clear;

disp('DEFINE THICKNESS TO YIELD FREQUENCY')
disp('Resistivity (Ohm-m)')
rho = 5
disp('Magnetic permeability (H/m)')
mu = (4*pi)*1e-7
```

```
disp('Body thickness')
x_in_inch = 20
x_in_m = x_in_inch*(0.0254)
disp('Depth of penetration')
h_in_m = x_in_m/2
h_in_inch = x_in_inch/2
disp('Frequency (Hz)')
f = rho/((h_in_m^2)*pi*mu)

% To plot a graph of how frequency varies with depth of
penetration
figure(1);
clear;
for n = 50:1:200;
   x_in_inch(n)=.1*n;
   rho = 5;
   mu = (4*pi)*1e-7;
   f(n)= rho/((((.1*n)*(0.0254))/2)^2*pi*mu);
   x_axis(n) = .1*n;
end
semilogy(x_axis,f);
axis([5 20 10^7 10^9]);
grid;
xlabel('Body Thickness: Typical Range (inches)');
ylabel('Frequency (Hz)');
title('Frequency vs. Body Thickness');

clear;
figure(2);
for n = 100:1:500;
   h_in_m(n)=.001*n;
   rho = 5;
   mu = (4*pi)*1e-7;
   f(n)= rho/((.001*n)^2*pi*mu);
   x_axis(n) = .001*n;
end
semilogy(x_axis,f);
axis([.1 .5 0 14e7]);
grid;
xlabel('Depth of Penetration: Typical Range (m)');
ylabel('Frequency (Hz)');
title('Frequency vs. Depth of Penetration');

figure(3);
clear;
for n = 1:1:10000;
   f = n*10^4;
```

```
   rho = 5;
   mu = (4*pi)*1e-7;
   h_in_m(n) = (rho/(pi*mu*n*10^4))^0.5;
   x_axis(n) = n*10^4;
end
semilogx(x_axis,h_in_m);
grid;
ylabel('Depth of Penetration (m)');
xlabel('Frequency (Hz)');
title('Depth of Penetration vs. Frequency');

figure(4);
x_in_inch = 2*h_in_m*39.37008;
semilogx(x_axis,x_in_inch);
grid;
ylabel('Body Thickness (inches)');
xlabel('Frequency (Hz)');
title('Body Thickness vs. Frequency');
```

Matlab Results

```
» Frequency1
DEFINE FREQUENCY TO YIELD THICKNESS
Resistivity (Ohm-m)
rho =
     5
Magnetic permeability (H/m)
mu =
  1.2566e-006
Frequency (Hz)
f =
      400000
Depth of penetration
h_in_m =
    1.7794
h_in_inch =
   70.0554
Body thickness
x_in_m =
    3.5588
x_in_inch =
  140.1107
DEFINE THICKNESS TO YIELD FREQUENCY
Resistivity (Ohm-m)
rho =
     5
Magnetic permeability (H/m)
```

```
mu =
  1.2566e-006
Body thickness
x_in_inch =
    20
x_in_m =
    0.5080
Depth of penetration
h_in_m =
    0.2540
h_in_inch =
    10
Frequency (Hz)
f =
  1.9631e+007
»
```

Appendix C: Mathematic Notes

$$
\begin{aligned}
B^2 &= \vec{B} \bullet \vec{B} \\
&= \left(\frac{\mu_0^2 N_P^2 R_P^4 [i(t)]^2}{4r^6} \cos^2\theta \right) + \left(\frac{\mu_0^2 N_P^2 R_P^4 [i(t)]^2}{16r^6} \sin^2\theta \right) \\
&= \left(\frac{3\mu_0^2 N_P^2 R_P^4 [i(t)]^2}{16r^6} \cos^2\theta \right) + \left(\frac{\mu_0^2 N_P^2 R_P^4 [i(t)]^2}{16r^6} \left[\sin^2\theta + \cos^2\theta \right] \right) \\
&= \left(\frac{\mu_0^2 N_P^2 R_P^4 [i(t)]^2}{16r^6} \right) \left(3\cos^2\theta + 1 \right)
\end{aligned}
$$

$$
\begin{aligned}
&\rho = (z_1 + z_2)\tan\psi \\
&d\rho = (z_1 + z_2)\sec^2\psi d\psi \\
&0 \le \rho \le (z_1 + z_2) \\
&0 \le \psi \le \frac{\pi}{4}
\end{aligned}
$$

$$
E(t) = \frac{\pi\mu_0 N_P^2 R_P^4 [i(t)]^2 L}{16} \int_0^{\frac{\pi}{4}} \left[\begin{array}{l} \dfrac{[(z_1 + z_2)\tan\psi][(z_1 + z_2)\sec^2\psi]}{(z_1 + z_2)^6 \sec^6\psi} + \\ \dfrac{[3(z_1 + z_2)^2][(z_1 + z_2)\tan\psi][(z_1 + z_2)\sec^2\psi]}{(z_1 + z_2)^8 \sec^8\psi} \end{array} \right] d\psi
$$

$$
\begin{aligned}
&= \frac{\pi\mu_0 N_P^2 R_P^4 [i(t)]^2 L}{16} \int_0^{\frac{\pi}{4}} \left[(z_1 + z_2)^{-4} \sin\psi\cos^3\psi \right] + \left[3(z_1 + z_2)^{-4} \sin\psi\cos^5\psi \right] d\psi \\
&= \frac{\pi\mu_0 N_P^2 R_P^4 [i(t)]^2 L}{16(z_1 + z_2)^4} \left[-\frac{\cos^4\psi}{4} - \frac{\cos^6\psi}{2} \right]_0^{\frac{\pi}{4}} \\
&= \frac{\pi\mu_0 N_P^2 R_P^4 [i(t)]^2 L}{16(z_1 + z_2)^4} \left[-\frac{1}{16} - \frac{1}{16} + \frac{1}{4} + \frac{1}{2} \right] \\
&= \frac{5\pi\mu_0 N_P^2 R_P^4 [i(t)]^2 L}{128(z_1 + z_2)^4}
\end{aligned}
$$

$$\Phi_S = \int \vec{B} \bullet d\vec{A}$$
$$= \int \left(\vec{\nabla} \times \vec{A}\right) \bullet d\vec{A}$$
$$= \oint \vec{A} \bullet d\vec{\ell}$$
$$= \frac{\mu_0 A_P N_P i(t) k}{8\pi\sqrt{2}(z_1 + z_2)^2} \oint d\vec{\ell}$$
$$= \left[\frac{\mu_0 A_P N_P i(t) k}{8\pi\sqrt{2}(z_1 + z_2)^2}\right][2\pi(z_1 + z_2)]$$
$$= \frac{\mu_0 A_P N_P i(t) k}{4\pi\sqrt{2}(z_1 + z_2)}$$

This is the flux for one loop, so for the total flux in the secondary coil, multiply by N_S:

$$\Phi_S = \frac{\mu_0 A_P N_P N_S i(t) k}{4\pi\sqrt{2}(z_1 + z_2)}$$

Appendix D: Matlab Script, Determine Coil Designs

M-File Script

```
% To solve for Ap, Np, and Ns:

% Take the following equation
% Vs = [mu_not*omega*Ap*Np*Ns*I*k]/[8(z1+z2)]
% and set Ap, Np, and Ns equal to one variable for now:
% X = ApNpNs.
% Later, one combination which yields X may be chosen.
% So, the new equation to be solved is:
% es = [mu_not*omega*X*I*k]/[8(z1+z2)].
% Solving for X yields:
% X = [8Vs(z1+z2)]/[mu_not*omega*I*k].
% where

alpha1 = 7.124;
z1 = 0.254;
k = exp(-alpha1*z1);
Vs = 3e-6;
mu_not = 4*pi*1e-7;
omega = 1.3e8;
I = 8e-4;

X = [8*Vs*z1]/[mu_not*omega*I*k]

% X = 2.8488e-4

% Now, define Ap, Np, and Ns based on this value X.
% Ap depends on the diameter of the primary coil.  If the
diameter of the
% primary coil is restricted to 1 cm, then the area is equal to
7.85e-5.
% Say Np is restricted to 2 turns, then...

Np = 2;
d = 1e-2;
Ap = pi*(d/2)^2;
Ns = X/(Ap*Np)

% Then Ns = 1.8136, or approximately 2 turns.  This will produce
the minimum signal.
% More turns will of course yield higher signal levels.
```

Matlab Results

```
» Coil
X =
  2.8488e-004
Ns =
    1.8136
»
```

Appendix E: Matlab Script, Determine Lumped Resistance

M-File Script

```
% To solve for the resistance terms:

clear all;
close all;

% Variable Definition:
alpha1 = 7.124
z1 = 0.254
k = exp(-alpha1*z1)
mu_not = (4*pi)*1e-7
omega = 1.3e8
Np = 2
dp = 1e-2
rp = dp/2
Ap = pi*(rp)^2
dwirep = 1e-3
h = dwirep*Np
Ns = 20
ds = 2*z1
rs = ds/2
As = pi*(rs)^2
dwires = 1e-3
L = dwires*Ns
Awire = (pi*(dwirep)^2)/4
rho = 1.7e-8
Km = 1.1

% Attenuation Term:
R1 = (1-
k^2)*[(5*omega*mu_not*(Np^2)*(Ap^2)*L)/(64*pi*sqrt(2)*0.254^4)]

% Coil Term:
R2 = [2*pi*rho*Np*rp]/Awire

% Core Term:
R3 = [(Km-1)*mu_not*(Np^2)*pi*(rp^2)*omega]/[h*2*sqrt(2)]

% Total Resistance:
R = R1 + R2 + R3
```

Matlab Results

```
» Resistance
alpha1 =
```

```
    7.1240
z1 =
    0.2540
k =
    0.1637
mu_not =
  1.2566e-006
omega =
   130000000
Np =
     2
dp =
    0.0100
rp =
    0.0050
Ap =
  7.8540e-005
dwirep =
    0.0010
h =
    0.0020
Ns =
    20
ds =
    0.5080
rs =
    0.2540
As =
    0.2027
dwires =
    0.0010
L =
    0.0200
Awire =
  7.8540e-007
rho =
  1.7000e-008
Km =
    1.1000
R1 =
  3.3144e-007
R2 =
    0.0014
R3 =
    0.9073
R =
    0.9086
```

Appendix F: Matlab Script, Determine Power Source Capacity

M-File Script

```
% To determine battery lifetime:

clear all;
close all;

disp('Telemetry burst time, b (s)')
b = 300e-3
disp('Transmit interval, t (s)')
i = 300
disp('Standby mode power drain, s (A)')
s = 7e-6
disp('Transmit mode power drain, t (A)')
t = 8e-4
disp('Demand, D (A)')
D = ((i/(i+b))*s)+((b/(i+b))*t)
disp('Lifetime (days)')
Days = 28
disp('Necessary battery capacity given a lifetime (A-h)')
Capacity = (Days*D)/24

% To determine battery lifetime given two operating modes
disp('Battery lifetime in short transmit interval mode, L1
(years)')
L1 = (1/365)
disp('Battery lifetime in long transmit interval mode, L2
(years)')
L2 = 2.5
disp('Number of days on short interval mode per year, A (days)')
A = 45
disp('Number of days on long interval mode per year, B (days)')
B = 365-A
disp('Battery lifetime overall, Lt (years)')
Lt = ((A/365)*L1) + ((B/365)*L2)
```

Matlab Results

```
» Lifetime
Telemetry burst time, b (s)
b =
    0.3000
Transmit interval, t (s)
i =
   300
```

```
Standby mode power drain, s (A)
s =
  7.0000e-006
Transmit mode power drain, t (A)
t =
  8.0000e-004
Demand, D (A)
D =
  7.7922e-006
Lifetime (days)
Days =
    28
Necessary battery capacity given a lifetime (A-h)
Capacity =
  9.0909e-006
Battery lifetime in short transmit interval mode, L1 (years)
L1 =
    0.0027
Battery lifetime in long transmit interval mode, L2 (years)
L2 =
    2.5000
Number of days on short interval mode per year, A (days)
A =
    45
Number of days on long interval mode per year, B (days)
B =
   320
Battery lifetime overall, Lt (years)
Lt =
    2.1921
»
```